약학박사학위논문

A study on low molecular weight heparin conjugates for cancer chemoprevention and chemotherapy based on angiogenesis inhibition

혈관 신생 억제 작용을 기반으로 한 화학적 암 예방 및 치료를 위한 헤파린 유도체의 개발에 관한 연구

2014년 8월

서울대학교 대학원

약학과 약제과학전공

김 지 영

Abstract

A study on low molecular weight heparin conjugates for cancer chemoprevention and chemotherapy based on angiogenesis inhibition

Ji-young Kim

Physical Pharmacy Major

Department of Pharmacy

The Graduate School

Seoul National University

The important role of angiogenesis over the whole process of cancer development has been extensively studied. Conventionally, angiogenesis is defined as a new vessel formation from pre-existing vascular structures and triggered at tumor size of 1-2 mm^3 for further growth. A numerous cytokines and growth factors are involved in this process, and thus they are good targets for cancer treatment. Consequently, a number of angiogenesis inhibitors with different mechanisms have been approved and widely used in the clinics. On the other hand, recently, increasing number of preclinical and clinical evidences also shows that angiogenic switch is already turned

on in the premalignant stage including hyperplasia and dysplasia, which provides a rationale to target angiogenesis for cancer chemoprevention. Cancer chemoprevention, which is defined as a pharmacological intervention to impede, arrest, or reverse carcinogenesis at its earliest stage, is well-accepted as a promising strategy for cancer controlling strategy. By targeting angiogenesis, not only the transformation from premalignant lesions to malignant tissues, but the further progression of malignant tumors can also be properly prevented and inhibited. In addition, the development of inventive drug delivery systems targeting vascular structures might be required for the further improve the therapeutic efficacy of antiangiogenic drugs while reducing toxicity.

Low molecular weight heparin is a polydisperse and highly sulphated glycosaminoglycan with molecular weight about 5000 Daltons. It has been widely used as an anticoagulant drug in the clinics. However, due to electrostatic interactions with various growth factors and cytokines, its application into anticancer therapy also has been extensively studied. In this context, a series of LMWH-bile acid conjugates was synthesized as antiangiogenic drugs in the previous studies. Through the chemical modification of LMWH, while side effect such as hemorrhage was avoided, the therapeutic efficacy was enhanced. They demonstrated both significant anticancer effects by angiogenesis inhibition and pharmacokinetic properties via different administration routes.

In the first part of this research, we introduce a newly developed oral heparin

derivative (LHTD4) for use as an inhibitor of angiogenesis and evaluate its antiangiogenic and preventive effects in an animal model of lung cancer. The antiangiogenic activities of LHTD4 were evaluated using tube formation and Matrigel assays. VEGF- and bFGF-induced tube formations were reduced by up to 77.2 and 67.3%, respectively, by LHTD4. Hemoglobin content was also significantly decreased by LHTD4 in the Matrigel plugs that were transplanted into mice. We also observed that the VEGF- and bFGF-mediated phosphorylation of the receptors VEGFR-2 and FGFR-1 was also inhibited by LHTD4. The *in vivo* anticancer effects of LHTD4 that developed following oral administration were also verified in a tumor xenograft model of human A549 lung cancer cells; most especially, tumor volume (60.2%). The expression of CD34 and Ki-67 in LHTD4-treated group was also affected. Finally, in our chemically induced lung carcinogenesis model, the number and area of each nodule were significantly reduced in the LHTD4-treated groups by 49.2% and 30.1%, respectively. In addition, the degree of angiogenesis in the lung tissue itself was affected in the treatment group. Taken together, these results suggest that LHTD4, which is an orally active heparin derivative, could be a promising candidate for the prevention of cancer by inhibiting angiogenesis.

Secondly, the combination effect of celecoxib and newly developed oral angiogenesis inhibitor, LHD4, on chemoprevention was evaluated to achieve a clinically rational regimen for cancer chemoprevention with improved efficacy and safety. The chemopreventive effects of celecoxib, LDH4, and the combination of celecoxib and LHD4 were evaluated in a murine colorectal carcinogenesis model.

After 17 experimental weeks, mouse colon tissues were collected and examined in terms of polyp volume and degree of carcinogenesis, inflammation and angiogenesis. Mice in the celecoxib- or LHD4-treated groups bore total polyp volumes of 47.0 ± 9.7 and 120.1 ± 45.2 mm^3, respectively, which represented decreases of 65.6% and 22.3% from the control (154.5 ± 33.5 mm^3). However, the polyp volume in the combination group was 22.8 ± 9.3 mm^3, a decrease of 85.2% from the control. In the comparison of carcinogenesis, the percentage of normal tissue (i.e., excluding proliferative tissue) was found to be 40.6% in the control, 51.7% in the celecoxib, 56.9% in the LHD4, and 81.7% in the combination group. In accordance with attenuated carcinogenesis, both inflammation and angiogenesis were also well controlled. Together, these results suggest that combinatory use of celecoxib and a newly developed oral heparin conjugate could be a promising regimen for chemoprevention by intervening both inflammation and angiogenesis.

Third, we have studied the COX-2 inhibition effect on antiangiogneic therapy. In present study, the induction of hypoxia and COX-2 overexpression were observed at tumor tissues that were treated with a multi-targeting angiogenesis inhibitor named as LHT7. In addition, while the recruitment of macrophage was also increased under angiogenesis inhibition, it was well-controlled by combination use of celecoxib and LHT7. On the other hand, the combination effect on tumor vasculature was also studied. The in vitro tube formation was inhibited by either LHT7 or celecoxib, but the inhibition effect was further enhanced by using them together. In addition, the in vivo tumor vessel formation and structure were also altered by treatment with LHT7,

celecoxib, and combination use. However, even though the combination therapy was effective enough to inhibit tumor angiogenesis, it did not further enhance the inhibitory effect on tumor growth in terms of volume than single drug use. Moreover, even though this regimen could not significantly increase cellular apoptosis at tumor tissues, it retarded the tumor growth by affecting cell proliferation. Taken all, COX-2 inhibition might enhance the therapeutic effect of antiangiogenic drugs both by inhibiting the inflammatory reactions induced by hypoxia and by altering the vascular stabilization that is mediated by assembly with mural cells.

Finally, we have studied on the tumor vascular structure-targeted delivery of antiangiogenic drug. We found that the systemic administration of LHT7 in cationic nanolipoplex could substantially enhance the anticancer effects. Moreover, we found that co-delivery of LHT7 with suberoylanilide hydroxamic acid (SAHA), a histone deacetylase inhibitor, in nanolipoplex could provide synergistic antitumor effect. LHT7/SAHA nanolipoplex was formulated by encapsulating SAHA inside cationic liposomes, followed by complexation of negatively charged LHT7 onto the cationic surfaces of SAHA-loaded liposomes (SAHA-L). The nanolipoplex form of LHT7 could alter its pharmacokinetics with 1.9-fold increased mean residence time compared to the free form of LHT7. LHT7/SAHA nanolipoplex showed highest antitumor efficacy in SCC-bearing mice, compared to LHT7, SAHA-L and sequential co-administration of LHT7 and SAHA-L. Consistent with the enhanced antitumor effect, the reduction of abnormal vessels in the tumor site was also the highest in the LHT7/SAHA nanolipoplex-treated group. These results suggested the potential of

LHT7/SAHA nanolipoplex for enhanced tumor vasculature targeting, and the importance of nanolipoplex-mediated co-delivery with a histone deacetylase inhibitor for maximal anticancer effect.

In conclusion, a series of LMWH-bile acids conjugates could be promising cancer chemopreventive and therapeutic agents via angiogenesis inhibition in the future. In addition, the antiangiogenic potency might be further improved by utilizing a functionalized drug delivery system such as tumor vascular targeting carrier.

Keywords: angiogenesis, heparin conjugate, cancer chemoprevention, cancer chemotherapy, cyclooxygenase-2, combination therapy, nanocomplex

Student number: 2009-30460

Table of Contents

List of Tables

List of Figures

Optical images were obtained at 40× magnification. (B, D) The number of branched points in cells that were treated with different concentrations of LHTD4 was counted using a microscope at 40× magnification. Each bar indicates the mean ± SD (n = 3). *$p < 0.05$ vs. control. **$p < 0.01$ vs. control.

Figure 2.3 Inhibitory effects of LHTD4 on VEGF-, bFGF-, and mixture-induced angiogenesis in Matrigel plugs. Mice were subcutaneously injected with 637 μL of the Matrigel mixture that contained growth factors and LHTD4. (A) After 10 days, the mice were sacrificed, and the Matrigel plugs were excised and photographed. (B) The hemoglobin content of each Matrigel plug was determined using Drabkin's method. Data are presented as the means ± SD. *$p < 0.05$ vs. no drug-treated group.

Figure 2.4 VEGF- and bFGF-dependent phosphorylation of VEGFR-2 and FGFR-1. HUVECs were incubated with 50 μg/mL LHTD4 for 1 hour, then treated with $VEGF_{165}$ (100 ng/mL) or bFGF (100 ng/mL) for 5 minutes. Proteins were separated by electrophoresis using SDS-PAGE and transferred to PVDF membranes. The phosphorylated proteins were probed using antiphospho-VEGFR-2 (panel A) and FGFR-1 (panel B). β-actin was used as the loading control.

Figure 2.5 *In vivo* inhibitory effects of LHTD4 on tumor growth in the A549 xenograft model. Mice were inoculated with A549 cancer cells (1×10^7 cells per mouse) at the dorsal flank and administered LHTD4 at different doses (0, 2.5, 5, 10 mg/kg; n number = 10). (A) Tumor volume of the control (○), and the daily oral administration of LHTD4 at 2.5 mg/kg (●), 5 mg/kg (□), and 10 mg/kg (▼). After 24 days, the mice were sacrificed and the tumors were isolated, and (B) weighed. Then, tumor tissues were paraffined in blocks, sectioned, and immunostained with the anti-CD34 and Ki-67 antibodies to examine the vessel formation and cell proliferation. (C, D) The immunostained slides were observed under a microscope at 40× magnification and photographed. (E) The expression of CD34 positive blood vessels and (F) Ki-67 positive proliferating cells were quantitatively analyzed using image analysis software. Data are expressed as the means ± SEM. *$p < 0.05$ *vs.* control. **$p < 0.01$ *vs.* control.

Figure 2.6 Evaluation of the chemopreventive effects of LHTD4 in a urethane-induced lung cancer carcinogenesis model. (A) Female A/J mice were injected with 1 mg/kg urethane, then treated with 5 mg/kg LHTD4 for 20 weeks. Mice were sacrificed at the intended time point (n number = 5 for the week of 3, 6, 9 and 15; n number = 25 for the week of 21), and

their lung tissues were collected and examined to determine (B) The morphologies of the lung tissues were determined and photographed, and (C) images of the cross-sectioned lung tissue following hematoxylin and eosin staining were obtained. (D) The number of nodules on the surface and (E) the cross-sectional area of the nodules. *$p < 0.05$ and **$p < 0.01$ *vs.* control on the same week. (F) Representative histological image of a murine lung adenocarcinoma observed in this study (100× magnification). (G) Vessel formation at lung tissues was compared between control and treatment groups by immunohistochemistry of CD34 and (H) quantification of CD34-positive area on cross-sectional lung tissue. *$p <$ 0.05 *vs.* control.

Figure 3.1 The experimental protocol and clinical observations. (A) Drug treatment schedule for LHD4 and celecoxib using AOM/DSS-induced colorectal carcinogenesis in ICR mice. Mice were treated with no drug (Group 1, n = 29), celecoxib alone (Group 2, n = 20), LHD4 alone (Group 3, n = 27), and the combination of celecoxib and LHD4 (Group 4, n = 20). LHD4 (10 mg/kg) and celecoxib (10 mg/kg) were orally administered once a day. (B) Body weight progression over the course of the study. No significant difference in body weight was observed among the various groups. (C) The incidence of prolapse during 17 weeks of experiment.

infiltration of macrophages and the integrity of the mucosa, submucosa and muscularis mucosa layers of the large intestine (scale bar = 200 μm). (C) Intensity of F4/80-positive macrophages expression was compared among groups (scale bar = 100 μm).

Figure 3.5 Degree of angiogenesis according to carcinogenesis. (A) Colon tissues of normal, hyperplasia, low- and high-grade adenoma and adenocarcinoma were also examined by using CD34 IHC as a biomarker of microvessel density (scale bar = 100 μm). (B) The intensity and distribution of CD34-positive cells were compared among groups (scale bar = 100 μm). (C) Then, the intensity of CD34 expression per field was quantitated by image analyzing software. *$p < 0.05$ vs. Group 1. **$p < 0.01$ vs. Group 1.

Figure 4.1 Dose-dependent effect of LHT7 on tumor growth inhibition. (A) SCC7-bearing mice were treated with LHT7 at 0, 0.5, 1, and 5 mg/kg/2 day, and their tumor volume on day 25 were compared. (B) Mice were intraperitoneally injected with Hypoxyprobe™-1 to detect hypoxic area at tumor tissues. *$p < 0.05$ and **$p < 0.01$, *vs. control.*

Figure 4.2 COX-2 expression under hypoxia at tumor tissues. Tumor tissues were collected from SCC7-bearing mice after Hypoxyprobe™-1 injection and were further stained with anti-COX-2 antibodies. The relationship between hypoxia and COX-2 expression was observed under confocal

Figure 5.4 Immunohistochemistry of tumor tissues isolated from mice treated with LHT7/SAHA nanolipoplex. (A) Microphotographs of anti-CD34 antibody immunostaining against microvessels on the isolated tumor tissue sections of various groups. (B) Microphotographs of anti-PCNA antibody immunostaining against proliferating cells on the isolated tumor tissue sections of various groups. (C) The numbers of anti-CD34 immunostained microvessels on the isolated tumor tissues. Data were expressed as mean ± SEM (n=3). (D) The numbers of PCNA immunostained proliferating cells on the isolated tumor tissues. Data were expressed as mean ± SEM (n=3). *$p < 0.05$ *vs.* control. **$p < 0.01$ *vs.* control

Abbreviations

LMWH	Low molecular weight heparin
UFH	Unfractionated heparin
AT	Antithrombin
HUVECs	Human umbilical vein endothelial cells
DOCA	Deoxycholic acid
TCA	Taurocholic acid
tetraDOCA	Tetrameric DOCA
DCK	N^{α}-deoxycholyl-$_{L}$-lysil-methylester
Et-STC	Ethylenediamine taurocholate
DMSO	Dimethyl sulfoxide
DCC	*N,N'*-dicyclohexylcarbodiimide
EDAC	Ethyl-3-(3-dimethylaminopropyl)carbodiimide
HOSu	*N*-hydroxysuccinimide
DMF	*N, N*-dimethylformamide
THF	Tetrahydrofuran

FITC	Fluorescein isothiocyanate
COX-2	Cyclooxygenase-2
PGs	Prostaglandins
NSAIDs	Non-steroidal anti-inflammatory drugs
AOM	Azoxymethane
DSS	Dextran sulfate sodium
SDS-PAGE	Sodium dodecyl sulphate
ASBT	Apical sodium-dependent bile acid transporter
EPR	Enhanced permeability and retention
PEG	Polyethylene glycol
SAHA	Suberoylanilide hydroxamic acid
PCNA	Proliferating cell nuclear antigen
TUNEL	Terminal deoxynucleotidyl transferase dUTP nick end labeling
AUC	Area under the curve
Cl	Clearance
AUMC	Area under the momentum curve

Vss	Volume of distribution at steady state
MRT	Mean residence time
BSA	bovine serum albumin
PBS	phosphate-buffered saline
TBST	Tris-buffered saline containing 0.1% Tween 20
EBM-2	Endothelial Basal Medium-2
EGM	Endothelial Growth Medium
SEM	Standard error of the mean
ANOVA	One-way analysis of variance
H&E	Hematoxylin and Eosin
IHC	Immunohistochemistry

Chapter I. Introduction

1.1. Angiogenesis

1.1.1. Angiogenesis in physiological and pathological conditions

Mammalian cells should reside within a distance of 100 to 200 μm, which is known to be the diffusion limit for oxygen, from blood vessels for the supply of oxygen and nutrients that is required for their survival and growth [1, 2]. If the amount of oxygen at tissues is not enough for cellular level, the formation of new blood vessels begins, which is called vasculogenesis and angiogenesis. This process is regulated by a tightly controlled balance between pro- and anti-angiogenic growth factors (Table 1.1 and 2) [3]. This new vessel formation occurs in physiological conditions for embryonic development and homeostasis maintenance of our body as well in pathological conditions of various diseases [4]. For example, physiological angiogenic process is involved in the formation of primitive blood vessels inside the embryo, the process of implantation on maternal uterine wall, normal cyclical ovarian function, and wound healing process after injury. On the other hand, angiogenesis also occurs in pathological conditions of various diseases such as rheumatoid arthritis, asthma, diabetes and its complications, dysfunctional uterine bleeding, Alzheimer's diseases, and cancer [1].

Even though the same pro- and anti-angiogenic growth factors are involved in both physiological and pathological angiogenesis, there is a substantial difference between physiological and pathological angiogenesis. In physiological conditions, when the oxygen level is recovered from ischemia or hypoxia by vascular perfusion through newly formed vessels, the molecular events of angiogenesis recede

automatically. However, the angiogenic process in pathological conditions such as tumor is abnormally persistent, uncontrolled, and is even fuelled by tumor tissue-derived molecules. These molecules are secreted by the tumor cells themselves, by stromal cells or by cells of immune system. In this context, the comprehensive understanding on physiological angiogenesis might provide a clue to intervene pathological angiogenesis to normalize it.

1.1.2. Angiogenesis and cancer

In 1971, Folkman *et al.* raised a new hypothesis that tumor growth is dependent on angiogenesis [5]. They also reported that most tumors require new blood vessels to grow beyond a microscopic size of 1−2 mm^3, and also secrete diffusible angiogenic molecules. After this remarkable publication that initiated new field of angiogenesis research, angiogenesis has been widely and extensively studied as a therapeutic target in cancer treatment up to now.

The initiation of angiogenesis depends on whether the angiogenic switch is 'off' when the effect of pro-angiogenic molecules is well-balanced by that of anti-angiogenic molecules or 'on' when the balance is tipped in favor of angiogenesis [6]. The activation of angiogenic switch is mediated by a diversity of signals that are derived from either cancer cell itself or its microenvironmental factors. For example, tumor microenvironment-derived factors include low pO_2, low pH, hypoglycaemia, and mechanical pressure, which attributes to the excessive proliferation of cancer cells. In addition, angiogenic switch is also affected by immune- and inflammatory-

cells that have infiltrated the tumor microenvironment. On the other hand, the activation of oncogenes or deletion of tumor-suppressor genes on cancer cell itself generally enables the angiogenic switch to be triggered. Once the angiogenic switch is turned on, new blood vessels are sprouted from pre-existing vessels and support the tumor growth and metastasis. Furthermore, recently, it is also reported that angiogenesis also contribute to the tumor rebound after successful treatment and activation of cancer stem cells [7, 8].

Furthermore, it is interesting that the pattern of production and secretion of angiogenic factors changes in amount and kind according to the carcinogenesis. Due to the unstable genome of cancer cells, genetic mutations of cancer cells are continuously accumulated over the whole span of carcinogenesis. Consequently, tumor tissues are dynamically altered and finally characterized with heterogeneous cell populations. Thus, the amount and kind of angiogenic factors that are secreted from tumor tissues also varies with cancer progression [9]. In other words, while tumors on early stage only secret one or two angiogenic factors like VEGF and bFGF, those on the end stage of carcinogenesis usually produce multiple angiogenic factors [10].

1.1.3. Anti-angiogenic drugs for cancer treatment

Tumor angiogenesis is ‘endothelial disorder’ in regards to abnormal vascular growth and remodeling by mural cells. In other words, while most healthy vasculatures are quiescent, where only less than 0.01% of endothelial cells are

activated and under cellular division, the tumor vessels are characterized with excessive proliferation of endothelial cells [11]. Thus, an abnormal increase in endothelial cell proliferation and migration could be an indicator that angiogenic switch has been turned on and initiated angiogenesis. In addition, in cancer, multiple sources and various modes of vascular remodeling also contribute to tumor development. All of these excessive and abnormal angiogenic processes substantially support the further progression of cancer. In this context, it is mandatorily required to intervene or inhibit the abnormal activation of vascular structure for successful cancer treatment.

Above all, compared to cancer cells, endothelial cells are genetically more stable and less inclinable to evolve into resistant ones under cytotoxic therapy. This genetic stability of endothelial cells might impose a superiority as a cancer therapeutic on antiangiogenic drugs that target endothelium to cytotoxic drugs that directly kills cancer cells in terms of drug resistance of [12]. Furthermore, when both cancer and endothelial cells are targeted at the same time by combination therapy using cytototoxic drugs and angiogenesis inhibitors, the therapeutic efficacy could be synergistically improved [13].

In this context, anti-angiogenic drugs have been extensively studied to develop them as anti-cancer therapeutics. As a result, a number of angiogenesis inhibitors are now on the clinical trials, and some of them are already approved from FDA and launched in the market with indications in various types of cancer (Table 1.3) Especially, VEGF-targeted drugs has been most actively studied as angiogenesis inhibitors. Vascular endothelial growth factor (VEGF) is a homodimeric glycoprotein

with a molecular weight of approximately 45 kDa, and known to be the most abundant and common pro-angiogenic factor that involved in tumor angiogenesis [14]. It can bind to its receptors like VEGFR-1 or -2, which are receptor tyrosine kinases, and then trigger the intracellular angiogenic cascades for new vessel formation. Since the VEGF and its receptors-mediated signaling pathway in angiogenesis occur via the serial and multifactorial steps, anti-VEGF therapeutics relies on a variety of molecular mechanisms. For example, VEGF signalling pathways can be disturbed either by monoclonal antibodies for VEGF-A or VEGF recetors, VEGF-trap (chimaeric soluble receptors), pegaptanib (aptamers that bind with heparin-binding domain of VEGF165), a variety of small-molecule VEGF receptor tyrosine kinase inhibitor, or antisense and siRNA targeting VEGF-A or its receptors [4].

1.1.4. Limitations of antiangiogenic therapy

Even though the concept of antiangiogenic therapy has been accepted as an innovative and hopeful strategy, there are still definite limitations and shortcomings of antiangiogenic drugs that hinder a sustainable and successful clinical outcome [15, 16]. First of all, its therapeutic efficacy of angiogenesis inhibitor is not sufficient to be applied as a single drug. Thus, it is usually used as an adjuvant in the combination chemotherapy for cancer treatment with other cytotoxic drugs. Second, not every type of cancer is susceptible to anti-angiogenic therapy. Thus, cancer patients who are diagnosed with the intrinsically resistant cancer lines usually do not respond to any

kind of antiangiogenic drugs. Moreover, some types of cancer are initially shrunk by anti-angiogenic therapy, but they evolved to resistant one under chronic inhibition of angiogenesis by eliciting evasive pathways from antiangiogenic drug in different ways [17, 18]. For example, angiogenic tumors can evade from the VEGF-targeted antiangiogenic therapy by up-regulating alternative proangiogenic factors, recruiting vascular progenitor cells and pro-angiogenic monocytes from the bone marrow, protecting tumor vascular structures by increasing the pericyte coverage, and triggering host-mediated response to fortify a prometastatic and invasive microenvironments for primary tumors [18]. In particular, since tumor tissues can shift from VEGF-dependent pathways to alternative pathways under VEGF-targeted antiangiogenic therapy, it might be preferred to suppress multiple angiogenic factors together rather than targeting one pathway of angiogenesis [3]. Even though various resistant mechanisms of anti-angiogenic drugs are clarified up to now, the clinical strategy to overcome these obstacles has not clearly answered yet.

1.2. Cancer chemoprevention and angiogenesis

1.2.1. Cancer chemoprevention

Since the declaration of war on cancer to defeat it completely from the earth by National Institute of Cancer in US in 1971, we have achieved a great advance in cancer science [19]. However, cancer still remains the leading cause of death worldwide. What is interesting is that it might not be due to lack of primary response or initial induction of remission, but rather it comes from the relapse or recurrence

including second primary cancer after successful cancer treatment [20]. In this context, the chemoprevention, which is defined as the use of pharmacological agents to impede, arrest, or reverse carcinogenesis at its earliest stages, has been emerging as a promising cancer-controlling strategy. Actually, the concept of cancer chemoprevention was firstly proposed by Sporn MB in 1976 [21]. After that, a variety of natural and pharmacological agents with different mechanisms have been evaluated as a chemopreventive agent, and some of them have been already approved by FDA as chemopreventive agents (Table 1.4) [22, 23]. Currently, together with early detection and proper treatment, cancer chemoprevention is required to achieve the successful cancer controlling strategy.

1.2.2. Classifications and requirements of cancer chemoprevention

To achieve a rational and practical cancer chemoprevention, it is mandatory to classify subjects into subcategories according to cancer risk as well to assess safety and efficacy of chemopreventive agents. Cancer chemoprevention can be subcategorized according to the target of intervention (Fig. 1.2) [24, 25]. Primary prevention, which is addressed to healthy individuals, particularly aims to prevent the occurrence of the malignant diseases by inhibition of mutation and cancer initiation and promotion. Since secondary prevention is addressed to patients in preclinical or early stage, its primary goal is the inhibition of progression of a timely diagnosed benign tumor towards malignant one. Finally, tertiary prevention, which is addressed to cancer patients after successful treatment, mainly target both prevention of relapse

and inhibition of invasion or metastasis.

On the other hand, cancer chemopreventive agents must be qualified with general requirements such as efficacy, safety, cost, and practicality of use. First of all, the balance between efficacy and safety should be considered [24]. According to the gradient of cancer risk of subject between primary and tertiary prevention, the level of acceptable safety would be determined. As the cancer risk of individual increases, the need for targeted chemoprevention based on clarified molecular mechanisms is also increased. For the practical use of chemopreventive agents for long-term period, both low cost and high practicality of use must be guaranteed [26].

1.2.3. Combination chemoprevention

Since carcinogenesis is the multistep, multipath, and multifocal process by which normal cells are transformed into cancerous cells [27]. A variety of molecular, physiological and histological changes occur on cells and tissues over the whole span of carcinogenesis. The complexity of the carcinogenesis provides a strong rationale for combination chemoprevention just as combination chemotherapy has been so important in the treatment of end-stage of malignant tumors [28]. Even though the basic concept of combination chemoprevention was first proposed by Sporn in 1980 [29], but a clinically applicable regimen with remarkable results was only recently reported by Meyskens et al. in 2008 [30, 31]. In this paper, they showed that the combination use of sulindac and difluoromethylornithine was enough to successfully prevent colorectal adenomas with acceptable safety. Taken all, a clinically

meaningful cancer chemoprevention with increased efficacy and safety might be achieved by combination use of more than two drugs at reduced dose.

1.2.4. Clinical cancer chemoprevention by delay

Even though the most ideal expectation on cancer chemoprevention might be the complete eradication of cancer risk, enormous preclinical and clinical studies have proved that chemopreventive agents rarely will prevent the progression of cancer development completely and permanently [32]. Consequently, the concept of "slowing the process of carcinogenesis" emerged as a clinically practical approach to cancer chemoprevention [33]. Thus, when it comes to clinical cancer chemoprevention, it is not truly prevention, but rather suppression or delay of an undesirable clinical outcome such as painful symptoms. In other words, if the onset of undesirable outcome can be suppressed during our life time by proper intervention with chemopreventive agents, people would not suffer from advanced cancer at least [28]. Consequently, their quality of life would be improved by living healthy without any clinical symptoms. Even though the phenotypic suppression by cancer delay seems not to be the ultimately desirable way to prevent cancer, but it is now accepted as a practical approach to cancer prevention by extending the latency period.

1.2.5. Angiogenesis as a target for cancer chemoprevention

As aforementioned, angiogenesis is conventionally defined as a new vessel formation for the further growth of malignant tumor at the volume of 1-2 mm^3.

However, increasing number of clinical and experimental evidences show that angiogenic switch is already turned on in the very early stages of carcinogenesis including hyperplasia and dysplasia, and it plays a critical role in the transformation of premalignant lesions into malignant tumors [34]. In other words, abnormal lesions, which are distinguished from normal healthy tissues with increased risk of cancer but without any clinical symptoms, can progress into malignant tumors only when they are continuously exposed to favorable conditions such as accumulation of mutations, inflammation, and angiogenesis [34].

On the other hands, if those abnormal premalignant lesions are properly treated with antiangiogenic drugs, they would remain asymptomatic and dormant forever [35]. In this context, angioprevention, which derived from angiogenesis and cancer chemoprevention, can be a promising strategy for cancer chemoprevention. Clinically, the purpose of angiogprevention is to maintain transformed cells in a dormant stage by keeping their microenvironment healthy and unfavorable for further progression by various stimuli. Recently, an increasing number of preclinical and clinical reports support the angioprevention as a practical approach in cancer chemoprevention.

1.3. Low molecular weight heparin-bile acid conjugates as an angiogenesis inhibitor

1.3.1. Unfractionated heparin and low molecular weight heparin

Heparin is a polydisperse and highly sulphated glycosaminoglycan (GAG) that is extracted from porcine intestinal mast cells for therapeutic purpose [36]. It consists

of polymeric chains of alternating disaccharide units of D-glucosamine and uronic acid, either glucuronic acid and iduronic acid. Heparin can be classified into two types according to its average molecular weight, unfractionated heparin (UFH) and low molecular weight heparin (LMWH) [37]. While UFH is heterogeneous mixture of polysaccharide chains with molecular weight ranging from 3,000 to 30,000 Da, LMWH is a fragment of UFH with average molecular weight about 5,000 Da. Various types of LMWHs with different physicochemical properties regarding average molecular weight and anti-Xa: anti-IIa ratio are produced from UFH by controlled enzymatic or chemical degradation methods including peroxidative depolymerization, nitrous acid depolymerization, benzylation and alkaline depolymerization, and heparinase digestion. Through this depolymerization of UFH into LMWH, the whole length of pentasaccharide (a unique sequence that is required for binding with antithrombin)-containing heparin chain was decreased to less than 18 saccharide units, which made LMWH unable to interact with thrombin (Fig 1.2) [37]. Thus, unlike UFH can interact with both Factor Xa and thrombin in the anticoagulant cascade, LMWH shows its anticoagulant activity only against Factor Xa with enhanced affinity. On the other hand, LMWH obtained several pharmacokinetic and pharmacodynamics advantages over UFH. For example, LMWH possesses less binding affinities to non-anticoagulant proteins including endothelial cells, macrophages, and acute phase reactant, which enabled LMWH to achieve a more predictable and reproducible anticoagulant response than that of UFH. LMWH also shows a better bioavailability at low doses, dose-independent clearance, longer half-life, less inhibition of platelet function, and lower risk of

thrombocytopenia compared to UFH (Table 1.5). Thus, LMWH have largely replaced UFH in the clinics as an anticoagulant drug.

1.3.2. LMWH and cancer

Even though LMWH has been widely used as an anticoagulant drug, it also has been actively investigated for its further clinical applications including anti-inflammatory, anti-angiogenic, and anti-cancer effects [36]. Thus, LMWH has been used for non-anticoagulant applications both in experimental and clinical trials. These diverse pharmacological effects of LMWH include AT-dependent plasmatic effect, AT-independent vascular effect, interaction with cell adhesion molecules, modulation of fibrinolytic system, interaction with inflammatory mediators, and inhibition of extracellular matrix degrading enzymes.

Particularly, LMWH can be an appealing anti-cancer drug in regards to its inhibitory effects on cancer cell proliferation, angiogenesis, and metastasis [38, 39]. It has been reported that heparin can interfere with proto-oncogene, protein kinase C activity, and mitogen-activated protein kinase phosphorylation which are required for cancer cell proliferation. In addition, the tissue factor pathway inhibitor, which is natural coagulant inhibitor, is also release by LMWH and can give an anticancer effect. Especially, since LMWH is a glycosaminoglycan chain with numerous functional moieties including sulfate, carboxylic acid, and amine groups, it can bind to a variety of bioactive molecules such as cytokines and growth factors involved in tumor pathogenesis via electrostatic interaction.

1.3.3. Heparin-bile acid conjugates as an angiogenesis inhibitor

Due to the anticancer effect of LMWH, the development of heparin-based new drug has been an important issue in the field of cancer therapeutics. However, there are two big hurdles to overcome in the application of LMWH into cancer therapy and in the development of a new anticancer drug form LMWH, that is, insufficient therapeutic efficacy and side effect such as hemorrhage. Thus, chemical modification of LMWH to make it strong enough to treat cancer with acceptable safety has been tried in different ways. For example, heparin-steroid conjugates, heparin-polystyrene conjugates, and heparin-bile acid conjugates have been synthesized and tested as anticancer drugs with various mechanisms and clinical applications.

Among them, a variety of LMWH-bile acid conjugates have been investigated extensively as an anticancer drug. According to kind of bile acid attached to LMWH, they demonstrated a different therapeutic effect on tumor growth and pharmacokinetic characteristics. Most interestingly, while chemically modified LMWH with bile acid showed a potentiated antiangiogenic activity, which led to the substantially enhanced antitumor efficacy in tumor bearing animal models, the anticoagulant activity was significantly decreased.

In case of LHD4, which is LMWH-deoxycholic acid (DOCA) conjugates at molar ratio 1:4, it showed a much stronger anticancer effect via angiogenesis inhibition than LMWH both *in vitro* and *vivo* [40]. Moreover, it also obtained oral bioavailability through the chemical conjugation. However, since DOCA was

conjugated to the pentasaccharide sequence of LMWH, it cannot interaction with antithrombin anymore, thus it lost its anticoagulant activity completely. It allows LHD4 to be utilized as an oral angiogenesis inhibitor without unexpected side effect such as hemorrhage (Fig 1.2A).

On the other hand, LHT7, where LMWH is conjugated with taurocholic acid (TCA) at molar ratio 1:7, showed the highest antiangiogenic activity among various LMWH-bile acid conjugates with negligible anticoagulant activity [41]. The excellent antiangiogenic activity of LHT7 contributed to the increased structural rigidity and net anionic charge by introducing two sulfate groups of taurocholic acid. Furthermore, the interaction between pentasaccharide sequence of LMWH and antithrombin was sterically hindered by the sterane core from taurocholic acid, which resulted in the complete loss of anticoagulant activity of LMWH [42] (Fig 1.2B).

Experimental studies on antiangiogenic LHT7 were further expanded through introducing various functional moieties that impose targeting effect to tumor site on LHT7. It was reported that the tumor therapeutic efficacy of LHT7 was further enhanced by localization to tumor sites when LHT7 was chemically modified by either cRGDyk (cyclic pentapeptides consisting of arginine, glycine, asparagine, tyrosine, and lysine; interact with $\alpha_v\beta_3$ integrin expressed on tumor endothelium) [43] or ApoPep-1 (hexapeptide consisting of cysteine, glutamine, arginine, proline (CQRPPR), tumor apoptotic and necrotic area binding peptide) [44].

1.3.4. Orally active heparin-bile acid conjugates

Even though LMWH-bile acid conjugates are effective and safe enough to be used as antiangiogenic therapeutics, if it is still available only through invasive route including subcutaneous or intravenous routes, its clinical applications might be limited. Especially when it is applied to outpatients or chronic use for treatment and prevention, the convenience of intake must be guaranteed such as oral administration.

In this context, the development of orally active LMWH-bile acid as an angiogenesis inhibitor has been tried in numerous studies (Fig 1.3). Particularly, the chemical modification with DOCA enabled LMWH and its derivatives to be absorbed with different pharmacokinetics and pharmacodynamics. As aforementioned, the conjugation of DOCA to pentasaccharide sequence of LMWH produced a high antiangiogenic and low anticoagulant LMWH derivatives named as LHD4, which is available via the oral route. It was mainly absorbed at the ileum part of intestine either by transcelluar pathway due to enhanced hydrophobicity or by bile acid transporters. Especially, the absorption via the bile acid transporter is mediated by DOCA part of LHD4 [40].

Actually, apical sodium-dependent bile acid transporter (ASBT)-mediated drug delivery has been actively investigated for successful oral absorption of various drugs that have low bioavailability and target the liver. Thus, more recently, various oligomeric bile-acids with higher affinity to ASBTs were synthesized to be used as a functional moiety for oral delivery of macromolecules such as LMWH and LMWH derivatives. Among them, a tetrameric DOCA (tetraDOCA), which is characterized

with eight hydroxyl and one focal primary amine groups, demonstrated the highest binding affinity for transporter-binding pocket of ASBT[45]. The specific mechanism of tetraDOCA-mediated oral absorption of macromolecules was also well clarified [46]. The interaction between tetraDOCA and ABST induced a functional transformation of ASBTs followed by cellular internalization in vesicular form, and finally tetraDOCA-conjugated molecules were delivered into the blood stream. By utilizing this system, LHT7 became orally active while preserving its potent antiangiogneic activity [47]. Consequently, clinical applications of heparin-based antiagiogenic drugs could be expanded more widely.

1.4. Drug delivery system for anti-angiogenic drugs

1.4.1. Nanoparticles as a drug delivery system

Nanoparticles are particles with diameter in the range of 10−100 nm comprised of therapeutic agents and components that assemble with therapeutic agents [48]. They have been studied in a number of preclinical and clinical trials as a part of drug delivery systems. By varying the physicochemical characteristics such as particle size, surface charge, and surface properties, they can be utilized successfully as a drug carrier in a variety ways. Furthermore, recently, nanoparticles become newer and sophisticated multifunctional and more frequently available in the clinics (Table 1.6).

The important advantages of nanoparticles might be the enhancement of therapeutic efficacy, which attributes to improved pharmacokinetic and pharmacodynamics properties, with reduced side effects. In addition, recently,

nanoparticles are emerging as a new strategy to overcome efflux pump-mediated multi drug resistance of cytotoxic therapy [48, 49].

Furthermore, the complexity of tumor biology supports the need for co-delivery systems for anticancer therapeutics. It is reported that more than 20 different growth factors and cytokines are expressed and produced in the process of angiogenesis for tumor progression [9]. In this context, targeting multiple growth factors by combination therapy using more than two drugs might take advantages over a one drug use. The comprehensive understanding of various structure of nanoparticles might be required to utilize it a as a co-delivery system for more than two anticancer drugs with different mechanisms. For example, both cytotoxic and antiangiogenic drugs can be loaded into nanoparticles at the same time and generate a synergic or additive effect on cancer treatment. Consequently, while the therapeutic efficacy could be improved due to both combination use and formulating effect by means of nanoparticles, the overall side effects might be reduced.

1.4.2. Pathological characteristics of tumor vascular structure and EPR effect

The physiological conditions of tumor tissues are substantially distinguished from those of normal tissues due to the excessive and dynamic cell proliferation [50]. However, these abnormalities might provide critical clues for the development of drug delivery system for anticancer drugs. For example, tumor tissues are usually characterized by irregular and immature vascular structures, variable permeability of blood vessels, high interstitial fluid pressure, and overexpression of p-glycoproteins.

Based on these unique pathological characteristics of tumor tissues, well-elaborated drug carriers with varied physicochemical properties have been investigated to deliver drugs to tumor sites and further achieve a successful tumor therapeutic efficacy.

Especially, the porosity of vascular structures with an average pore size about 100-600 nm, which is significantly larger size than that of normal healthy endothelium (< 6 nm), enables the selective uptake of nano-sized particles encapsulated with anticancer therapeutics [51, 52]. Thus, anticancer drugs formulated into nanoparticles can be preferentially accumulated and then retained for longer time at tumor tissues due to limited lymphatic drainage. Since this unique phenomenon, which is well-known as the enhanced permeability and retention (EPR) effect, is related to passive targeting and mainly affected by pathological conditions of tumor tissues, particles must survive and circulate for a long time in the blood stream [53]. In this context, the physicochemical characteristics of particles including size, surface charge, structural stability and rigidity, and coverage with biocompatible polymer should be fine-tuned to effectively enhance drug localization via the EPR effect. It was reported that particles with smaller size, especially less than 100 nm, showed the higher accumulation effect at tumor sites [54]. On the other hand, in terms of *in vivo* longevity in plasma, it was reported that particles with negative or neutral surface charge take advantages over those of positivity due to avoidance of being collapsed by interaction with negative plasma proteins. In addition, particles can be camouflaged with hydrophilic polymers such as polyethylene glycols to protect them from being recognized by reticuloendothelial system [55].

1.4.3. Vascular targeted delivery of anticancer drugs using nanoparticles

Ttumor vascular structure also possesses its own pathological characteristics in regards to overexpression of various surface receptors and antigens, negatively charged macromolecules such as glycoproteins, anionic phospholipids and proteoglycans [56, 57]. These unique features can be also utilized to invent a new drug delivery system by active targeting of nano-carriers.

At first, since the charge density of tumor vascular structure is usually altered by abnormal expression of molecules, it might be suggested that positively charged nanoparticles be utilized as a drug carrier to selectively deliver antiangiogenic drugs to tumor sites [58, 59]. Compared to the neutral or anionic particles, the cationic particles can be captured by negatively charged vascular glycocalyx overexpressed on endothelium in pathological conditions such as inflammation and cancer, which strikingly prolonged the retention time of particles at tumor tissues. However, the enhanced therapeutic effect of particles might be explained in different ways according to surface charge. In other words, while neutral and anionic particles can extravasate from tumor vasculature, diffuse into tumor tissues, and then exert their therapeutic effects, cationic particles tend to stay at endothelium. Thus, once anticancer drug-loaded cationic particles are captured by tumor endothelium, the incorporated drugs can be slowly released out from the particles and then form a concentration gradient to facilitate the drug absorption. In this context, cationic liposomes might be the most suitable drug carriers for antiantiognic drugs to reach

their endothelial target. However, it was reported that the interactions of cationic particles with plasma proteins are more frequent than that of neutral and anionic particles. Thus, the balance between targeting effect and plasma stability should be considered to avoid the rapid clearance from the body [60].

Secondly, nanoparticles can be manipulated using functional targeting moieties, which can interact with specific receptors or antigens that are particularly expressed on cancer cells or endothelial cells at tumor tissues, to increase the localization effect [51]. It was reported that the expression of tumor-specific receptors and molecules are substantially increased and varied at the tumor sites, which make it clearly distinguished from normal tissues. Thus, it could be a promising strategy to make an antibody- (whole or fragmentary antibody) or peptide- (natural or synthetic) conjugated nanoparticles to target the desired sites of action characterized with the unique pathological biomarkers [61]. For example, the modification of pegylated cationic liposome with bevacizumab, which is a humanized monoclonal antibody for VEGF, showed a significant enhancement in tumor growth inhibition [62]. On the other hand, there are various kinds of small size-peptides that can interact with integrins and enzymes particularly expressed at tumor site. These specific peptides such as Arg-Gyl-Asp (RGD; bind to $\alpha_v\beta_3$ integrin), Asn-Gly-Arg (NGR; bind to aminopeptidase N), and Cys-Arg-Glu-Lys-Ala (CREKA; bind to fibrinogen or fibrin) can be used to impose targeting effect on nanoparticles. More interestingly, it was reported that the convergent system using more than two targeting moieties was able to further improve the suppression effect on tumor growth [63].

1.5. Research rationale

Since angiogenesis plays a pivotal role in cancer development from the earliest stages of carcinogenesis to the end-stage of cancer, it could be an important target in both cancer chemotherapy and prevention. Thus, a number of angiogenesis inhibitors have been developed up to now. In addition, some of them such as bevacizuman, sorafenib, sunitinib, and pazopanib have been approved from FDA as anticancer therapeutics, and widely used in the clinics. On the other hand, numerous natural and synthetic pharmacological agents have been also studied as chemopreventive agents based on angiogenesis inhibition.

Previously, we have developed three different kinds of heparin-based new angiogenesis inhibitors named as LHD4, LHT7, and LHTD4. It is well-known that LMWH, which is a widely used anti-coagulant drug, also has a binding affinity to various angiogenic growth factors such as VEGF, bFGF and PDGF, which led to the anti-angiogenic properties of LMWH. For the further enhancement of antiangiogenic efficacy, LMWH was modified with different kinds of bile acid such as monomeric- and tetrameric-deoxycholic acid and taurocholic acid. According to the type of bile acid and molar ratio of conjugation, the pharmacological characteristics of LMWH-bile acid conjugates varied in regards to oral bioavailability and antiangiogenic potency. What is interesting is that, through this chemical conjugation, while the antiangiogenic and anticancer efficacy was substantially increased, the anticoagulant activity became negligible. Above all, LMWH-bile acid conjugates have a binding affinity with multiple growth factors. Since the secretion of

angiogenic growth factors are altered according to progression of cancer, it might be superior to the other conventional drugs. In addition, both LHD4 and LHTD4 were available via the oral route, which enables the long-term intake with patient convenience.

Based on these backgrounds, in this study, we have experimentally evaluated the efficacy of these LMWH-bile acid conjugates on cancer chemoprevention and chemotherapy. In chapter II and III of this study, we showed that both LHD4 and LHTD4, which are orally active angiogenesis inhibitors, were effective in the prevention of colorectal and lung cancers, respectively, in chemically induced animal model. The substantial effect of LMWH-bile acid conjugates on cancer chemoprevention in experimental animal models might provide a rationale to apply them into human beings for chemoprevention of various kinds of cancer that is characterized with high angiogenic potentials in the early stage of carcinogenesis. By intervening angiogenesis from the earliest stage of cancer development, the morbidity and modality of cancer might be successfully controlled.

Two of the major obstacles in utilizing cancer therapeutics in the clinics might be development of resistance and severe toxicity. To overcome this, we have studied the combination effect of two drugs in Chapter III and IV of this study. In Chapter IV, we have clarified the COX-2 inhibition effect on anti-angiogenic therapy using LMWH-taurocholic acid conjugates. We found that celecoxib, a selective COX-2 inhibitor, could inhibit the COX-2 activity at hypoxic area of tumor tissues. Furthermore, combination use of celecoxib and LHT7 demonstrated a substantial effect on vascular formation and stabilization both *in vitro* and *vivo*. On the other

hand, in Chapter V, we achieved a synergistic effect of LHT7 and SAHA, a histone deacetylase inhibitor, by co-loading them into nanolipocomplex. The cationic nanolipocomplex exhibited both localization at tumor sight and sustained release in a murine animal model. The results from these two studies might provide a rationale to apply these strategies into clinics to solve the practical problems of cancer therapeutics.

Taken all, this study showed that LMWH-bile acid conjugates are promising antiangiogenic drugs in regards to efficacy and safety. Furthermore, their antiangiogenic efficacies might be further improved through the combination use or formulation using various drug delivery systems. Consequently, this study might provide a clue that LMWH-bile acid conjugates could be applied in the clinics for cancer chemoprevention and chemotherapy in diverse ways.

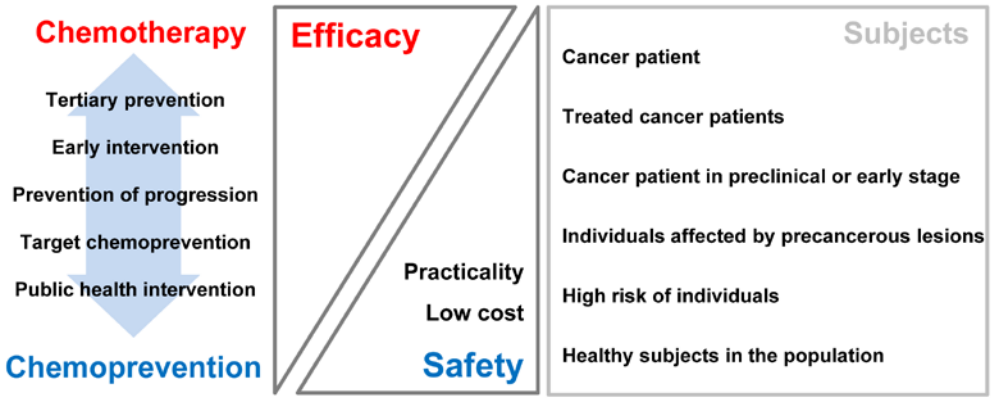

Figure 1.1 Classification and requirements for cancer chemopreventive agents according to intervention strategies and target populations

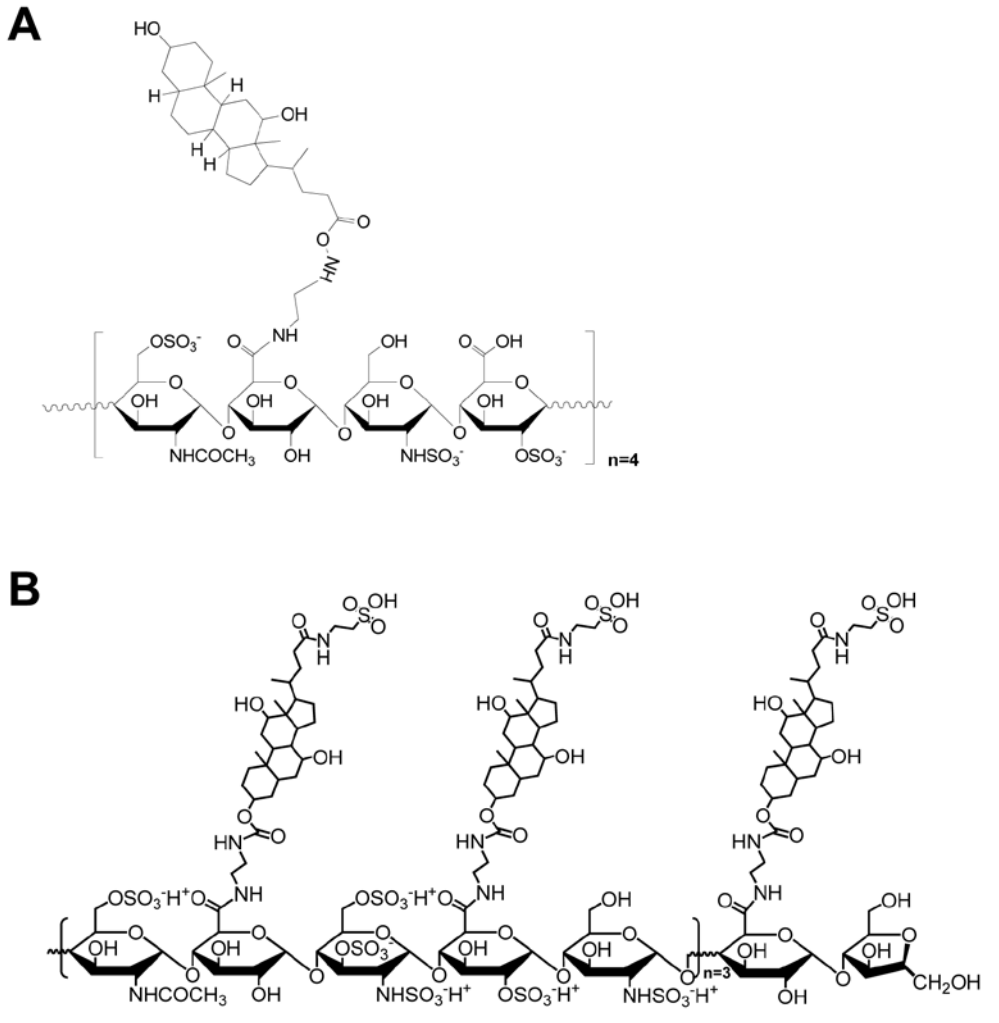

Figure 1.2 Molecular structures of LMWH-bile acid conjugates as angiogenesis inhibitors. (A) LHD4, (B) LHT7

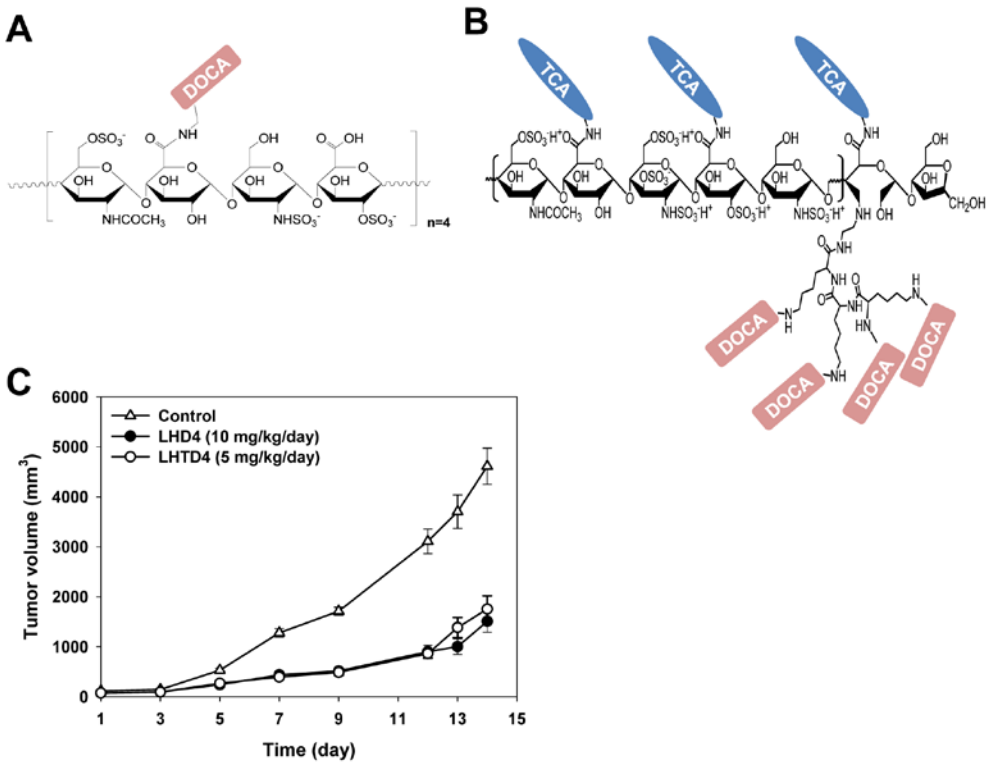

Figure 1.3 Scheme of molecular structure of orally active LMWH-bile acid conjugates (A) LHD4, LMWH was conjugated with deoxycholic acid at molar ratio 1:4, (B) LHTD4, LHT7, which is a LMWH-taurocholic acid conjugate at molar ratio 1:7, was further conjugated with tetrameric deoxycholic acid for oral administration. (C) The therapeutic efficacy of LHD4 and LHTD4 was compared in terms of tumor growth inhibition in SCC7-bearing mice.

Table 1.1 Pro-angiogenic factors

	Function
VEGF family members	Stimulate angio/vasculogenesis, permeability, leukocyte adhesion
VEGFR, NRP-1	Integrate angiogenic and survival signals
Ang1 and Tie2	Stabilize vessels, inhibit permeability
PDGF-BB and receptors	Recruit smooth muscle cells
TGF-β1, endoglin, TGF-β1 receptors	Stimulate extracellular matrix production
FGF, HGF, MCP-1	Stimulate angio/arteriogenesis
Integrins	Receptors for matrix macromolecules and proteinases
VE-cadherin, PECAM (CD31)	Endothelial junctional molecules
Ephrins	Regulate arterial/venous specification
Plasminogen activators, MMPs	Remodel matrix, release and activate growth factors
PAI-1	Stabilize nascent vessels
NOS, COX-2	Stimulate angiogenesis and vasodilation
AC133	Regulate angioblast differentiation
Chemokines	Pleiotropic role in angiogenesis
Id1/Id3	Determine endothelial plasticity

Table 1.2 Anti-angiogenic factors

	Function
VEGFR-1, soluble VEGFR-1, soluble NRP-1	Sink for VEGF, VEGF-B, PIGF
Ang-2	Antagonist of Ang-1
TSP-1, -2	Inhibit endothelial migration, growth, adhesion, and survival
Angiostatin and related plasminogen kringles	Suppress tumor angiogenesis
Endostatin (collagen XVIII fragment)	Inhibit endothelial survival and migration
Vasostatin, calreticulin	Inhibit endothelial growth
Platelet factor-4	Inhibit binding of bFGF and VEGF
TIMPs, MMP inhibitors, PEX	Suppress pathological angiogenesis
Meth-1, -2	Inhibitors containing MMP, TSP and disintegrin domains
IFN-α, -β, -γ; IP-10; IL-4, -12, -18	Inhibit endothelial migration, down-regulate bFGF
Prothrombin kringle-2, antithrombin III fragment	Suppress endothelial growth
Prolactin	Inhibits bFGF/VEGF
VEGI	Modulate cell growth
Fragment of SPARC	Inhibit endothelial binding and activity of VEGF
Osteopontin fragment	Interfere with integrin signaling
Maspin	Protease inhibitor
Canstatin, proliferin-related protein, restin	Mechanisms unkown

Table 1.3 Examples of FDA-approved VEGF-targeted angiogenesis inhibitors

Drug name		Mechanisms of action	Indications	Trade name
Bevacizumab	VEGFR-specific humanized antibody	blocks antigen-receptor binding	colon, lung, breast, glioblastoma, kidney	Avastin (Genentech/Roche)
Sorafenib	TKI targets VEGFR-2, -3, Raf, PDGFR, KIT and RET	inhibits signaling of the VEGFR receptor tyrosine kinase	kidney, liver	Nexavar (Bayer and Onyx)
Sunitinib	TKI targets VEGFR-1, -2, -3, PDGFR, KIT and FLT3	inhibits signaling of the VEGFR receptor tyrosine kinase	kidney, gastrointestinal stromal tumor	Sutent (Pfizer)
Pazopanib	c-KIT, FGFR, PDGFR, VEGFR-1, -2, -3	multi-targeted receptor tyrosine kinase inhibitor	advanced/metastatic renal cell carcinoma, advanced soft tissue sarcomas	Votrient (GlaxoSmithKline)

Table 1.4 Examples of FDA-approved chemopreventive agents

Target cancer	Drug	Mechanism	Trade name/ Manufacturer	Year first approved
Breast	Tamoxifen	Selective estrogen receptor modulator (SERM)	Nolvadex (AstraZeneca) Valodex(Samarth Pharma) Istubal	1998
	Raloxifene		Evista (Eli Lilly)	2007
Cervix Vulva Vagina/Anus	HPV vaccine	Human papillomavirus (HPV)-induced immune reaction	Gardasil (Merck) Cervarix (GSK)	2006
Esophageal (Barrett's esophagus)	Porfimer sodium + photodynamic therapy (PDT) & omeprazole	a photosensitizing agent	Photofrin (Axcan)	2003
Skin	Fluorouracil	Interferes with DNA synthesis and leads to cell death	Efudex (Valeant) Fluoroplex (Aqua) Carac (Dermik Laboratories)	1970
	Diclofenac sodium, 3%	Exact mechanism is unknown	Solaraze (PharmaDerm)	2000
	5-aminolevulinic acid + PDT	Solution kills precancerous actinic keratoses cells when exposed to light	Levulan® Kerastick® (DUSA)	1999
	Imiquimod	immune response modifier	Aldara (5 %, 3M) Zyclara (3.75%, Medicis)	2004

Table 1.5 Advantages of LMWH over UFH

Advantages	Mechanisms	
More predictable anticoagulant response	Reduced binding to a variety of non-anticoagulant proteins: plasma proteins, platelet factor 4, von Willebrand	*No need for laboratory monitoring Availability for outpatient therapy
Better bioavailability at low doses	Reduced binding to plasma proteins and endothelium	*Recovery of anti-factor Xa activity after s.c. injection: LMWH (100%), UFH (30%)
Reduce risk of bleeding and thrombocytopenia	Less inhibition of platelet function by reduced binding affinity No increase in microvascular permeability Less interference with the interaction between platelets and vessel wall	
Longer plasma half-life Dose-independent clearance mechanism	Less binding to macrophages	*UFH (hepatic cleaerance, half-life: 0.5-2 hr) *LMWH (renal clearance; half-life: i.v. 2-4 hr, s.c. 3-6 hr)
Increase anticancer effect	Increased release of tissue factor pathway inhibitor (TFPI) Increased inhibition effect on angiogenesis and metastasis via higher binding affinities to VEGF, bFGF, chemokines, and selectins Increased inhibition of heparanase	

Table 1.6 Nanoparticles for systemic cancer therapy

Platform	Examples		Latest stage of development
Liposomes	DaunoXome (daunorubicin liposomal, Galen)		Approved
	Doxil (doxorubicin HCl liposome injection, Janssen)		
Albumin-based particles	Abraxane (protein-bound paclitaxel, Celgene)		Approved
PEGylated proteins	Oncaspar (PEG-L-asparaginase, Sigma-Tau)		Approved
	PEG-Intoron (PEG-interferon α-2b, Merck)		
	PEGASYS (PEG-interferon α-2a, Genentech)		
	Neulasta (pegfilgrastim, PEG-rh GCSF, Amgen)		
Biodegradable polymer-drug composites	Doxorubicin Transdrug (Livatag®, Phase III, BioAlliance Pharma)		Clinical trials
Polymeric micelles	Genexol-PM (paclitaxel-loaded polymeric micelle)	*South Korea, Samyang	Approved
		Cynviloq™, Lupin	Clinical trials
	SP1049C, NK911, NK012, NK105, NC-6004		

Polymer-drug conjugate-based particles	XYOTAX™ (CT-2103, paclitaxel poliglumex, paclitaxel and poly-L-glutamic acid) CT-2106 (camtothecin and poly-L-glutamate) IT-101 , AP5280, AP5346, FCE28068 (PK1), FCE28069 (PK2), PNU166148, PNU166945, MAG-CPT, DE-310, Pegamotecan, NKTR-102, EZN-2208	Clinical trials
Dendrimer	Polyamidoamine (PAMAM, Dendritech, Inc)	Preclinical
Inorganic or other solid particles	Carbon nanotubes, silica particles	Preclinical
	Aurimune™ (CYT-6091, rhTNF-PEG-gold nanoparticles, CytImmune Inc.)	Clinical

Chapter II. Chemoprevention effect of an orally active low-molecular-weight heparin conjugates on urethane-induced lung carcinogenesis via the inhibition of angiogenesis

2.1. Introduction

Low molecular weight heparin (LMWH) is a polydispersed sulfated glycosaminoglycan that consists of repeating disaccharide units with an approximately average molecular weight of 5,000 Da. LMWH is widely used as an anticoagulant drug because it binds to antithrombin III (ATIII) via a unique pentasaccharide motif [64]. Beside of this affinity for binding to ATIII, LMWH can bind to a wide range of molecules and proteins via electrostatic interactions with glycosaminoglycan chains, which enables the application of LMWH in various clinical purposes, including anticancer therapy [65]. Most especially, LMWH interacts with a variety of vascular growth factors including vascular endothelial growth factor (VEGF) and basic fibroblast growth factor (bFGF) [66]. However, when it comes to using LMWH in anticancer therapy, the anticoagulant efficacy should be considered in order to avoid unexpected side effects such as bleeding. Accordingly, we previously conjugated LMWH with various kinds of bile acids at different molar ratios and evaluated their anticancer (primarily antiangiogenic) and anticoagulant effects [67-71]. We found that LHT7 (where LMWH is conjugated with taurocholic acid at a molar ratio of 1:7) demonstrates the most potent anticancer and antiangiogenic activities and negligible anticoagulant activities [42, 70]. These properties of LHT7 contribute to the selective blocking of interactions with ATIII while also enhancing binding with VEGF and bFGF. Furthermore, we synthesized LHTD4, where LHT7 is conjugated with a newly developed bile acid-derived moiety that consists of 4 molecules of deoxycholic acid (tetraDOCA), in order to achieve the

administration of LHT7 via the oral route [47]. It was proven that this conjugation imposed high binding affinity to membrane transporters on LHTD4, which enabled it to be orally absorbed through the apical sodium-dependent bile acid transporters (ASBT)-mediated pathway [45, 46]. In addition, in order to further enhance the oral bioavailability of LHTD4, a cationic oral absorption carrier, N^{α}-deoxycholyl-$_{L}$-lysil-methylester (DCK), was also utilized to prepare the LHTD4/DCK complex as part of the final formulation before oral administration (Fig. 1) [72-74]. Thus, due to its convenience of intake, this newly developed orally active angiogenesis inhibitor can be used in the clinics, where a long-term drug administration is required such as follow up medication after discharge from hospital and both treatment and prevention of chronic diseases.

Angiogenesis is conventionally recognized as the formation of new vessels in order to allow the further growth of a malignant tumor [5]. Recently, however, several studies reported that angiogenesis is initiated and can be observed in premalignant stages [75, 76]. Moreover, these abnormal lesions demonstrate not only elevated angiogenesis, but a high risk of progression to malignancy when continuously exposed to favorable conditions [34, 77]. Because chemoprevention could involve pharmacological interventions that block the accumulation of mutations, as well as treatments that inhibit or eradicate the preinvasive precursors to invasive cancer [20, 78, 79], angiogenesis is considered a promising target for the chemoprevention of cancer.

In this regard, the incidence of lung cancer could be controlled by inhibiting angiogenesis. The premalignant lesions of lung cancer are usually diagnosed as

angiogenic squamous dysplasia (a premalignant lesion where the capillaries invade the overlying dysplastic endobronchial epithelium) in the central airways of high-risk patients such as current or ex-smokers [80, 81]. Lung cancer is the second-most common new cancer and the most common cause of cancer death [82]. This is probably due to the relatively lower 5-year survival rate of lung cancer patients (approximately 16%) in comparison with patients with other types of cancer (approximately 68%). This also means that once a patient is diagnosed with lung cancer, it is difficult to treat and recover from the disease [83]. In addition, lung cancer relapse frequently develops in patients who have been successfully treated using chemotherapy [84]. Taken together, the development of chemopreventive approaches is strongly needed in order to reduce both lung cancer-associatied morbidity and mortality. Consequently, we expect that if patients at high risk of lung cancer are diagnosed with highly angiogenic premalignant lesions and properly treated with an antiangiogenic regimen, the incidence of life-threatening lung cancer could be well-controlled.

In this study, we introduce a newly developed angiogenesis inhibitor named LHTD4, which demonstrates antiangiogenic effects following oral administration, as a promising chemopreventive agent. The antiangiogenic activities of LHTD4 were studied using various *in vitro* and *in vivo* studies. The chemopreventive effects of LHTD4, in terms of carcinogenesis and angiogenesis, were also evaluated in a urethane-induced murine lung cancer model.

2.2. Materials and Methods

2.2.1. Materials

Low molecular weight heparin (LMWH; Fraxiparine®; 4500 Da) was obtained from Nanjing King-Friend Biochemical Pharmaceutical Company (Nanjing, China). Taurocholic acid (TCA), deoxycholic acid (DOCA), dimethyl sulfoxide (DMSO), *N*,*N*'-dicyclohexylcarbodiimide (DCC), *N*-hydroxysuccinimide (HOSu), 1-ethyl-3-(3-dimethylaminopropyl)carbodiimide (EDAC), formamide, sodium cyanoborohydride ($NaBH_3CN$), tetrahydrofuran (THF), ethyl chloroformate, *N*-methylmorpholine, H-Lys(Boc)-OMe·HCl, and urethane were purchased from Sigma (St. Louis, MO). *N, N*-dimethylformamide (DMF) was obtained from Merck (Darmstadt, Germany). Poloxamer188 was obtained from BASF (Ludwigshafen, Germany). All reagents were analytical grade and used without further purification.

2.2.2. Synthesis and characterization of LHT7, LHTD4, and DCK

The synthesis of LHT7 was performed according to a previously published method [70]. Briefly, sodium taurocholate (STC, 0.5 g) was introduced with ethylenediamine at molar feed ratio 1:100 using 4-nitrophenylchloroformate (0.937g) in the presence of triethylamine (0.565 g) and 4-methylmorpholine (0.144 g). After 16 hours of agitation, the solution was precipitated with cold acetonitrile to obtain sodium ethylenediamine taurocholate (Et-STC). The obtained Et-STC was washed with cold acetonitrile and freeze dried to obtain the final product. Then, LMWH (500

mg) was dissolved in distilled water, to which HOSu (126.6 mg) was added. This solution was then further consecutively reacted with EDAC (310 mg) and Et-STC (686 mg). After reacting overnight, the solution was precipitated, washed with cold methanol, and freeze dried. The final product, LHT7, was obtained as a white powder.

LHTD4 was then synthesized by end-site conjugation of LHT7 with tetraDOCA following the previous procedure [47]. At first, LHT7 was oxidized by using potassium metaperiodate (57.5 mg) in acetate buffer at pH4.5. Then, LHT7 (30 g) was dissolved in mixed solution of formamide and DMF, and agitated at 50°C. The ethyl-tetraDOCA solution was prepared by dissolving ethyl-tetraDOCA (41.63 mg) in formamide (0.535 mL) and DMF (0.662 mL). Then, this ethyl-tetraDOCA solution was slowly added to the LHT7 solution and reacted for 3 hours at constant temperature. Then, sodium cyanoborohydride ($NaBH_3CN$, 1.6 mg) was added to this mixture, and the chemical reaction was allowed to react for 18 hours. The temperature was constantly maintained at 50°C throughout the whole reaction. This solution was precipitated by cold ethanol, centrifuged, and vacuum dried. This product was dissolved in distilled water and lyophilized in order to obtain a powder. Prior to using LHTD4 in this study, it was characterized using sulfuric acid and anti-FXa chromogenic assays (Chromogenix, Milano, Italy), as previously described [71], in order to confirm the conjugation ratio and anticoagulant activities.

Preparation of the absorption enhancer (DCK) was performed according to a previously detailed method [72]. Deoxycholic acid (26 g) was dissolved in THF (800 mL), to which ethyl chloroformate (6.4 mL) and 4-methylmorpholine (7.4 mL) were

added; this mixture was then agitated for 30 minutes at 4°C. The reaction was continued for 2 hours at room temperature. Then, H-Lys (Boc)-OMe·HCl (20 g) and 4-methylmorpholine (7.4 mL) were added into this mixture and heated for 2 hours under refluxing conditions. The chemical reaction was continued overnight at room temperature. The precipitates were obtained by filtration and solvent evaporation. The products were further purified by column chromatography (chloroform/methanol), then dissolved in a solution of acetyl chloride (23.4 mL) and methanol (100 mL) under mild agitation and allowed to react overnight at room temperature. The solvent was removed under reduced pressure, and the residue was dissolved in water and washed with chloroform. The final product was obtained as a powder by lyophilization (Fig. 2.1).

2.2.3. Tube formation assay

The *in vitro* endothelial tube formation assay was performed as described in previous studies [71, 85]. Briefly, 100 μL Matrigel (growth factor-reduced and phenol red-free; BD Bioscience, Billerica, MA) was loaded into each well of a 96-well plate and polymerized for 30 minutes at 37°C. Then, 1.5×10^4 human umbilical vein endothelial cells (HUVECs), which were suspended in 100 μL Endothelial Basal Medium-2 (EBM-2) containing either VEGF (50 ng/mL; Peprotech, NJ) or bFGF (50 ng/mL; ReliaTech GmbH, Germany), was added onto each well. To assess the dose-dependent inhibitive effects of LHTD4 on endothelial tube formation, the cells were treated with LHTD4 at different concentrations, including 0, 0.01, 0.1, 1, 10,

and 50 μg/mL. After 6 hours of incubation in 5% CO_2 at 37°C, the number of branch points in each capillary-like tube in each well were counted at 40× magnification using a microscope (Eclipse TE2000-S; Nikon, Japan) and statistically analyzed (n = 3).

2.2.4. Matrigel plug assay

The Matrigel plug assay was used to evaluate the *in vivo* antiangiogenic activities of LHTD4, as previously described with some modifications [70, 85]. Each C57BL/6 mouse (7-week-old males) received the subcutaneous injection of a 637.7 μL Matrigel-PBS mixture that contained 500 μL Matrigel, 86 μg/mL unfractionated heparin (UFH), 500 ng/mL VEGF, 500 ng/mL bFGF, and 50 μg/mL LHTD4, which was administered to the abdominal flank. Each group contained 3 mice. The mice were fed commercial rodent chow (Samyang Co., Seoul, Korea) and water *ad libitum* and housed in climate-controlled quarters (24ºC at 50% humidity) under a 12-hour light-dark cycle. All animal experiments were conducted according to the standard operating procedures established by the Committee for Ethics in Animal Experimentation of Seoul National University. Animals were raised under standard pathogen-free conditions, as established by the Animal Center for Pharmaceutical Research of Seoul National University. After 10 days, all mice were sacrificed, and the Matrigel plugs were removed and frozen in liquid nitrogen. To measure the hemoglobin content in the new blood vessels within the Matrigel plugs, samples were homogenized in hypotonic lysis buffer (250 μL 0.1% Brij-35 per plug) and

centrifuged for 20 minutes at 15,000 rpm. The supernatant was incubated in 0.5 mL Drabkin's solution for 15 minutes at room temperature, and absorbance was measured at 540 nm. Absorbance is proportional to the total hemoglobin content, thus the relative hemoglobin content was calculated and compared with the negative and positive controls.

2.2.5. Western blot

To assess the inhibitory effects of LHTD4 on the VEGF- and bFGF-mediated signaling pathways via the receptors that are expressed on HUVECs, the amount of phosphorylated VEGFR-2 and FGFR-1 was analyzed using western blot analysis [70]. HUVECs were fasted in serum-free media without other supplements for 12 hours at 37ºC under 5% CO_2, then treated with 50 μg/mL LHTD4. After 1 hour of incubation, either 100 ng/mL $VEGF_{165}$ or 500 ng/mL bFGF was added to the cells to stimulate them, then they were further incubated for another 5 minutes. Treatment was terminated by removing the media and washing with cold phosphate-buffered saline and 0.2 mM Na_3VO_4. Cells were harvested by scraping and solubilization in a lysis buffer (Pro-prep™ Protein Extraction Solution; Intronbio, Seongnam, Korea) that contained 20 mM of β-glycerophosphate, 50 mM NaF, and 200 μM Na_2VO_3 for 1 hour on ice. Insoluble materials were removed by the centrifugation at 4ºC for 10 minutes at 12,000 *g*. Then, the supernatant was collected and boiled in sodium dodecyl sulphate (SDS) sample loading buffer (0.5 M Tris-HCl, glycerol, 2-mercaptoethanol, 1% bromophenol blue) at 95ºC for 10 minutes. Protein (60 μg)

was separated using 7% SDS-PAGE and transferred to polyvinylidene difluoride membranes. After blocking with 5% bovine serum albumin (BSA) in Tris-buffered saline containing 0.1% Tween 20 (TBST) at room temperature for 1 hour, the membranes were probed with either rabbit polyclonal antiphospho-VEGFR-1 antibody (R&D Systems, Minneapolis, MN) or rabbit polyclonal antiphospho-FGFR-2 antibody (Cell Signaling Technology, Boston, MA) followed by goat anti-rabbit IgG horseradish peroxidase-conjugated secondary antibody. The transferred proteins were visualized using an enhanced chemiluminescent detection kit (ECL kit; Pierce, Rockford, IL).

2.2.6. Tumor growth inhibition test

The anticancer effects of LHTD4 were investigated in a tumor xenograft model that used the A549 human lung cancer cell line (American Type Culture Collection, Manassas, VA). Cells were cultured in Dulbecco's Modified Eagle's Medium (DMEM; Sigma Aldrich, St. Louis, MO) supplemented with 10% fetal bovine serum and 1% penicillin-streptomycin at 37°C under 5% CO_2. Athymic nude mice (7-week-old males; Orient Bio Inc., Seungnam, South Korea) received the subcutaneous injection of 1×10^7 A549 cells to the right flank. When the tumor volume was approximately 150–200 mm^3, the mouse was orally administered different concentrations of LHTD4, including 2.5, 5, and 10 mg/kg, once per day via an oral gavage (200 μL).

For oral administration, LHTD4 was formulated into the LHTD4/DCK complex, which was prepared by mixing LHTD4 with 3 mg/kg DCK, and labrasol (10 μL/mg LHTD4) and poloxamer 188 (2.16 mg/kg-body weight) as a solubilizer. Mice were fasted for 4 hours, and the stomach was neutralized with 3% sodium bicarbonate before drug administration. Tumor size was measured in two dimensions using slide calipers every 3 days. The tumor volume was calculated as $a \times b^2 \times 0.5$, where a is the largest and b is the smallest diameter. Mice were treated with drugs for 3 weeks and sacrificed by the inhalation of carbon dioxide. Tumor tissues were collected, weighted, and immunostained using anti-CD34 and anti-Ki67 antibodies to determine blood vessel formation and cell proliferation, respectively. The number of microvessels and proliferating cells were imaged and counted by using microscope (Olympus BX43, Hamburg, Germany).

2.2.7. Urethane-induced lung carcinogenesis model

A murine model of chemically induced lung carcinogenesis was used in this study, as previously described [80, 86]. To induce tumors by using urethane as the carcinogen, 6-week-old female A/J mice (Jackson Laboratory, Bar Harbor, ME) weighing between 20–25 mg were intraperitoneally injected with a single dose of 1 mg/kg urethane (Sigma Aldrich) that had been dissolved in normal saline. The mice were then divided and placed into either the control or treatment group. One week after urethane injection, the mice in the treatment group were treated with once-daily

5 mg/kg LHTD4. Over the entire 21-week experimental period, the clinical conditions of the mice, such as body weight, were closely observed.

2.2.8. Histological and serological evaluations

During this 21-week experiment, lung tissues were collected from the mice according to the time schedule for the histological examinations. To determine the tumor burden in the lungs of each mouse, the number of nodules on the surface was counted and the cross-sectional nodule area was determined. At weeks 1, 3, 6, 9, 15, and 21, the lung tissues were harvested after sacrificing the mice by cervical dislocation under light ether anesthesia and washed with cold PBS. First, the number of nodules on the surface of each lung was counted. Then, all left-side lobes were fixed in 10% neutral buffered formalin for subsequent histopathological analyses. The formalin-fixed left-lung lobes were routinely processed, embedded in paraffin, and cut to 4-μm-thick section for hematoxylin and eosin (H&E) staining and CD34 immunohistochemical analysis. Following H&E staining, in order to determine the degree of carcinogenesis in the lung tissues, all of the cross-sectioned lung tissues were closely examined by a pathologist and the nodule area was calculated using a slide image analyzer (Panoramic Scan; 3D Histech, Hungary) and software (Panoramic viewer; 3D Histech). To compare the degree of angiogenesis between the control and treatment groups at week 21, the lung tissues were also immunostained with rat polyclonal anti-mouse CD34 antibody (Thermo Scientific). The CD34

expression on the cross-sectioned lung tissue was also observed and imaged by using microscope.

2.2.9. Statistical analysis

All data are reported as the mean ± standard error of the mean (SEM). The data of the tube formation assay, Matrigel assay, and tumor growth inhibition study were statistically analyzed by the student *t* test. The Mann-Whitney test was used to compare nodule number and area. All p values < 0.05 were considered significant.

2.3. Results

2.3.1. Characterization of LHTD4 as an angiogenesis inhibitor

We evaluated the antiangiogenic activities of LHTD4 using both *in vitro* and *in vivo* experiments. First, we observed tube formation in HUVECs following treatment with LHTD4 for 6 hours at different concentrations (Fig. 2.2). We found that VEGF- and bFGF-induced tube formation is inhibited by LHTD4 in a dose-dependent manner without demonstrating significant cytotoxicity. In the control groups, in which endothelial cells were treated with either VEGF or bFGF alone, well-organized and multibranched tubular structures were observed. However, in the LHTD4-treated groups, which were treated with either VEGF or bFGF, tube formation was reduced in a dose-dependent manner. Relative tube formation among VEGF-induced endothelial cells decreased by 3.2% (0.01 μg/mL-LHTD4), 15.4%

(0.1 μg/mL-LHTD4), 34.0% (1 μg/mL-LHTD4), 55.1% (10 μg/mL-LHTD4), and 67.3% (100 μg/mL-LHTD4) in comparison with the control group (Fig. 2.2A, B). On the other hand, under bFGF-induced conditions, relative tube formation decreased by 6.7% (0.01 μg/mL-LHTD4), 16.1% (0.1 μg/mL-LHTD4), 30.9% (1 μg/mL-LHTD4), 51.7% (10 μg/mL-LHTD4), and 77.2% (10 μg/mL-LHTD4) in comparison with the control group (Fig. 2.2C, D).

Second, the Matrigel plug assay was used to investigate the *in vivo* antiangiogenic activities of the LMWH conjugates. We found that LHTD4 significantly inhibited EGF- and bFGF-induced angiogenesis in the Matrigel plugs that were transplanted into the study mice. As shown in Fig. 2.3A, while the Matrigel plugs treated with either VEGF or bFGF alone or a mixture were dark red in color; in contrast, plugs treated with LHTD4 together with either VEGF or bFGF alone or a mixture were pale. This indicates a substantial decrease in microvessel formation within the Matrigel plugs due to drug treatment. The hemoglobin content was decreased by 31.8%, 52.0%, and 55.0% in VEGF-, bFGF-, and mixture-treated groups, respectively, following co-administration with LHTD4 (Fig. 2.3B).

Finally, in order to study how LHTD4 affects the VEGF- and bFGF-mediated pathways involved in endothelial cell growth, we observed the effects of LHTD4 on the phosphorylation of VEGFR-2 and FGFR-1, which are the most representative receptors for VEGF and bFGF, respectively. As shown in Fig. 2.4, both VEGF and bFGF phosphorylated VEGFR-2 and FGFR-2 in HUVECs. However, the treatment of LHTD4 significantly blocked both the VEGF- and bFGF-induced phosphorylation of VEGFR-2 and FGFR-1 in these cells. Therefore, VEGF- and bFGF-mediated

phosphorylation of VEGFR-2 and FGFR-1 were inhibited by LHTD4 in HUVECs, which led to decreased angiogenesis.

2.3.2. Antiangiogenic effects of LHTD4 on tumor growth were observed in the A549 human lung cancer xenograft model

The dose-dependent inhibitory effects of LHTD4 on tumor growth were tested in a tumor xenograft model that used A549 human lung cancer cells. As shown in Fig. 2.5A, there was no significant difference in tumor volume on day 25 between the groups that received 5 mg/kg or 10 mg/kg LHTD4. Compared with the control group, the tumor volumes of these groups had decreased by 60.2% and 56.8%, respectively. Regarding tumor weight, the inhibitory effects determined for the groups that received 5 mg/kg LHTD4 were similar to those of the group that received 10 mg/kg LHTD4; tumor weight decreased by 60.5% in both of these groups in comparison with the control ($p < 0.01$; Fig. 2.5B). Drug treatment with LHTD4 did not affect body weight change over the whole experiment period (data not shown).

In the examination of new vessel formation by immunohistochemistry of CD34, even though the number of vessel was decreased by treatment with LHTD4 in all groups, there was no significant difference among these groups at different doses (Fig. 2.5C, E). In addition, in the observation of proliferating cells based on the immune-stained cells with Ki-67, the number of proliferating cell was significantly decreased in all LHTD4-treated groups. However, the proliferating cell number of group that is treated with 5 mg/kg LHTD4 was similar with that of group that is administered with 10 mg/kg LHTD4 (Fig. 2.5D, F). Therefore, based on these results,

we determined 5 mg/kg/day LHTD4 to be the appropriate regimen to use in the subsequent analyses.

2.3.3. LHTD4 demonstrates chemopreventive effects by decreasing nodule formation and the degree of angiogenesis in lung tissue

The time-dependent manner of the tumor burden of urethane-induced lung cancer was determined in terms of both nodule number and area (Fig.2.6A). As shown in Fig. 2.6B and D, even though the nodule number demonstrated a time-dependent increase in both the control and treatment groups, the value of the treatment group was lower than that of the control. Most especially, the mean number of nodules decreased from 28.4 to 14.4, corresponding to a significant reduction of 49.2%. In addition, when comparing cross-sectional nodule area, the results demonstrate a similar pattern to that of the nodule number (Fig. 2.6C, E). While the nodule area percentage—which was calculated by dividing the whole lung area by the tumor area—of the control group was 6.9% versus 4.8% for the treatment groups, corresponding to a significant reduction of 30.1%. Fig. 2.6F shows the degree of carcinogenesis of each nodule. Every nodule was classified bronchiolo-alveolar adenoma stage both in control and treatment groups, which is the major type of lung tumors induced by carcinogens in mouse carcinogenesis model. However, in the examination of blood vessel formation at nodule site of lung tissues by immunohistochemistry using anti-CD34 antibody, the blood vessel formation was affected and reduced by LHTD4 treatment (Fig. 2.6G and H).

Treatment with LHTD4 for 20 weeks did not affect the body weight or other physical conditions of the mice. There was no significant difference in body weight between the control and the treatment groups (data not shown).

2.4. Discussion

The present study demonstrates that a newly developed oral heparin conjugate named LHTD4 shows antiangiogenic effects both *in vitro* and *vivo*, leading to chemopreventive effects in a chemically induced murine lung carcinogenesis model. LHTD4 was synthesized by conjugating tetraDOCA, a tetrameric structure of deoxycholic acid, at the end saccharide of LHT7, which consists of an average of 7 sodium taurocholate molecules bound to each of the carboxyl groups of LMWH [47]. As a result of this conjugation, LHTD4 becomes orally active while retaining potent antiangiogenic effects with a negligible anticoagulant activity [42, 70]. Both *in vitro* and in *vivo* experiments verified that the antiangiogenic activity of LHTD4 was still maintained throughout the chemical conjugation. Above all, orally available LHTD4 could be applied to a long-term use such as cancer chemoprevention, where convenience of intake, therapeutic efficacy, and chronic safety of drug should be fully satisfied, with the mechanism of angiogenesis inhibition.

At first, both VEGF- and bFGF-induced tube formations in HUVECs were effectively inhibited by LHTD4 in a dose-dependent manner without demonstrating significant cytotoxicity. Since demonstrating tube formation in HUVECS is the most well-established *in vitro* assay for the 3-dimensional modeling of the vessel

formation involved in angiogenesis, this significant reduction in tube formation could be an indicator of the *in vivo* antiangiogenic effects of LHTD4. Furthermore, as demonstrated by the quantification of hemoglobin content in the Matrigel plugs, LHTD4 inhibited the migration of endothelial cells to the Matrigel plugs, which led to reduced angiogenesis. Thus, this study demonstrates that LHTD4 inhibits the activities of VEGF and bFGF that is recruitment of endothelial cells, thereby leading the inhibition of angiogenesis. To assess the inhibitory effects of LHTD4 on the molecular signaling pathways involved in angiogenesis, we measured the degree of phosphorylation of VEGFR-2 and FGFR-1 that occurred following stimulation with VEGF and bFGF. Intracellular signaling for angiogenesis is initiated by the binding of angiogenic growth factors to receptors, such as VEGFR-2 and FGFR-1, which is followed by phosphorylation. We found that the phosphorylation of VEGFR-2 and FGFR-1, considered the most representative receptors in angiogenesis, were significantly inhibited by LHTD4.

Both the end site-specific conjugation of tetraDOCA and the physical complexation with DCK could increase the oral bioavailability of LHTD4, and its absorption mechanism could be explained in different ways. Firstly, it was proven that the conjugated tetraDOCA could carry LHTD4 via oral route by the newly proposed vesicular transport mechanism [45, 46]. In other words, the specific and strong binding of tetraDOCA (tetrameric deoxycholic acid) to apical sodium dependent bile acid transporter (ASBT), which is a highly expressed membrane transporter in the ileum, induced the functional transformation of ASBT like receptors, thereby forming the vesicles containing LHTD4 and finally enabled the

delivery of LHTD4 across the cell membrane. On the other hand, the electrostatic interaction of anionic LHTD4 and cationic DCK resulted in the increased hydrophobicity of the drug by masking the net charge. Thus, it enabled the transcellular uptake of LHTD4 at the duodenum, where it cannot be absorbed by itself due to the lack of ASBT expression. It was also proven that the structure of LHTD4/DCK complex was well retained until it reaches the site of absorption. In addition, enteric coating capsules or tablets might be utilized to achieve oral absorption of LHTD4/DCK complex in the clinics. Consequently, LHTD4 can now be absorbed both in the ileum and the duodenum, with 34.3% bioavailability, 7.39 μg/mL C_{max}, and a half-life of 6.04 hours following the oral administration of the LHTD4/DCK complex [47]. This was enough to maintain a therapeutic concentration (1–2 μg/mL) when administered once daily.

Based on these pharmaceutical characteristics of LHTD4, we verified the antiangiogenic effects of LHTD4 at different doses in a tumor xenograft model using the A549 human lung cancer cell line. As shown in Fig. 5, even though tumor growth was not completely inhibited or reduced, it was significantly inhibited by LHTD4 in a dose-dependent manner. However, the effects were not increased by administering above 5 mg/kg. This might be explained by the complex biology of cancer; in other words, there are angiogenic as well as other factors that are involved in the progression of cancer. Thus, even though we blocked the angiogenic signaling pathways using doses > 5 mg/kg LHTD4, tumor growth still continued via other pathways in areas where the inhibition of angiogenesis by LHTD4 was already saturated. In the histological analysis of tumor tissues by immunohistochemistry

using anti-CD34 antibody, we observed a slight decrease in the number of blood vessels between control and LHTD4-treated groups without a statistical difference. However, the size and morphology of blood vessels of the control group were different from those of LHTD4-treated group. While the vessels were observed to be well-structured and macro-sized in the control group, the maturation and development of blood vessels were markedly inhibited by LHTD4 in the treatment group. Thus, the results of the tumor growth inhibition study on the A549 human lung cancer cell line illustrate that LHTD4 could also work as an antiangiogenic drug when it is applied to lung cancer patients in the clinics.

Based on the antiangiogenic activity of LHTD4, we further investigated the chemopreventive effects of LHTD4 in a murine carcinogenesis model of lung cancer, using urethane as carcinogen. This murine model is commonly used in pathological studies evaluating lung cancer development and chemopreventive agents since there are histological similarities between the murine lung adenomas and the papillary stage of human adenocarcinomas. That is, if a candidate compound demonstrates chemopreventive effects in the animal model in terms of its effects on nodule number or size, it might also be expected to prevent lung cancer in humans. As shown in Figure 6, the formation of nodules in lung tissue time-dependently increased subsequent exposure to the carcinogen. However, the number of nodules on the surface of the lung tissue was significantly reduced by treatment with LHTD4. Accordingly, the cross-sectional area of the nodule also increased in a time-dependent manner; however, the cross-sectional area was also significantly reduced in the treatment group. In addition, the nodules were diagnosed as

bronchiolo-alveolar adenoma (Fig. 6F), which is referred as virtually any adenoma and carcinoma of lung that are derived from the peripheral lung structures such as terminal bronchioles, alveolar ducts, and alveoli [87]. In the cancer chemotherapy, angiogenesis inhibitors do not directly kill the malignant cells but foster unfavorable microenvironment conditions for tumor growth by inhibiting new vessel formation. Thus, the therapeutic effect of LHTD4 can be evaluated by measuring not the shrinkage of tumor size but the degree of retardation or delay of tumor growth. In the same way with cancer chemotherapy, the chemoprevention effect of LHTD4 might be also related with slowing down the progression rate of cancer. Thus, the number and size of nodule, which was diagnosed with early stage of lung cancer, can be a good indicator for the evaluation of chemopreventive effect of LHTD4 on lung cancer development, which might satisfy the objective of this study. In other words, the administration of LHTD4 as a chemopreventive agent could prevent and inhibit the formation of premalignant lesions and its further progression to malignant tumors. This might satisfy the requirements for clinical chemoprevention, which is defined as the delay of clinically invasive and painful symptoms during a patient's lifetime [88]. In addition, in the immunohistoglogial analysis of nodules on lung tissue, we found that the expression of CD34-positive cells was prominently reduced by administration with LHTD4. The inhibition of new vessel formation at the nodule of lung tissue by LHTD4 might contribute to the delayed progression of nodules. Previously, it was reported that intervention with vandetanib, which is an angiogenesis inhibitor that targets VEGFR-2 tyrosine kinase, could decrease the incidence or delay the progression of urethane-induced lung cancer [80]. However,

because the secretion of angiogenic factors proportionally increases the degree of carcinogenesis [10], the binding activity of LHTD4 to multiple angiogenic factors, including VEGF, bFGF, and PDGF, would make it superior to vandetanib as a chemopreventive agent. Moreover, since combination chemoprevention using more than two drugs was proven to be more effective and less toxic [89], the chemopreventive effect of LHTD4 might also be further enhanced by using other drugs together. In this context, LHTD4, as a multitargeting angiogenesis inhibitor, could be a promising drug for the chemoprevention of lung cancer.

2.5. Conclusions

The newly developed oral angiogenesis inhibitor named as LHTD4, synthesized by the conjugation of LHT7 with a bile acid moiety to achieve oral absorption, still retained its antiangiogenic activity after oral administration both *in vitro* and *vivo*. Its bioavailability and therapeutic efficacy also indicate that LHD4 could be applied as an antiangiogenic drug in the clinics. Above all, because of high patient convenience of intake guaranteed by its route of administration, we expect that LHD4 can serve well in cancer chemoprevention requiring chronic administration.

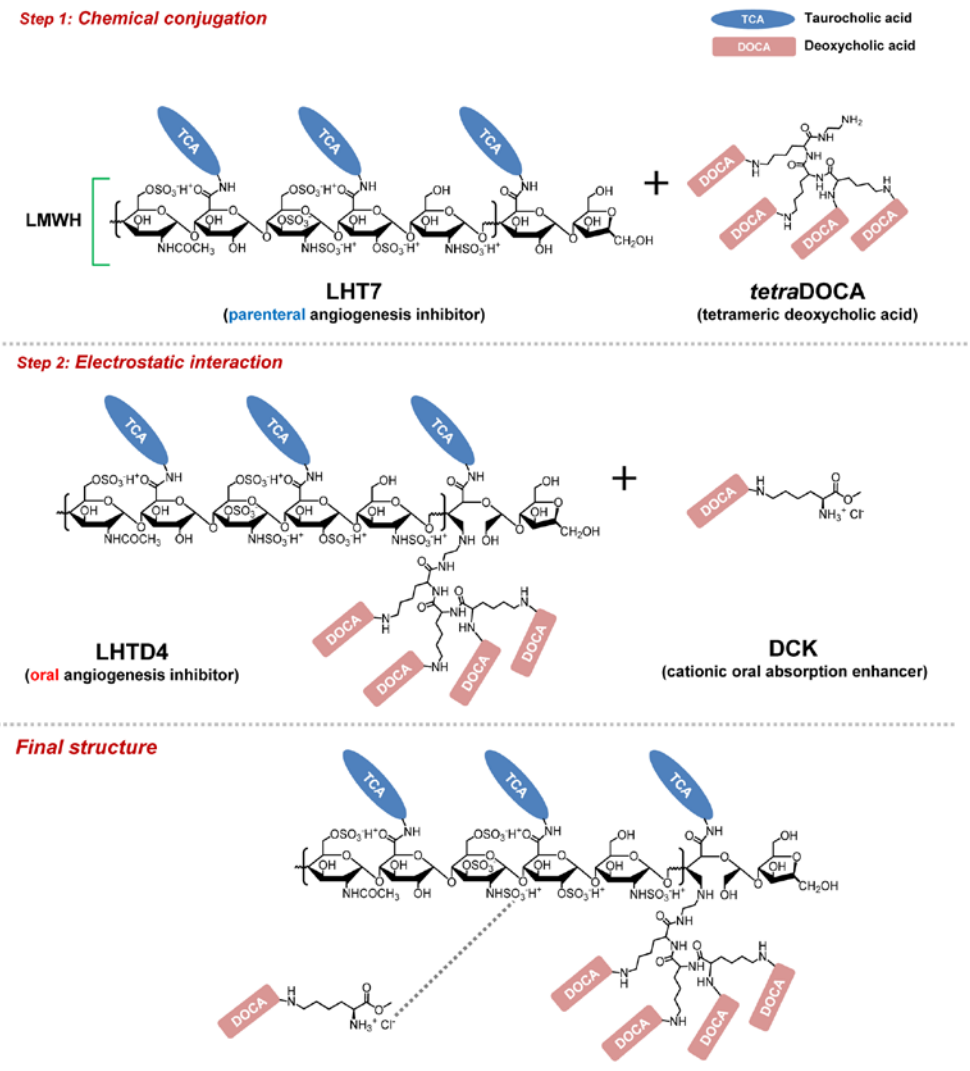

Figure 2.1 Scheme of molecular structure of LHTD4/DCK complex

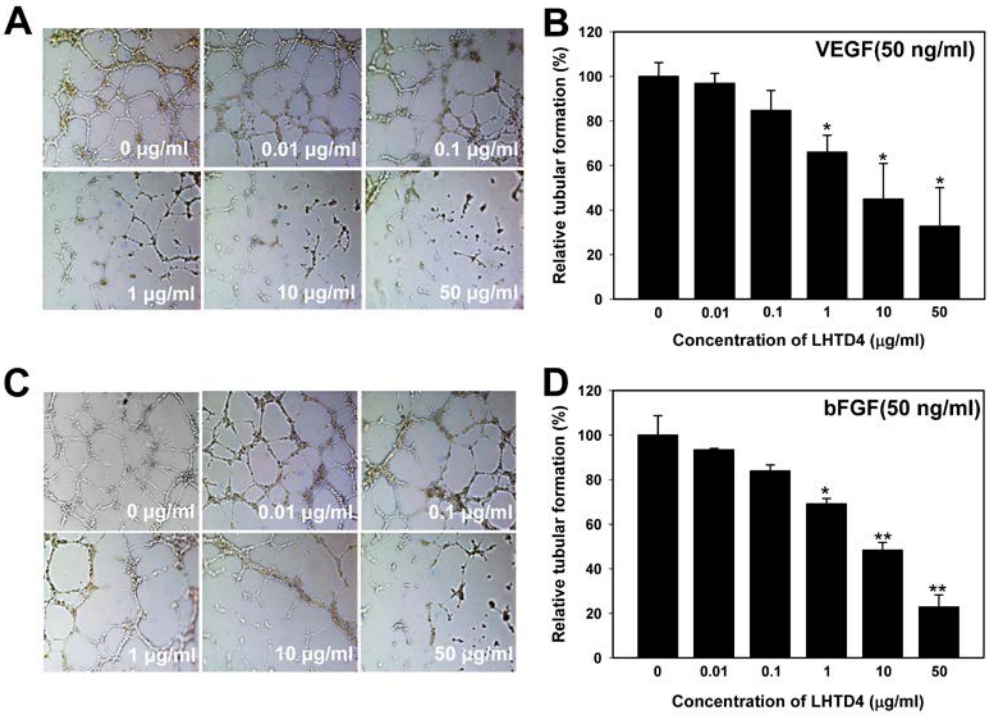

Figure 2.2 Dose-dependent effects of LHTD4 on tube formation (0.01−50 μg/mL) induced by VEGF (50 ng/ml; A, B) and bFGF (50 ng/ml; C, D). HUVECs (1.5 × 104 cells per well) were seeded onto polymerized Matrigel plugs and incubated for 6 hours at 37°C in an atmosphere with 5% CO2. (A, C) Optical images were obtained at 40× magnification. (B, D) The number of branched points in cells that were treated with different concentrations of LHTD4 was counted using a microscope at 40× magnification. Each bar indicates the mean ± SD (n = 3). *p < 0.05 vs. control. **p < 0.01 vs. control.

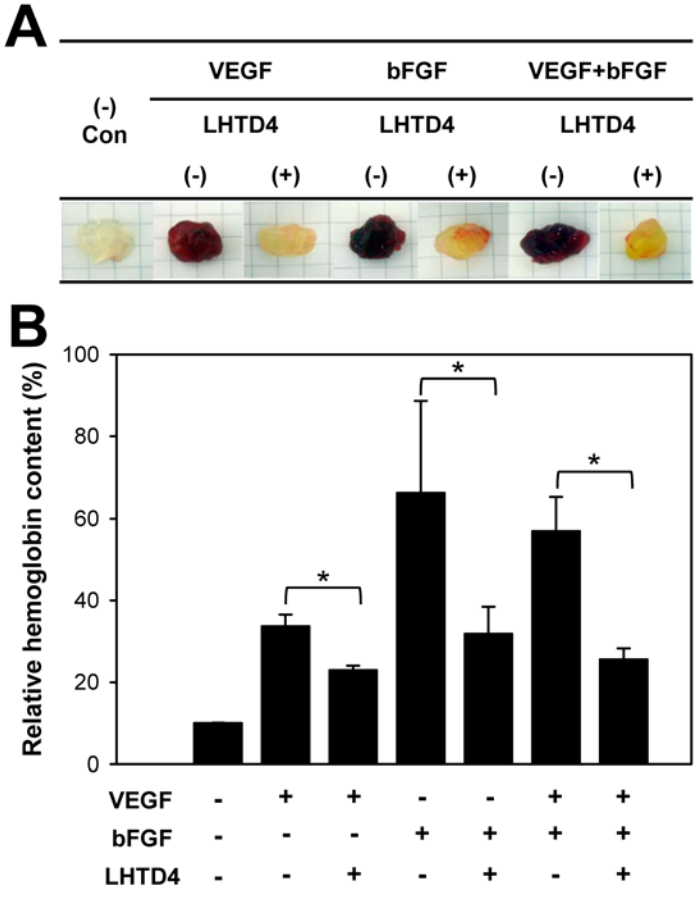

Figure 2.3 Inhibitory effects of LHTD4 on VEGF-, bFGF-, and mixture-induced angiogenesis in Matrigel plugs. Mice were subcutaneously injected with 637 μL of the Matrigel mixture that contained growth factors and LHTD4. (A) After 10 days, the mice were sacrificed, and the Matrigel plugs were excised and photographed. (B) The hemoglobin content of each Matrigel plug was determined using Drabkin's method. Data are presented as the means ± SD. *$p < 0.05$ vs. no drug-treated group.

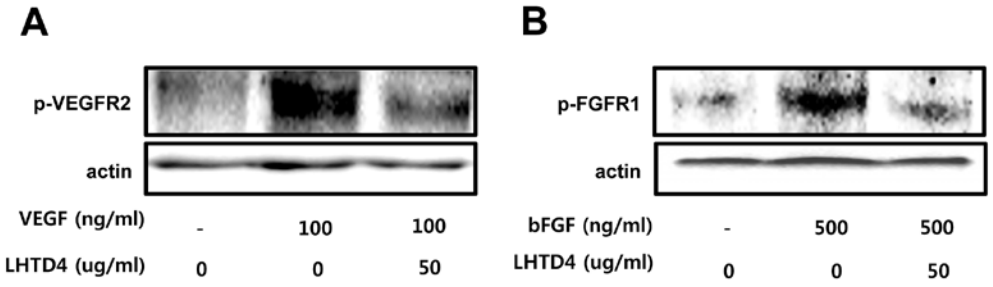

Figure 2.4 VEGF- and bFGF-dependent phosphorylation of VEGFR-2 and FGFR-1. HUVECs were incubated with 50 μg/mL LHTD4 for 1 hour, then treated with $VEGF_{165}$ (100 ng/mL) or bFGF (100 ng/mL) for 5 minutes. Proteins were separated by electrophoresis using SDS-PAGE and transferred to PVDF membranes. The phosphorylated proteins were probed using antiphospho-VEGFR-2 (panel A) and FGFR-1 (panel B). β-actin was used as the loading control.

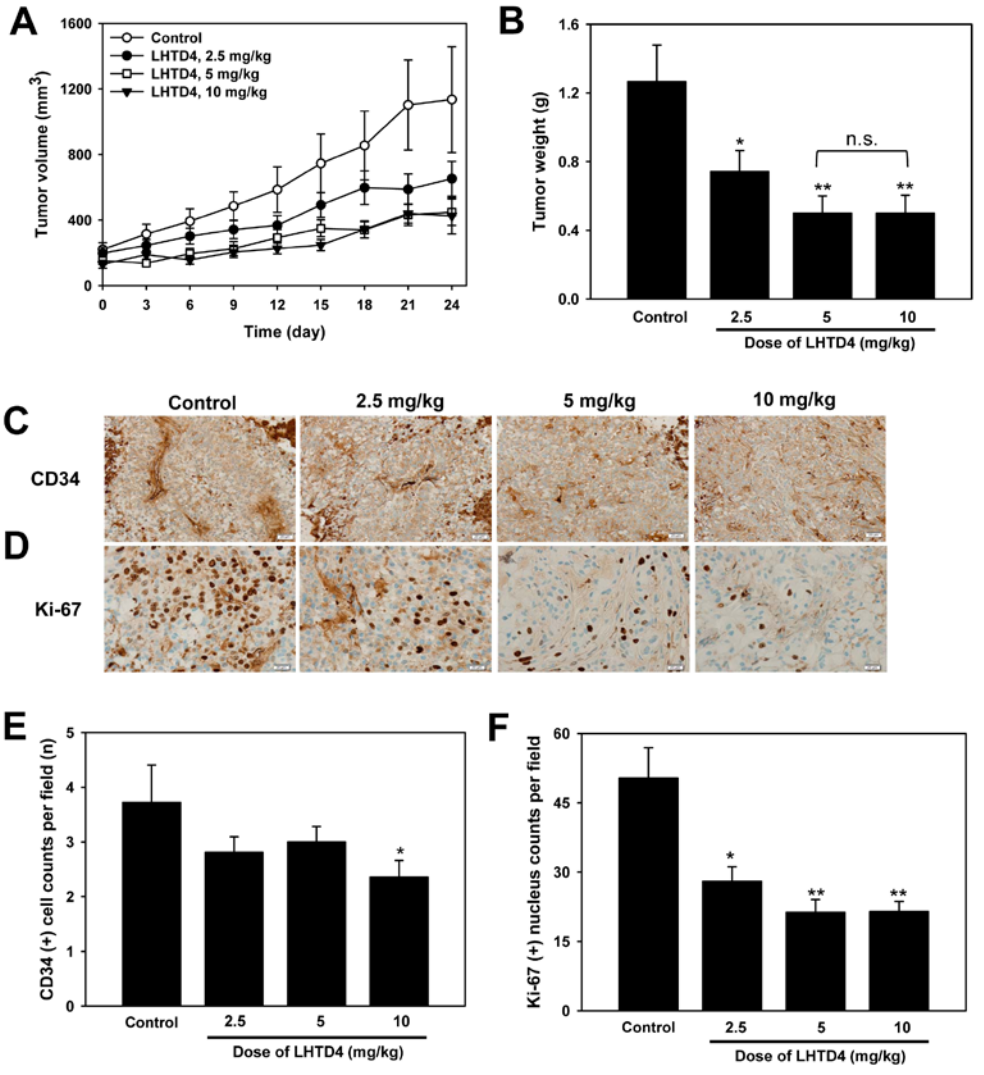

Figure 2.5 *In vivo* inhibitory effects of LHTD4 on tumor growth in the A549 xenograft model. Mice were inoculated with A549 cancer cells (1×10^7 cells per mouse) at the dorsal flank and administered LHTD4 at different doses (0, 2.5, 5, 10 mg/kg; n number = 10). (A) Tumor volume of the control (○), and the daily oral administration of LHTD4 at 2.5 mg/kg (●), 5 mg/kg (□), and 10 mg/kg (▼). After 24

days, the mice were sacrificed and the tumors were isolated, and (B) weighed. Then, tumor tissues were paraffined in blocks, sectioned, and immunostained with the anti-CD34 and Ki-67 antibodies to examine the vessel formation and cell proliferation. (C, D) The immunostained slides were observed under a microscope at 40× magnification and photographed. (E) The expression of CD34 positive blood vessels and (F) Ki-67 positive proliferating cells were quantitatively analyzed using image analysis software. Data are expressed as the means ± SEM. *$p < 0.05$ *vs.* control. **$p < 0.01$ *vs.* control.

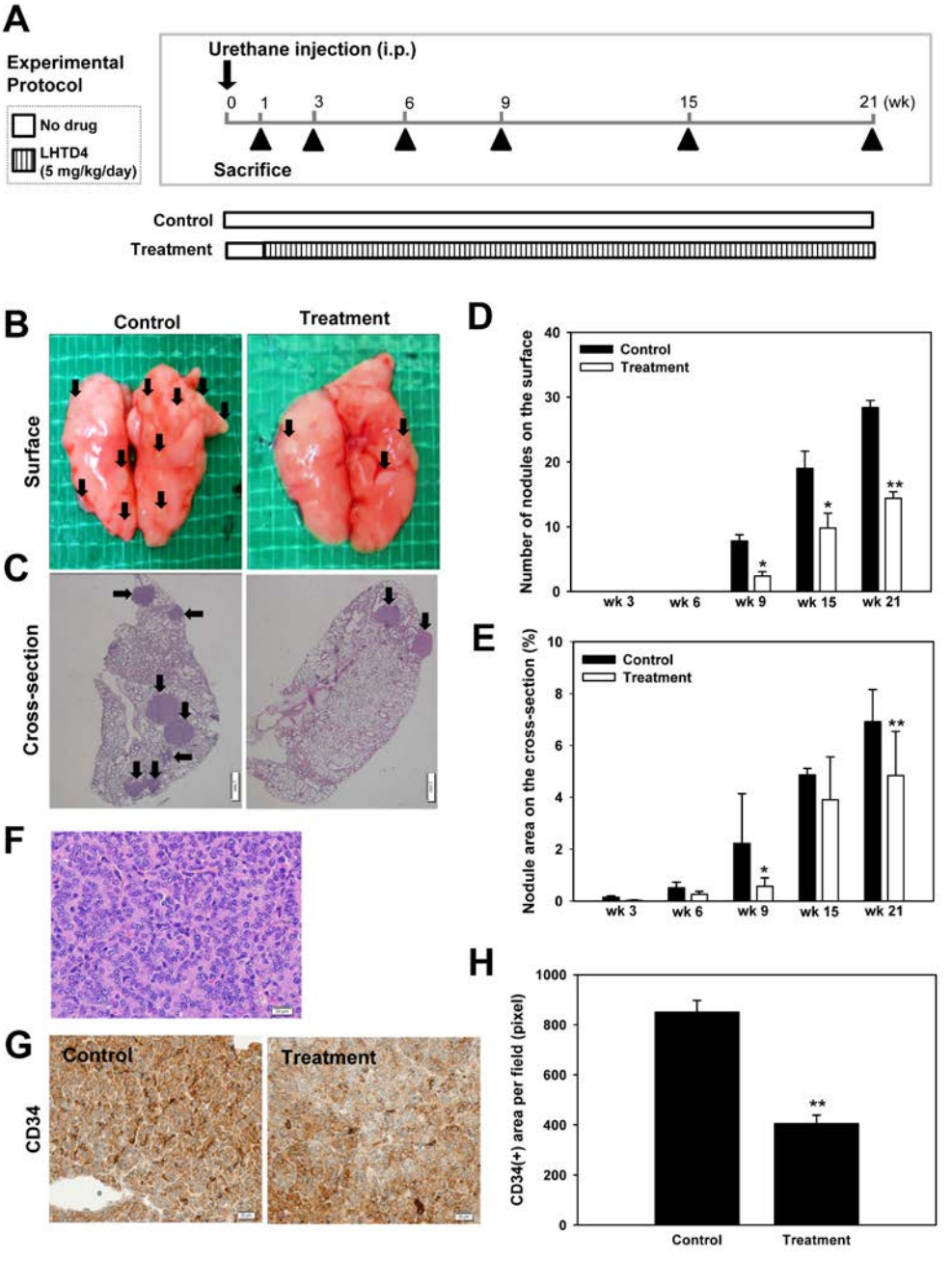

Figure 2.6 Evaluation of the chemopreventive effects of LHTD4 in a urethane-induced lung cancer carcinogenesis model. (A) Female A/J mice were

injected with 1 mg/kg urethane, then treated with 5 mg/kg LHTD4 for 20 weeks. Mice were sacrificed at the intended time point (n number = 5 for the week of 3, 6, 9 and 15; n number = 25 for the week of 21), and their lung tissues were collected and examined to determine (B) The morphologies of the lung tissues were determined and photographed, and (C) images of the cross-sectioned lung tissue following hematoxylin and eosin staining were obtained. (D) The number of nodules on the surface and (E) the cross-sectional area of the nodules. *$p < 0.05$ and **$p < 0.01$ *vs.* control on the same week. (F) Representative histological image of a murine lung adenocarcinoma observed in this study (100× magnification). (G) Vessel formation at lung tissues was compared between control and treatment groups by immunohistochemistry of CD34 and (H) quantification of CD34-positive area on cross-sectional lung tissue. *$p < 0.05$ *vs.* control.

Acknowledgement

This work was supported by Korea Foundation for Cancer Research (KFCR-2011-004).

본 연구는 2011년도 대한암연구재단 암 연구 박사학위논문 저술 지원사업 지원에 의하여 수행 되었음.

Chapter III. Combinational chemoprevention effect of celecoxib and an oral anti-angiogenic LHD4 on colorectal carcinogenesis in mice

3.1. Introduction

Even though a significant understanding of cancer biology has been achieved, cancer still remains as a leading cause of death worldwide. Thus, the concept of chemoprevention, referring to the use of pharmacological agents to inhibit, reverse or delay carcinogenesis in the early stages, has emerged, which, in conjunction with early detection and chemotherapy, represents a promising strategy for controlling the incidence of cancer [90].

In chemoprevention, the role of inflammation has been widely studied for its significance in cancer development and progression [91]. Pharmacological agents that target inflammatory mediators such as prostaglandins (PGs) and cytokines are expected to have anticancer effects [92]. Accordingly, non-steroidal anti-inflammatory drugs (NSAIDs), which mainly block the cyclooxygenase-mediated production of PGs, have been used in both cancer chemotherapy and chemoprevention [93]. Moreover, blocking inflammation through the use of NSAIDs is thought to be a successful way to prevent cancer incidence because inflammation is involved in the overall process of carcinogenesis, especially in the early initiation stage. For this purpose, various kinds of NSAIDs, such as aspirin [94], nimesulide [95], sulindac [96] and celecoxib [97] have been evaluated as chemopreventive agents. Among these, celecoxib is one of the most representative drugs of the selective cyclooxygenase-2 (COX-2) inhibitor, which is the most commonly prescribed in the treatment of chronic inflammatory diseases. Celecoxib has also been actively studied as a chemopreventive agent in different types of cancer

including colorectal, breast, and head and neck cancer [98]. However, it is disappointing that no clinical regimen has yet been proven to achieve both therapeutic efficacy and long-term safety although a number of experiments using NSAIDs have reported successful chemoprevention outcomes.

Angiogenesis has also been shown to play a pivotal role in the early stages of carcinogenesis [99]. It is widely accepted that the switching-on of angiogenesis is essential for progression from the pre-malignant to the malignant stage of cancer [100, 101]. In this context, intervening in the process of angiogenesis to inhibit may also be a way to reduce incidences of cancer. Here, we introduce a newly developed, orally active heparin conjugate named LHD4 as an angiogenesis inhibitor. In the previous studies, we reported that low molecular weight heparin (LMWH)-deoxycholic acid (DOCA) chemical conjugates show different molecular structures, anticoagulant activities and anticancer effects that depend on the LMWH:DOCA molar ratio. In addition, compared to LMWH, it also shows significantly increased oral bioavailability. DOCA was introduced to change the structure of the LMWH and permit transport through the bile acid transporter in the ileum and to increase the hydrophobicity of the molecule [67-69, 102]. Among these conjugates, LHD4, which is thus named because it consists of a 1:4 molar ratio of LMWH:DOCA, completely loses its anticoagulant activity, but shows increased binding affinity for angiogenic growth factors and oral bioavailability [71]. This new drug was proven to have angiogenesis inhibition-related anticancer effects both *in vitro* and *in vivo*, without side effects such as bleeding. Most of all, this new drug is

expected to be a promising chemopreventive agent due to its oral administration route.

Based on the well-established mechanism studies of chemopreventive agents reported up to now, the combination chemoprevention method of using more than one drug with different mechanisms is expected to be a practical and meaningful strategy. The basic concept of combined chemoprevention was first proposed by Sporn in 1980 [29], but it has only emerged as a clinically ideal method for preventing cancer since the report of the combination use of sulindac and difluoromethylornithine to successfully prevent colorectal adenomas in 2008 [30, 31]. Given the close relationship between inflammation and angiogenesis in cancer and their important respective roles in the early stages of carcinogenesis, the two processes could be an ideal target for cancer chemoprevention, and the combined use of celecoxib with an angiogenesis inhibitor might be a successful regimen [27, 90, 103, 104].

In this study, we hypothesized that the combined use of a selective COX-2 inhibitor (celecoxib) and an oral angiogenesis inhibitor (LHD4) would provide a clinically meaningful regimen for improving cancer chemopreventive effects in terms of delayed carcinogenesis through intervention of inflammation and angiogenesis. To evaluate this hypothesis, we used the azoxymethane (AOM) and dextran sodium sulfate (DSS)-induced colorectal carcinogenesis animal model, which mimics the pathological properties of human colitis-driven colorectal carcinogenesis. The chemopreventive effect was evaluated in terms of clinical symptoms such as prolapse

incidence and polyp volume. In addition, the pathohistological analysis of colon tissue was evaluated for signs of carcinogenesis, angiogenesis and inflammation.

3.2. Materials and Methods

3.2.1. Materials

LMWH (Fraxiparine®, 4500 Da) was obtained from Nanjing King-Friend Biochemical Pharmaceutical Company (Nanjing, China). DOCA, *N*,*N'*-dicyclohexylcarbodiimide (DCC), *N*-hydroxylsuccinimide (HOSu) , 1-ethyl-3-(3-dimethylaminopropyl) carbodiimide (EDAC), formamide, AOM, methylcellulose, and Tween 20 were purchased from Sigma (St. Louis, MO). DSS with a molecular weight of 36,000 to 50,000 Da was obtained from ICN Biochemicals (Aurora, OH). *N*, *N*-dimethylformide (DMF) was obtained from Merck (Darmstadt, Germany). Celecoxib (Celebrex® Capsule, 200 mg) was manufactured by Pfizer (New York, NY). For oral formulations, polyethylene polyoxypropylene block copolymer (poloxamer 407) was obtained from BASF (Ludwigshafen, Germany).

3.2.2. Synthesis of LHD4

LHD4 was synthesized according to the previous method [71]. Briefly, DOCA (10 g) was dissolved in 89.99 ml of DMF and reacted with DCC (8.4 g) and HOSu (4.7 g). The activated DOCA was precipitated in cold acetonitrile following

filtration, and 10 g of activated DOCA was dissolved in DMF (94 ml) and reacted with ethylenediamine (136 ml) solution for 5 h at room temperature to synthesize EtDOCA. Next, EtDOCA was conjugated to LMWH. For this reaction, 200 mg of LMWH was dissolved in 44 ml of formamide, and EDAC (204.48 mg) was added to activate the carboxylic acid of LMWH. After 10 min of chemical reaction, 386.4 mg of EtDOCA, which was dissolved in 40 ml of DMF, was added to the mixture. Then, 122.76 mg of HOSu dissolved in 4 ml of DMF was added. The reaction mixture was incubated for 12 h in an ice bath while stirring. The reacted solution was then precipitated in ethanol, centrifuged, and vacuum dried. The product was subsequently dissolved in water and lyophilized, and the final compound, LHD4, was obtained as a white powder. LHD4 was characterized by ^{1}H NMR and anti-FXa chromogenic assay (Chromogenix, Milano, Italy), as detailed previously [71], to confirm its amide bond formation and anticoagulant activity.

3.2.3. Animal treatment

Animals were treated with AOM and DSS to mimic colitis-associated colorectal carcinogenesis according to the protocol provided in the literature [105]. Male ICR mice (5-weeks old; Orient Bio, Sungnam, Korea) weighing from 20 to 25 mg were divided into 5 groups, with the first group receiving no treatment (negative control, n = 5) and all the other groups receiving one of the following treatments: a single intraperitoneal injection of AOM (10 mg/kg) followed by one cycle of 2.5% DSS ingestion in drinking water for 1 week (Group 1, n = 27); 10 mg/kg of celecoxib

(Group 2, n = 20); 10 mg/kg of LHD4 (Group 3, n = 29), and finally both celecoxib and LHD4 in combination (Group 4, n = 20) (Fig. 3.1A). Celecoxib was daily administered from the third week after AOM injection. For oral administration, celecoxib was suspended in 0.5% of methylcellulose with 0.025% of Tween 20 as a stabilizer. Daily oral administration of LHD4, which was dissolved in distilled water with 2.16 mg/kg poloxamer 407 as a solubilizer, was started on the same day as the AOM injection. Mice were fasted for 4 h before drug administration. The combined volume of 200 μl of suspended celecoxib and solubilized LHD4 were administered by oral gavage. In the case of Group 4, LHD4 was administered first, followed by celecoxib administration with 1 h time interval.

The mice were housed in climate-controlled quarters (24ºC at 50% humidity) with a 12-h light:dark cycle. During the entire 17-week experiment, the clinical phenotypes of the mice were closely observed (such as body weight and rectal prolapse). All animal experiments were conducted according to the standard operating procedures of the Committee for Ethics in Animal Experimentation of Seoul National University. Animals were raised under the standard pathogen-free conditions of the Animal Center for Pharmaceutical Research of Seoul National University. The mice were fed with commercial rodent chow (Samyang Co., Seoul, Korea) and water ad libitum.

3.2.4. Histopathological evaluation

After 17 weeks treatment, all mice were sacrificed by cervical dislocation.

Their colon tissues were removed, opened longitudinally, and washed with cold normal saline. The number, size and distribution of the polyps were closely examined through the use of a dissection microscope and a digital slide calipers. The volume of each polyp was calculated according to the equation, $a \times b^2$, where 'a' is the largest and 'b' is the smallest diameter. The total polyp volume per mouse was obtained by summing all the volumes of the individual polyps of each mouse. Next, the colon tissue was divided into three parts (distal, middle and proximal), spread on filter paper and fixed overnight in neutral 4% paraformaldehyde-phosphate-buffered saline (PBS). The fixed colon tissue was sectioned at 4 μm at 3 mm intervals, embedded in paraffin, and then mounted onto the slides. For the hematoxylin and eosin (H&E) staining and immunohistochemistry (IHC), the slides were deparaffinized by incubation at 60ºC for 2 h, submerged in xylene for 5 min and rehydrated in a graded alcohol series (100, 90, 80, 70, and 60%). After H&E staining, all the distal parts of the colon tissue were closely examined by a pathologist to measure the colon crypt height and determine the degree of carcinogenesis. The height of colon crypt was measured by using microscope and image analysis software (Eclipse, TE2000S, Nikon, Japan). On the other hand, all tissues were classified into five stages (normal, hyperplasia, low-grade adenoma, high-grade adenoma and adenocarcinoma) according to Gregory's method, which has previously been used for assessing the pathology of mouse models of intestinal cancer [106]. Those tissues were also classified at the same time into five different stages—normal, minimal, slight, moderate, and marked inflammation—according to previously defined criteria.

3.2.5. Immunohistochemical analysis

After rehydrating the slides according to the protocol used for the histopathological evaluation, antigen retrieval was carried out for IHC by heating the slides in a steamer for 1 h in 10 mM citrate buffer, pH 6.0, and then cooling to room temperature. After washing with distilled water, the slides were pre-incubated in blocking solution (Power block®, BioGenex, Fremont, CA) for 30 min to reduce nonspecific binding. Then, the slides were incubated for 12 h at 4°C with anti-PCNA (Thermo Scientific, Hudson, NH; dilution ratio at 1:1600), anti-CD34 (Affinity Bioreagents, Golden, CO; dilution ratio at 1:100), anti-F4/80(AbCam, Cambridge, MA; dilution ratio at 1:200), in a humidified chamber. After washing with PBS, the tissue sections were observed with a peroxidase-labeled polymer conjugated to goat anti-rabbit immunoglobulins (to anti-PCNA and CD34 antibodies) and goat anti-mouse immunoglobulins (to anti-F4/80 antibody) in Tris-HCl buffer (Envision+ System-HRP-labeled polymer; Dako, Glostrup, Denmark), which was incubated for 30 min at room temperature. The slides were washed and the chromogen was developed for 5 min with liquid 3, 30-diaminbenzidine (Dako). The slides were counterstained with Mayer hematoxylin. All of the negative controls were treated similarly except for that of the primary antibody, which was omitted. On the other hand, antigen-retrieved tissue slides were also subjected to terminal deoxynucleotidyl transferase dUTP nick-end labeling (TUNEL) assays according to the according to the manufacturer's manual (Millipore Corporation, Billerica, MA)

3.2.6. Statistical analysis

All data are reported as mean ± standard error of the mean (SEM). Statistical analysis of data was performed with the use of one-way analysis of variance (ANOVA) followed by the Dunnett's multiple comparisons procedure, in which several treatment groups were compared with a control. Differences of $P < 0.05$ were considered significant.

3.3. Results

3.3.1. Clinical symptoms were not observed in mice that were co-treated with celecoxib and LHD4

The chemopreventive effects of celecoxib, LHD4, or a combination of these two drugs were evaluated in an AOM and DSS-induced colorectal carcinogenesis animal model. During the period of 17 weeks, the mice were closely observed for clinical symptoms such as the presence of blood in the stool, prolapses, and reduced body weight. Even though body weight was temporarily reduced during the period of DSS treatment in Groups 2, 3 and 4 compared to Group 1, there were no significant statistical differences among all groups for 17 weeks of whole experiment (Fig. 3.1B). On the other hand, bloody stool were observed only in Groups 1 and 2, where mice were exposed to AOM and DSS without drugs, during the period of DSS treatment. However, the experimentally treated animals with LHD4 in Groups 3 and 4 were

similar to the negative control group with regard to bloody stool. Prolapses were clinically observed as an indicator of the massive development of polyps in the distal part of the colon. In the positive control group (Group 1), where mice were treated with both AOM and DSS without drugs, 28.5% of mice had prolapses. However, in the celecoxib- or LHD4-treated groups (Groups 2 and 3), the prolapse incidence significantly decreased to 10.5 and 18.5 %, respectively. Moreover, no prolapse was observed in Group 4, where the mice were co-treated with celecoxib and LHD4 (Fig. 3.1C).

After 17 weeks, the mice were sacrificed and their colon tissue was removed for subsequent examination of polyp size and distribution as shown in Figure 3.2A. In concurrence with the previously measured prolapse incidence, the polyp volume of each group showed a similar pattern (Fig. 3.2B). The incidence of polyp formation was 100 % in all groups, where mice were exposed to AOM and DSS. In addition, there was no significant difference in multiplicity among groups. In the positive control (Group 1), the average polyp volume of each mouse was around 154.5 ± 33.5 mm^3. However, the polyp volumes of the celecoxib- or LHD4-treated groups (Groups 2 and 3) were 47.0 ± 9.7 and 120.1 ± 45.2 mm^3, respectively, showing a reduction of 65.6 and 22.3% compared to Group 1, respectively. Moreover, following co-treatment with both celecoxib and LHD4, the polyp volume was around 22.8 ± 9.3 mm^3, which was 85.2% smaller than that of Group 1.Though there were no statistical differences in polyp volume in Groups 2 and 3, compared to Group 1, the polyp volume of Group 4 was significantly smaller than that of Group 1 (mean ± SEM,

$p<0.05$).

On the other hand, the average colon crypt height of Group 1 was around 2.82 ± 0.34 mm. However, it was decreased by treatment with either celecoxib or LHD4 to 1.86 ± 0.31 ($p<0.05$) and 2.11 ± 0.22 (*no statistical significance*) mm, respectively. Moreover, the colon crypt height of Group 4 was around 1.17 ± 0.24, which was 58.7% smaller than that of Group 1 ($p<0.01$) (Fig. 3.2C). As more than 80% of the polyps in all the groups were located in the distal part of the large intestine (data not shown), only the distal part of the colon was selected for subsequent pathohistological evaluations.

3.3.2. The malignant progression of polyps was significantly attenuated by the combined use of celecoxib and LHD4

The histopathological stage of proliferation in colon tissues was examined according to Gregory's classification method, which is recommended for the study of intestinal neoplasia in mouse models of colorectal carcinogenesis. Gross examination (x40 magnification) was conducted followed by microscopic examination (x200 magnification) for all tissues, and then classified into five stages, namely, normal, hyperplasia, low-grade adenoma, high-grade adenoma, and adenocarcinoma, based on the architecture and degree of cytologic atypia. The proliferative lesions such as hyperplasia, low- or high-grade adenoma, and adenocarcinoma based on the percentage of normal tissue were used as an indicator of the chemopreventive effect of each regimen. While the percentage of normal tissue was 40.6% in the positive

control (Group 1), those in the celecoxib-treated (Group 2) and LHD4-treated groups (Group 3) increased to 51.7 and 56.9%, respectively. Moreover, the celecoxib and LHD4 co-treatment group showed a two-fold increase in the normal tissue since 81.7% of the tissues had been classified as normal. Of the proliferative lesions, most were classified as high-grade adenoma in all groups. Interestingly, adenocarcinoma, which is a malignant neoplasm, was observed only in Groups 1 and 3, and the percentages of herniation, in which the glands penetrated through the muscularis mucosae, were 2.9 and 2.8%, respectively (Fig. 3.3A).

Figure 3.3B shows the histological changes according to each carcinogenesis stage. The cytological observation at high magnification (x200) shows more elongated and crowded neoplastic crypts when tissues diagnosed were in higher malignant stages of carcinogenesis. In addition, the degree of nuclear atypia and polarity became progressively more severe and herniation was evident with higher stage of malignancy.

The drug effect on both cell proliferation and apoptosis in colonic epithelium was evaluated by immunohistochemistry using anti-PCNA antibody and TUNEL assay. As shown in Figure 3.3C, the expression of PCNA of Group 1 was much higher than those of other groups, and evenly distributed throughout the whole colonic epithelium. However, in Groups 2 and 3, even though the abnormalities of colon tissues with considerable malignancy were still observed, the intensity of PCNA expression was significantly decreased. Above all, in Group 4, where the highest ratio of non-proliferative tissues was observed, the intensity of PCNA

expression was observed the least. On the other hand, there was no significant difference in the intensity of apoptotic cells that was examined by TUNEL assay among all groups.

3.3.3. The degree of inflammation and angiogenesis was correlated with carcinogenesis and was regulated by co-treatment with celecoxib and LHD4

All of the tissues were evaluated based on inflammation and were classified into five stages: normal, minimal, slight, moderate and marked. No marked stage of inflammation was observed in this study. The anti-inflammatory effect of drug regimen was determined by the ratio of normal tissues. While the percentage of normal tissue was 58.0% in the control group, the percentages in the celecoxib- and the LHD4-treated groups increased to 68.3 and 62.5%, respectively (Fig. 3.4A, B). Moreover, in the group receiving co-treatment of celecoxib and LHD4, 86.7% of the tissues were classified as normal tissue in terms of inflammation, which was a 49.5% increase compared to the control group. In addition, the expression of F4/80, which indicates the recruitment of inflammatory macrophages, was also affected by drug treatment as shown in Fig. 3.4C.

The degree of angiogenesis for each stage of carcinogenesis was determined through IHC for CD34, which is considered to be a marker of microvascular density of colorectal cancer according to malignant progression [71, 107]. The intensity of the CD34 expression of normal tissue was almost non-existent or very weak, as shown in Figure 3.5A. However, the expression was different in the proliferative

tissues (i.e., hyperplasia, low- and high- grade adenoma, and adenocarcinoma). In the case of hyperplasia, the highest intensity was seen at the stromal tissue and discontinuous and small-sized vessels were seen to have sporadically formed in the proliferative villus area. However, the continuity and size of the vessels were increased and correlated well with carcinogenesis. On the other hand, in the comparison of CD34 expression and distribution among groups, it was observed to be correlated with the degree of carcinogenesis (Fig. 3.5B, C). While the vascular structure of Group 1 was continuous and organized with the highest intensity, it was observed to be disorganized and weakly expressed in Groups 2 and 3. Moreover, the pattern of CD34 expression of Group 4 was almost similar to that of normal tissue. In the quantitative comparison of CD34 expression, only Groups 3 ($p < 0.05$) and Group 4 ($p < 0.01$) showed significantly decreased expression of CD34 compared to Group 1.

3.4. Discussion

Most studies of chemoprevention have largely focused on clarifying how historically well-accepted natural products show chemopreventive effects, which usually involve multifunctional and diverse mechanisms, including apoptotic, anti-proliferative, anti-inflammatory and anti-angiogenic effects [108]. Recently, however, the development and application of chemopreventive agents based on their scientifically clarified molecular mechanisms are emerging as a promising strategy in cancer chemoprevention [109]. Candidate drugs should be validated as a

chemopreventive agent in terms of efficacy, safety, and convenience of intake [110, 111]. In this context, we expect that our newly developed oral angiogenesis inhibitor named as LHD4 may meet these requirements.

Even though LMWH is widely used as an anticoagulant drug, it also acts as an anticancer agent through its inhibitory effects on angiogenesis and metastasis that are not related to its anticoagulant functions [64]. These effects involve various properties of LMWH, which include a binding affinity for angiogenic growth factors like VEGF and bFGF, and through interaction with metastatic adhesion molecules like sialyl-Lewis A and X [69]. However, when LMWH is used for cancer therapy, its anticoagulant effect must be carefully considered in order to avoid unexpected side-effects like bleeding, especially when it comes to a long-term application. On the other hand, LHD4, the newly developed oral angiogenesis inhibitor with no anticoagulant activity, shows no adverse effects like bleeding when it is used in cancer therapy and prevention. Moreover, in terms of the toxicity of the DOCA part of LHD4, it was also proven to be safe at the therapeutic dose, which indicates long-term safety [112]. In the present study, we administered a LHD4 from the initiation stage following the reference paper. In this paper, Gabriele Bergers et al. showed that the angiogenic therapy prevented the activation of angiogenic switch in the premalignant stage, which led to regression of cancer development [113].Thus, we treated mice with LHD4 from the AOM injection and for whole experimental period. On the other hand, we started the administration with celecoxib after DSS treatment according to the previous experimental procedure [114]. They evaluated a

chemopreventive effect of a traditional herbal medicine using the same animal model with our study, and proved that its chemopreventive effect came from the intervening tumor promotion by COX-2 inhibition. Thus, we decided to follow the same treatment schedule for celecoxib in our study. Consequently, LHD4 at the dose of 10 mg/kg was orally administered to mice for 17 weeks in Group 3 and 4. However, there was no significant toxicity observed in terms of overall clinical health conditions such as body weight and hair loss. Furthermore, the healthy conditions of mice in Group 4, which were treated with LHD4 and celecoxib at the same time for 14 weeks, were also well maintained. Considering all of these characteristics of LHD4, we expect that LHD4 would be a promising chemopreventive candidate that effectively blocks angiogenesis.

The AOM-DSS induced carcinogenesis animal model is commonly used not only in the pathological studies of colorectal cancer but also in the development of chemopreventive agents. It is because this animal model is characterized by mimicking histopathology of human colitis-related colorectal cancer with high incidence of neoplasm about 100% [105]. Thus, the chemopreventive effect can be evaluated with various indicators including multiplicity, size, and histological analysis of colonic neoplasms. In this study, at first, we chose to measure the height of colon crypt as an indicator for the evaluation of malignant progression. In addition, we also calculated the average polyp volume for each mouse by adding up all polyp volume to evaluate the chemopreventive effect of each regimen together with classification based on degree of carcinogenesis. The sum of polyp volume for each

mouse can be an indicator of tumor burden because it is derived from both tumor number and size. This can be explained with two different rationales. First, we observed that all mice both in control and treatment group were bearing neoplasm with no significant difference in number. In addition, the size of every neoplasm was not distributed evenly. In addition, since polyps grow in size with time, the multiplicity of polyp is not enough to indicate the degree of tumor development. In some cases, some large polyps are merged together, which make it impossible to count them separately. Second, even though two different neoplasms were observed with similar size, the degree of carcinogenesis did not always coincide in the pathohistological analysis. In other words, the progress in size did not always correspond to the degree of carcinogenesis in neoplasm. Thus, under this scheme, we found that, although the total volume of polyps in Group 2 was 60.9% smaller than that of Group 3, there was no significant difference in the histological degree of carcinogenesis. In addition, while Groups 2 and 4 showed no significant difference in polyp volume ($P > 0.05$), the percentage of normal tissue in Group 4 was 58% higher than that of Group 2. From these results, we conclude that while 10 mg/kg celecoxib can effectively prevent an increase in polyp volume, it cannot inhibit the initial formation and further progression to the malignant stage of these polyps. Similarly, 10 mg/kg LHD4 was not effective in inhibiting either the polyp formation or its further progression. Interestingly, however, when these two agents are administered together, we saw a much more significant cancer chemopreventive effect in terms of both polyp volume and degree of carcinogenesis in the colorectal tissues that were

exposed to the carcinogen and tumor promoter. In other words, the combined use of celecoxib and LHD4 could delay or inhibit carcinogenesis by blocking the transition of pre-malignant polyps to malignant tumors. Furthermore, in terms of colon crypt height and incidence of prolapse, the chemopreventive effect of combined use was more remarkable. On the other hand, in continuation with polyp volume and degree of carcinogenesis, the IHC for PCNA was also supportive of delayed carcinogenesis. However, while the intensity of PCNA was significantly decreased by drug treatment, there was no significant difference in intensity of apoptotic cells labeled by TUNEL assay among groups. These results indicate that both LHD4 and celecoxib inhibit or delay the progression of cancer development by slowing cell proliferation rather than by inducing cellular apoptosis.

These results are supported by recent reports showing that abnormal lesions with high risk of cancer, which are distinguishable from normal tissues, progressed to malignant lesions only under favorable conditions such as inflammation, angiogenesis, and the accumulation of mutations [90]. Other researches also point out that the angiogenic switch is already turned on in the pre-malignant stages like hyperplasia and dysplasia, and that it plays an important role in the transition of pre-malignant lesions to malignant tumors [34]. Thus, the earlier the angiogenesis inhibitor intervention is started, the higher the efficacy of the achieved cancer prevention will be. In addition, the secretion of angiogenic factors increases proportionally to the degree of carcinogenesis [10]. From this point of view, LHD4, which binds to multiple angiogenic factors, including VEGF, bFGF and PDGF,

would satisfy the requirement of a chemoprevention agent that targets angiogenesis.

Selective COX-2 inhibitors have been studied as chemopreventive agents in various types of cancer because the products of COX-2, such as PGs, are involved in essential processes of carcinogenesis, including cell proliferation, survival, invasion, and angiogenesis [115]. However, the long-term toxicity at high doses that is required for colorectal cancer prevention has remained an unsolved problem. To overcome this drawback, a variety of different regimens have been proposed, including short-term intermittent administration [116] and the combination of two or more agents at reduced doses [109]. In the present study, mice were orally administered celecoxib at the dose of 10 mg/kg, which is equal to 64 ppm of celecoxib mixed in diet [117]. This means that the amount of celecoxib used in the present study was comparatively lower than those used in previous cancer chemopreventive experiments [118, 119].

On the whole, the current combination regimen of celecoxib and LHD4 could improve the chemopreventive effects on colorectal cancer by inhibiting both the massive growth of polyps and their further progression from the pre-malignant to the malignant state. At the same time, in accordance with this attenuated carcinogenesis, we also observed that both inflammation and angiogenesis could be prevented or inhibited, reducing progression to more severe conditions. Taken together, these results surely prove that both inflammation and angiogenesis are the pivotal driving forces in cancer development from the very early stage, which makes these two processes the most attractive targets in cancer chemoprevention.

The present results strongly indicate its merits for clinical cancer prevention

but it should be noted that the present regimen could not fundamentally prevent the formation of polyps. Nevertheless, it significantly delayed the rate of progression to more severe malignant stages and the appearance of painful clinical symptoms such as prolapses, achieving phenotypic suppression by cancer delay, which defines clinical chemoprevention [32]. In this context, our results may provide a meaningful and successful clinical strategy for controlling the incidence of colorectal cancer.

3.5. Conclusions

In this study, we showed, using an AOM and DSS-induced colorectal carcinogenesis animal model, that the combination use of celecoxib, a selective COX-2 inhibitor, and LHD4, an angiogenesis inhibitor, could significantly enhance chemoprevention of colorectal cancer in terms of polyp formation and malignancy development. In addition, we also introduced a newly developed angiogenesis inhibitor, which can be absorbed via oral route, as a promising chemopreventive agent. This new regimen is a clinically rational strategy for overcoming the chemopreventive limitations of celecoxib treatment alone.

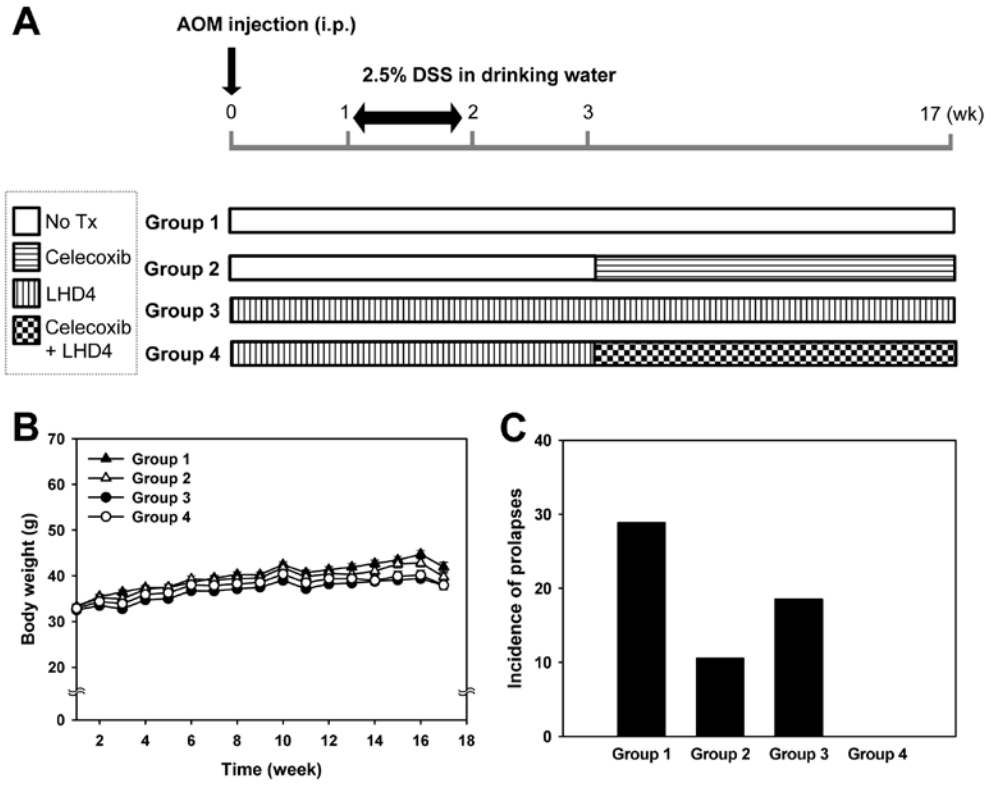

Figure 3.1 The experimental protocol and clinical observations. (A) Drug treatment schedule for LHD4 and celecoxib using AOM/DSS-induced colorectal carcinogenesis in ICR mice. Mice were treated with no drug (Group 1, n = 29), celecoxib alone (Group 2, n = 20), LHD4 alone (Group 3, n = 27), and the combination of celecoxib and LHD4 (Group 4, n = 20). LHD4 (10 mg/kg) and celecoxib (10 mg/kg) were orally administered once a day. (B) Body weight progression over the course of the study. No significant difference in body weight was observed among the various groups. (C) The incidence of prolapse during 17 weeks of experiment.

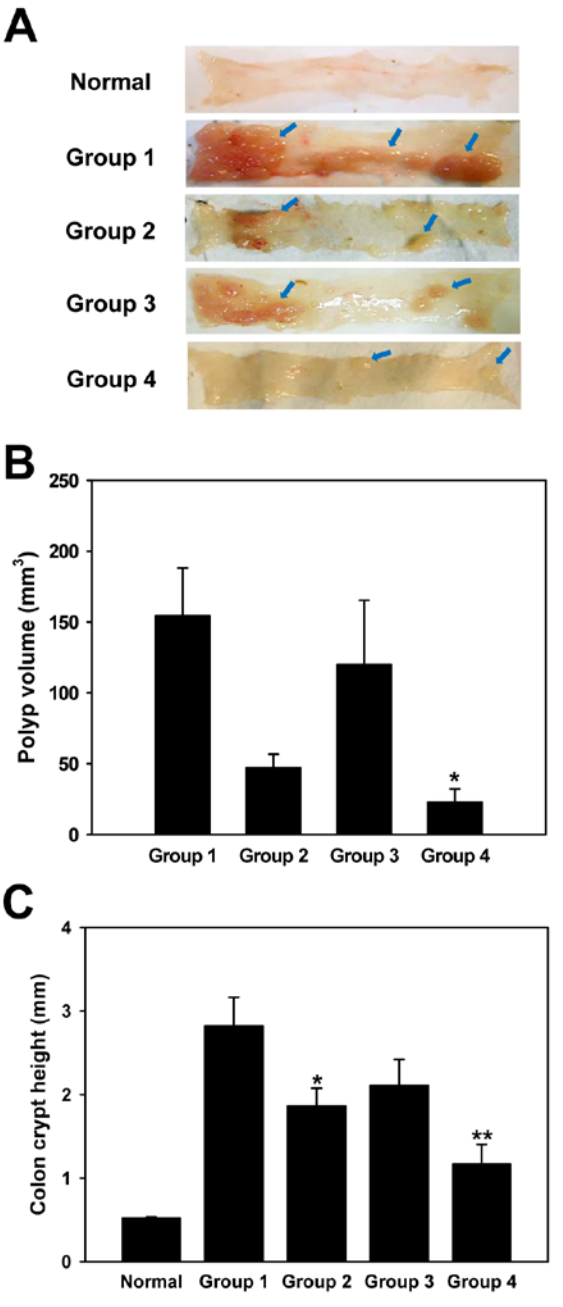

Figure 3.2 The comparison of chemoprevention effect in terms of polyp formation.

After 17 weeks of the experiment, mice were sacrificed and their colon tissues were

collected and photographed (A) and then polyp size was measured to calculate the polyp volume (B). Then, all the H&E stained colon tissues were examined to measure the crypt height by using microscope (C). Data represent mean ± SEM.

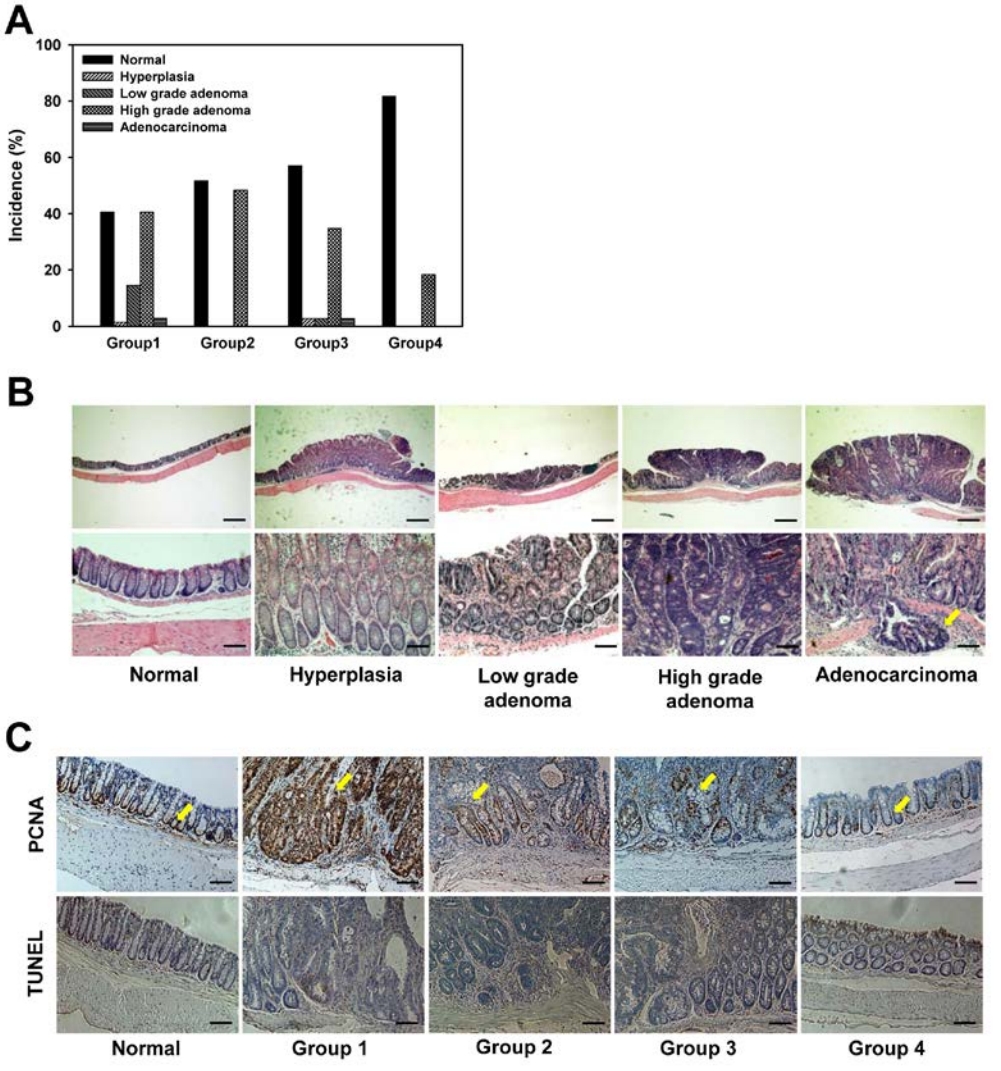

Figure 3.3 Pathohistological examination and classification into different stages according to the degree of carcinogenesis. (A) The H&E stained distal part of the colorectal tissues were classified into five stages: normal, hyperplasia, low-grade adenoma, high-grade adenoma, and adenocarcinoma. (B) Pathohistological changes indicative of carcinogenesis in the colorectal tissue, in terms of architecture (upper

panel; scale bar = 500 μm) and degree of cytologic atypia (lower panel; scale bar = 100 μm), were observed according to Gregory's classification method. (C) Intensity of proliferating cells and apoptotic cells labelled by immunohistochemistry for PCNA and TUNEL assay, respectively. Scale bar = 100 μm.

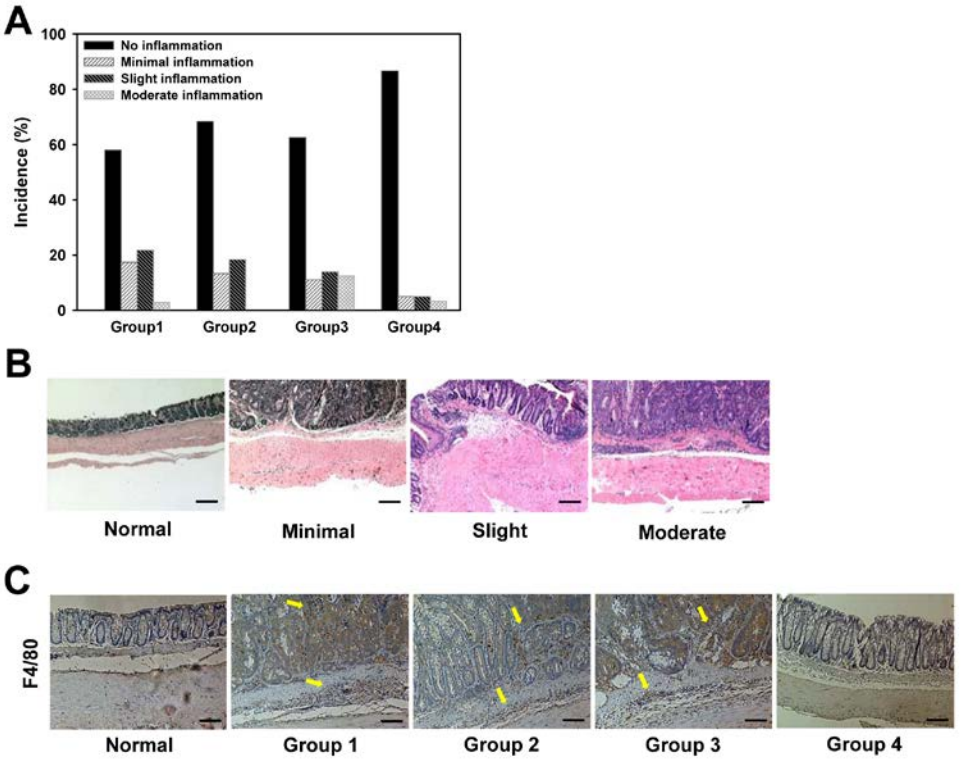

Figure 3.4 Degree of inflammation at the distal part of the large intestine. (A) All the H&E stained tissues were examined and then classified into four stages: normal, minimal, slight, and moderate inflammation. (B) Pathohistological differences in inflammation were observed in terms of infiltration of macrophages and the integrity of the mucosa, submucosa and muscularis mucosa layers of the large intestine (scale bar = 200 μm). (C) Intensity of F4/80-positive macrophages expression was compared among groups (scale bar = 100 μm).

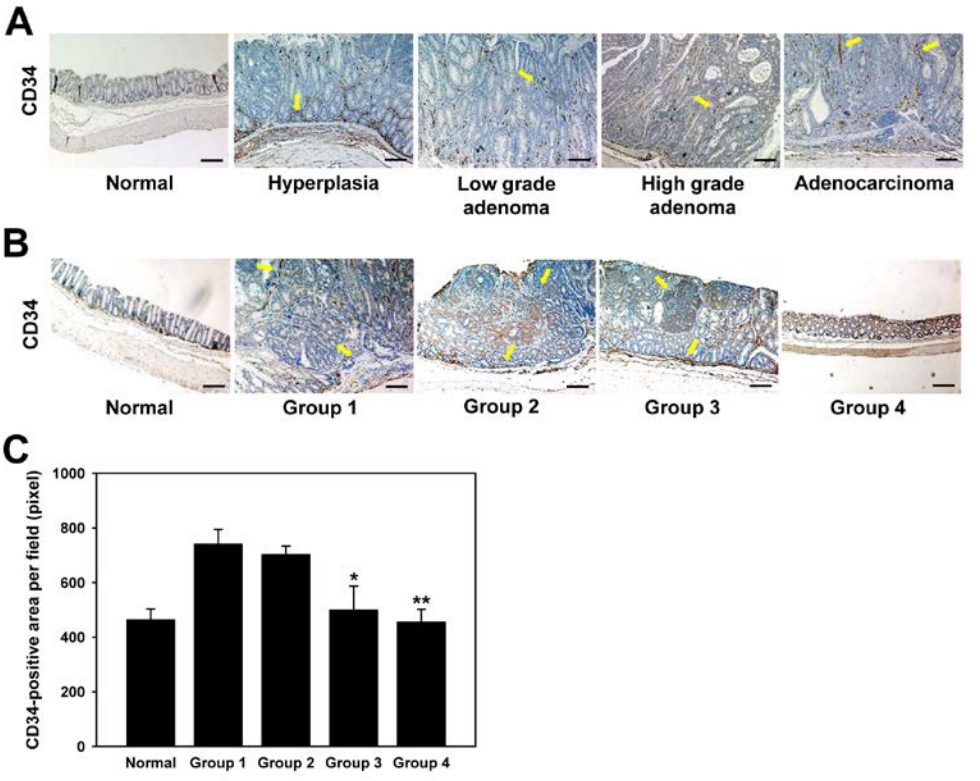

Figure 3.5 Degree of angiogenesis according to carcinogenesis. (A) Colon tissues of normal, hyperplasia, low- and high-grade adenoma and adenocarcinoma were also examined by using CD34 IHC as a biomarker of microvessel density (scale bar = 100 μm). (B) The intensity and distribution of CD34-positive cells were compared among groups (scale bar = 100 μm). (C) Then, the intensity of CD34 expression per field was quantitated by image analyzing software. *$p < 0.05$ *vs.* Group 1. **$p < 0.01$ *vs.* Group 1.

ChapterIV. COX-2 inhibition effect on tumor growth under anti-angiogenic therapy using heparin conjugates

4.1. Introduction

Since Folkman raised the involvement of angiogenesis in the tumor development for the first time [5], the role of angiogenesis in tumor pathogenesis has been actively studied up to now. As a result, a variety of angiogenesis inhibitors with different mechanisms have been developed and applied in the clinics together with other chemotherapeutics to treat cancer. However, it also has shown its limitations or shortcomings to achieve a sustainable and successful clinical outcome [15, 16]. For example, first, its therapeutic efficacy is not sufficient to be used as a single drug. Thus, it should be combined with other cytotoxic drugs to treat cancer properly. Second, not every type of cancer was susceptible to anti-angiogenic therapy. Moreover, some types of cancer were initially shrunk by anti-angiogenic therapy, but evolved to resistant one under chronic inhibition of angiogenesis by eliciting evasive pathways from anti-angiogenic drug in different ways [17, 18]. Even though diverse mechanisms how cancers become resistant to anti-angiogenic drugs are clarified, the clinical regimen how to overcome these obstacles has not developed yet.

It might be helpful to understand the close interactions between angiogenesis and inflammation in the tumor pathogenesis to overcome those limitations of anti-angiogenic drugs [104]. It is well-known that the inflammation and angiogenesis make a positive feedback cycle and closely cooperate on the further progression of cancer [120]. Inflammation is considered as a critical driving force for angiogenesis not only in the cancer but also in other diseases, since it can produce a variety of cytokines and growth factors that are involved in the angiogenesis [115, 121].

Especially, in case of cancer, the enormous role of inflammatory factors as positive regulators over the whole period of carcinogenesis is well-known. Among them, cyclooxygenase-2 (COX-2) and prostaglandins are known to be the most representative factors, and their expression can be used as an indicator for prognosis of cancer [122]. They not merely can induce the initial vessel formation, but they can also reinforce the vascular structure by assembling with vascular mural cells [123, 124]. In particular, in terms of evasive resistance to anti-angiogenic therapy, it was reported that these matured and stabilized vessels by mural cells do not respond to anti-angiogenic therapy since they pretend to function like a normal healthy vessel by restoring tumor perfusion [125]. Thus, if the maturation and stabilization of immature vessels are properly inhibited by pharmacological agent, the anti-angiogenic therapy might be continued for much longer period with higher efficacy.

Moreover, recently, it was reported that hypoxia at the tumor tissue was intensified by antiangiogenic therapy using sunitinib, which is a VEGFR/PDGFR kinase inhibitor, which led to a pro-inflammatory response to generate a favorable conditions for invasive and aggressive tumors [126, 127]. In addition, the expression of COX-2 was also correlated with the hypoxia induced by anti-angiogenic therapy [128]. On the other hands, the angiogenic growth factors produced by cancer cells and endothelial cells can also exacerbate COX-2 mediated inflammatory reaction at the tumor tissues. For example, vascular endothelial growth factor (VEGF) is one of stimulator to induce the expression of COX-2 and prostaglandins in the endothelial cells [129]. Thus, the blockade of VEGF-mediated pathway at the tumor tissues can

improve the therapeutic efficacy by intervening both inflammation and angiogenesis.

In this context, the combination use of angiogenesis inhibitors with anti-inflammatory drugs can be a strategy not only to improve the therapeutic efficacy, but also to prevent these adverse effects that might occur during anti-angiogenic therapy. Among a number of anti-inflammatory drugs, the selective COX-2 inhibitors might be the most promising agent to be utilized in cancer treatment due to its safety and efficacy. Actually, since COX-2 has multiple functions in the overall carcinogenesis, selective COX-2 inhibitors including celecoxib and nimesulide have been widely used not only in cancer therapy but also in cancer prevention as a single and combination therapies [130, 131]. A diversity of mechanisms how COX-2 inhibitors can give an additive or synergic effect on cancer therapy were clarified in many clinical experimental studies. Above all, the effect of COX-2 inhibitors on tumor vascular structures in different clinical conditions was also well reported in many studies [132].

In this study, we have observed the induction of hypoxia and COX-2 expression at tumor tissues under angiogenesis inhibition by using low molecular weight heparin (LMWH)-tauroholic acid conjugate as a multi-targeting angiogenesis inhibitor. Then, the effect of COX-2 inhibition by using a selective COX-2 inhibitor on inflammatory reactions, vascular structure and tumor growth was also evaluated in a tumor xenograft model.

4.2. Materials and Methods

4.2.1. Materials

LMWH (Fraxiparine®, 4500 Da) was obtained from Nanjing King-Friend Biochemical Pharmaceutical Company (Nanjing, China). Taurocholic acid (TCA), N,N'-dicyclohexylcarbodiimide (DCC), N-hydroxylsuccinimide (HoSu), 1-ethyl-3-(3-dimethylaminopropyl) carbodiimide (EDAC), formamide, methylcellulose, and Tween 20 were purchased from Sigma (St. Louis, MO). N, N-dimethylformide (DMF) was obtained from Merck (Darmstadt, Germany).

4.2.2. Synthesis of LHT7

LHT7 was synthesized according to the previous method [41]. Briefly, ethylenediamine taurocholic acid (5 g) was dissolved in methanol (150 ml) in the presence of sodium hydroxide (5 g) and agitated for 2 hr. The mixture was precipitated with cold acetonitrile, washed with cold acetonitrile and freeze-dried to obtain sodium ethylenediamine taurocholate (Et-STC). LMWH (500 mg) was dissolved in distilled water. Then, HOSu (126.6 mg), EDAC (310 mg) and Et-STC (686 mg) were added consecutively into this solution. After overnight reaction, LHT7 was finally obtained as white powder after precipitation and lyophilization.

4.2.3. Tube formation assay

The *in vitro* endothelial tube formation assay was performed as described in

previous studies [40]. Briefly, 100 μL Matrigel (growth factor-reduced and phenol red-free; BD Bioscience, Billerica, MA) was loaded into each well of a 96-well plate and polymerized for 30 minutes at 37°C. Then, 1.5×10^4 human umbilical vein endothelial cells (HUVECs), which were suspended in 100 μL Endothelial Basal Medium-2 (EBM-2) containing VEGF (50 ng/mL; Peprotech, NJ, USA), was added onto each well. To assess the inhibition effect on endothelial tube formation, the cells were treated with LHT7 (50 μg/ml), celecoxib (10 μg/ml), and the combination of those two drugs. After 6 hours of incubation in 5% CO_2 at 37°C, the number of branch points in each capillary-like tube in each well were counted at 40× magnification using a microscope (Eclipse TE2000-S; Nikon, Japan) and statistically analyzed (n = 3).

4.2.4. Tumor growth inhibition assay

Both the antiangiogenic effect on hypoxia induction and the combination effect on vascular formation and tumor growth were investigated in a tumor xenograft model using SCC7 murine squamous cancer cell line (American Type Culture Collection, Manassas, VA). Cells were cultured in RPMI 1640 medium (Sigma Aldrich, Saint Louis, MO) supplemented with 10% fetal bovine serum and 1% penicillin-streptomycin at 37°C under 5% CO_2. Seven-week-old male C3H/HeN mice (Orient Bio Inc., Seungnam, South Korea) subcutaneously injected with 1×10^6 SCC7 cells to the right flank. At the same time with cancer cell inoculation, mice were divided into two groups according to the experimental purpose, 1)

dose-dependent induction of hypoxia of LHT7 at doses of 0, 0.5, 1, and 5 mg/kg/2 days; 2) combination effect of LHT7 (1 mg/kg/2 days; intravenous injection) and celecoxib (10 mg/kg/day; oral administration). For oral administration, celecoxib was suspended in 0.5% of methylcellulose with 0.025% of Tween 20 as a stabilizer. The volume of 200 μl of suspended celecoxib was administered by oral gavage. When the tumor volume of control was approximately 50–80 mm^3, tumor size was measured in 2 dimensions using slide calipers every 3 days. Tumor volume was calculated as $a \times b^2 \times 0.5$, where a is the largest and b is the smallest diameter. The mice were housed in climate-controlled quarters (24ºC at 50% humidity) with a 12-h light:dark cycle. During the entire 25-day experiment, the body weight of the mouse was closely observed. All animal experiments were conducted according to the standard operating procedures of the Committee for Ethics in Animal Experimentation of Seoul National University. Animals were raised under the standard pathogen-free conditions of the Animal Center for Pharmaceutical Research of Seoul National University. The mice were fed with commercial rodent chow (Samyang Co., Seoul, Korea) and water ad libitum.

4.2.5. Hypoxic probe staining

After 25 days of drug treatment, all mice were sacrificed by cervical dislocation. To detect the degree of hypoxia on tumor tissues under antiangiogenic therapy, animals were injected intraperitoneally with Hypoxyprobe™-1 (pimonidazole hydrochloride; Hypoxyprobe Inc., Burlington, MA, USA).

Pimonidazole solution at a dose of 60 mg/kg body weight in saline was injected to mice 2 h prior to sacrifice. Then, the tumor tissues were isolated and fixed overnight in neutral 4% paraformaldehyde-phosphate-buffered saline (PBS). The fixed tumor tissue was embedded in paraffin, sectioned at 4 μm, and then mounted onto the slides. For the detection of hypoxic area that bound with pimonidazole through thiol groups, the slides were deparaffinized by incubation at 60ºC for 2 h, submerged in xylene for 5 min and rehydrated in a graded alcohol series (100, 90, 80, 70, and 60%). Then, antigen retrieval was carried out by heating the slides in a steamer for 1 h in 10 mM citrate buffer, pH 6.0, and then cooling to room temperature. After washing with PBS, the slides were pre-incubated in blocking solution (Power block®, BioGenex, Fremont, CA) for 30 min to reduce nonspecific binding. Then, the slides were incubated for 1 h at room temperature with FITC-conjugated mouse monoclonal antibody to pimonidazole adducts in a humidified chamber. The slides were counterstained with Hoechst (Life Science, OR, USA). The whole area of stained tissue was observed by tile scanning method using a confocal laser microscope (Carl Zeiss LSM710, Germany). For detection of COX-2 expression at hypoxic area, the slides were further incubated with anti-COX-2 antibody (Thermo Scientific, IL, USA; dilution ratio at1:200) followed by Alexa 594-conjugated anti-rabbit IgG secondary antibody (Life Science, OR, USA) and counterstaining with Hoechst.

4.2.6. Vessel staining with lectin perfusion

For microscopic imaging of functionalized vessels, 100 μg of FITC-lectin

was intravenously administered to SCC7-tumor bearing mice to visualize microvessels. Five minutes after lectin injection, tumor tissue was removed, embedded in OCT compound and snap-frozen in liquid nitrogen. Frozen tissue was sectioned in 5 μm-thickness, and then fixed with cold acetone for 10 min. After a proper drying and washing with PBS, the tissue slides were incubated with phycoerythrin (PE)-conjugated CD31 antibody (Life Science, OR, USA) overnight. After washing properly, slides were counter-stained by Hoechst for 5 min and then imaged by confocal laser scanning microscopy (Carl Zeiss LSM710, Germany).

4.2.7. Immunohistological evaluation

For histological analysis of tumor tissues, slides were processed in the same way with the aforementioned methods. Rehydrated slides were incubated with anti-F4/80 (AbCam, Cambridge, MA; dilution ratio at 1:200), anti-alpha smooth muscle actin (α-SMA) (AbCam; dilution ratio at 1:200), anti-collagen IV (AbCam; dilution ratio at 1:500), and anti-PCNA (Thermo Scientific, IL, USA; dilution ratio at1:1600) antibodies overnight at 4ºC in a humidified chamber. After washing with PBS, in case of immunofluorescence for F4/80, the tissue sections were incubated with an Alexa 594-conjugated anti-rabbit IgG secondary antibody. On the other hand, tissue slides were incubated with horseradish peroxidase (HRP)-conjugated goat anti-rabbit immunoglobulins (to collagen IV antibody) and goat anti-mouse immunoglobulins (to anti-SMA antibody) in Tris-HCl buffer (Envision^{+} System; Dako, Glostrup, Denmark) for 30 min at room temperature. The slides were washed

and the chromogen was developed for 5 min with liquid 3, 30-diaminbenzidine (Dako). The slides were counterstained with Mayer hematoxylin. On the other hand, antigen-retrieved tissue slides were also subjected to terminal deoxynucleotidyl transferase dUTP nick-end labeling (TUNEL) assays according to the according to the manufacturer's manual (Millipore Corporation, Billerica, MA).

4.2.8. Statistical analysis

All data are reported as mean ± standard error of the mean (SEM). Statistical analysis of data was performed with the use of one-way analysis of variance (ANOVA) followed by the Dunnett's multiple comparisons procedure, in which several treatment groups were compared with a control. Differences of $P < 0.05$ were considered significant.

4.3. Results

4.3.1. Induction of hypoxia and COX-2 expression under anti-angiogenic therapy

We evaluated the tumor growth inhibition effect of LHT7 in a dose-dependent manner (0, 0.5, 1, 5 mg/kg/day) in SCC7-bearing mice. After 25 days of treatment, mice were injected with pimonidazole before sacrifice to detect hypoxic area on tumor tissues. As shown in Fig. 4.1A, there was dose-dependent effect on tumor growth up to 1 mg/kg of LHT7, however, no further increase in therapeutic effect was observed between 1 and 5 mg/kg. On the other hand, the degree of

hypoxia was also increased in a dose-dependent manner. In case of the control, where mice were not treated with LHT7, even though the tumor volume was largest among four groups, the intensity of hypoxic area detected by FITC-conjugated pimonidazole was lowest (Fig. 4.1B).

The expression of COX-2 at the hypoxic area of the tumor tissues was observed by co-immunofluorescence. As shown in Fig. 4.2B, it was observed that the fluorescence image of FITC, which is conjugated to pimonidazole to detect hypoxic area, and Alexa594, which indicates the existence of COX-2, was well overlapped and correlated. This result showed that the expression of COX-2 was significantly increased at hypoxic area of tumor tissue that was exposed to antiangiogenic therapy.

4.3.2. Combination effect on macrophage recruitment on tumor tissue

The degree of inflammation at the tumor tissues was examined by quantifying the recruitment of macrophages through immunohistochemistry for F4/80. Compared to the control, the intensity of F4/80-positive cells was decreased in Group 2, where mice were treated with celecoxib, by 20% ($p > 0.05$, *vs.* control). However, it was observed that the recruitment of macrophage was increased by 66% at tumor tissues from LHT7-treated mice ($p < 0.05$, *vs.* control). Finally, the intensity of F4/80 in the co-treated with celecoxib and LHT7 group was observed to be similar with that of control and celecoxib-treated groups (Fig. 4.3A, B).

4.3.3. The combination effect of celecoxib and LHT7 on vessel formation in vitro and vivo

The drug effect on HUVEC activity was examined by *in vitro* tube formation assay. The drug effect was quantified by counting the number of tubular branches at every field. Even though tube formation in celecoxib- and LHT7-treated groups was inhibited by 35.6 and 39.6%, respectively ($p > 0.05$, *vs.* control), the inhibition effect was significantly enhanced by combination use of celecoxib and LHT7 (64.4%, $p < 0.05$, *vs.* control) (Fig. 4.4A, B).

The drug effect on vascular structure was also examined *in vivo* using tumor bearing mice. Tumor vessels were stained by perfusion using FITC-labelled lectin and then further labelled with PE-conjugated CD31 antibodies (Fig. 4.5A). While the functionality of vessels was well maintained in the control, it was almost disturbed either by single or combination therapy with celecoxib and LHT7 with no significant difference among drug-treated groups. On the other hand, the morphology of CD31-positive endothelial cells was observed a little bit different. Even though the number of endothelial cells was decreased either by celecoxib or LHT7, those of combination use were inhibited most significantly. In addition, while the CD31-positive endothelial cells in the control formed a regular structure, those of celecoxib-, LHT7-, and combination- treated groups were scattered and irregular.

To examine the combination effect of celecoxib and LHT7 on vascular stabilization in regard to defective assembly or recruitment of vascular mural cells, tumor tissues were also immune-stained for α-SMA and collagen type IV. As shown in Fig. 4.5B, in the control, both α-SMA- and collagen type IV-positive cells were

observed to be abundant and well-organized. However, those of celecoxib- and LHT7-treated groups were sparse and discontinuous. Moreover, the intensities of two markers were weak and scattered throughout tumor tissues in the combination group.

4.3.4. The effect of combination use of celecoxib and LHT7 on tumor growth

The drug effect on tumor growth was tested in SCC7 bearing-mice. As shown in Fig. 4.6A, there was no significant difference in tumor volume among celecoxib- and LHT7-groups on day 25. Compared to the control, the tumor volume was decreased by 69.5 and 70.0%, respectively. Moreover, the combination use did not further enhance the inhibitory effect on tumor growth compared to the single use of either celecoxib or LHT7 (77.5%; $p < 0.05$, *vs.* control, $p > 0.05$, *vs.* celecoxib- or LHT7-treated groups). Drug treatment with celecoxib, LHT7, or combination use did not affect body weight during experiment period (Fig. 4.6B).

In the immunohistochemistry of PCNA, while the cell proliferation was inhibited by celecoxib- or LHT7-treatement (35.8 and 40.8%, respectively), the highest inhibition effect was achieved by combination use (61.4%; $p < 0.01$, *vs.* LH7- or celecoxib-treated groups) (Fig. 4.6C, E). However, in the TUNEL assay, even though the number of apoptotic cells was significantly increased in all drug-treated groups, there was no further increase in combination group ($p > 0.05$, *vs.* celecoxib-treated group) (Fig. 4.6D, F).

4.4. Discussion

In present study, we observed the induction of hypoxia and COX-2 expression by anti-anangiogenic therapy using LHT7. In addition, COX-2 inhibition effect on antiangiogenic therapy in regard to tumor vascular structure and tumor volume were also studied. LHT7 was synthesized by conjugating a LMWH with taurocholic acid at molar ratio 1:7 [41]. Through this conjugation, while the anti-coagulant activity of LMWH became negligible, the binding affinity to various angiogenic growth factors was potentiated by introducing more sulfate moieties to the molecule [42]. Thus, LHT7 was proven to be a potent anti-angiogenic drug by neutralizing multiple targets including VEGF, bFGF, and PDGF. This might guarantee the superiority of LHT7 as an angiogenesis inhibitor compared to other drugs that target a specific single growth factor. Because even though tumors treated with VEGF-targeted anti-angiogenic drugs usually are able to shift from VEGF-dependence to other angiogenic pathways by producing alternative angiogenic growth factors including bFGF and PDGF. But LHT7 can also block those angiogenic growth factors at the same time.

Even though LHT7 is a multi-targeting angiogenesis inhibitor with a strong therapeutic efficacy, the tumor growth inhibition effect of LHT7 at dose of 5 mg/kg was not further increased than that of 1 mg/kg. This might contribute to the complexity of tumor pathogenesis that not only angiogenic factors but also other variety of factors are also involved in the cancer development. Moreover, while the tumor growth was inhibited by LHT7, the degree of hypoxia was dose-dependently

increased. In concurrence with exacerbated hypoxia by LHT7 treatment, the expression of COX-2 was also increased at hypoxic area of tumor tissue. Since angiogenesis is initiated for tumor tissues to overcome the harsh conditions induced by insufficient blood supply, the compulsory inhibition of angiogenesis can bring a rather conflicting effect on cancer therapy by intensifying the degree of hypoxia [133]. Thus, contrary to our expectations on anti-angiogenic drugs as a cancer therapeutic, it can worsen the pathological niches at tumor tissues and accelerate the tumor progression in COX-2 mediated pathways under hypoxia [16, 18, 134]. As a result, anti-angiogenic therapy can elicit evasive resistance mechanisms systemically or locally, thus finally shortened the progression-free or overall survival time of anti-angiogenic therapy.

In our study, the recruitment of F4/80-positive macrophages increased in LHT7-treated group compared to control. However, it was prevented by treatment with celecoxib. These phenomena might be explained either by hypoxia or COX-2 effect on macrophage activity at tumor tissues. Previously, it was reported that macrophages are recruited in the hypoxic area of tumor tissue [135]. In addition, it was also reported that the differentiation of monocytes into M2 type macrophages, which is also known as tumor associated macrophages, at tumor sites is mediated by locally expressed COX-2 [136, 137]. These M2 type macrophages can produce inflammatory cytokines and growth factors, which can facilitate the overall cancer progression [138]. Thus, if COX-2 is more activated at tumor tissues by anti-angiogenic therapy, it can worsen the tumor microenvironment through COX-2 mediated inflammatory reactions. This might provide a new rationale for the

combination use of a selective COX-2 inhibitor with anti-angiogenic drugs.

In this context, we decided to study the combination effect of a multi-targeting anti-angiogenic drug (LHT7) and a selective COX-2 inhibitor (celecoxib) on vessel formation and stabilization and finally on tumor growth. *In vitro* tubular formation assay, even though single use of celecoxib or LHT7 still inhibited the tube formation, the combination use of them further improved the inhibition effect. On the other hand, while the study on functional vessel formation by lectin perfusion showed no significant difference among drug-treated groups, the morphology of CD31-positive endothelial cells at tumor vascular structure was affected by each drug regimen in a different way. The number of endothelial cells was more significantly decreased by combination use than that of single drug treatment. Moreover, the immunohistochemistry of α-SMA and collagen IV also shows that the combination use further improved the inhibitory effect on vascular mural cell recruitment to tumor sites than single drug treatment. It is well known that new vessels are formed through a serial cascade including proliferation and recruitment of endothelial cells, tube formation and elongation by assembling endothelial cells, and finally maturation and stabilization by vascular mural cells [2, 139]. Thus, our results show that the combination use of LHT7 and celecoxib can inhibit tumor angiogenesis by intervening angiogenic process at multiple points. While LHT7 can disturb the extracellular action of angiogenic growth factors by capturing them, celecoxib can inhibit the intracellular activity of COX-2. On the whole, the combination use of LHT7 and celecoxib can inhibit the formation of finally functionalized vessels at tumor site.

However, the combination use did not further enhance the tumor growth in regard to volume. In addition, our drug regimen showed its therapeutic effect by retarding the tumor growth rather than shrinking or diminishing the tumor tissues. It was also supported by the histological analysis which showed that while cell proliferation was significantly inhibited by drug treatment with celecoxib and LHT7, the number of apoptotic cells was not significantly enhanced by combination therapy. This is because neither LHT7 nor celecoxib directly target cancer cells to eradicate, rather they intervene with tumor microenvironment to generate unfavorable conditions for cancer progression [34, 123]. Even though the combination use for primary tumor growth inhibition did not show a remarkable effect, this regimen could be applied as an adjuvant therapy to improve the efficacy of cancer chemotherapy using other cytotoxic drugs. Moreover, it can be utilized for caner chemoprevention by slowing down overall carcinogenesis and extending the latency with progression-free period.

4.5. Conclusions

Taken all, the new anti-angiogenic regimen combined with a selective COX-2 inhibitor could be applied in the clinics to prevent the evasive resistance to cancer treatment that comes from the chronic anti-angiogenic therapy. Thus, we expect that this new regimen improve the overall clinical therapeutic efficacy by prolonging the progression-free period and overall survival rate of cancer patients.

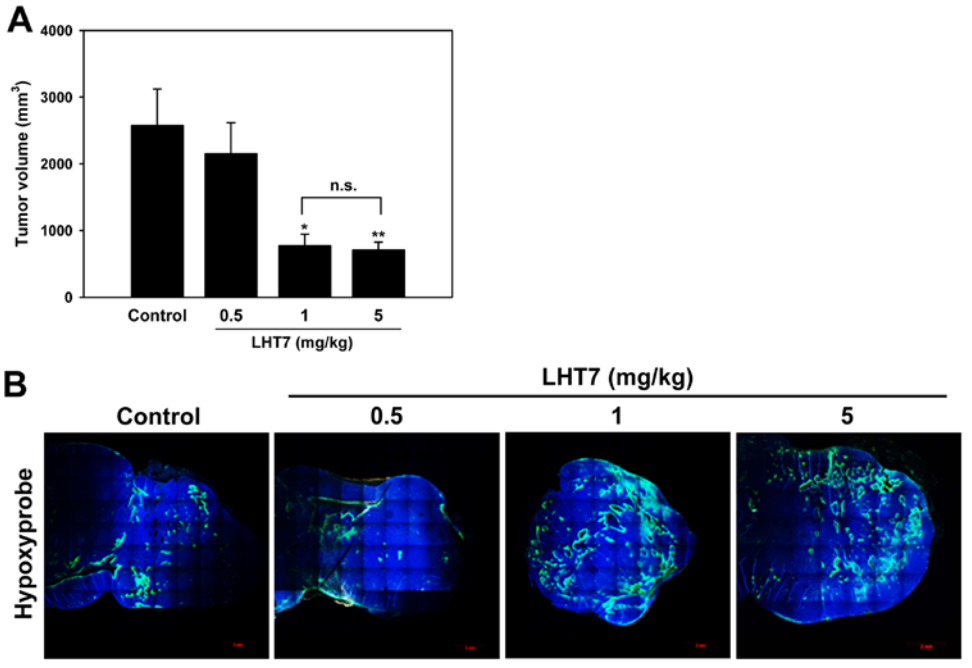

Figure 4.1 Dose-dependent effect of LHT7 on tumor growth inhibition. (A) SCC7-bearing mice were treated with LHT7 at 0, 0.5, 1, and 5 mg/kg/2 day, and their tumor volume on day 25 were compared. (B) Mice were intraperitoneally injected with Hypoxyprobe™-1 to detect hypoxic area at tumor tissues. *$p < 0.05$ and **$p < 0.01$, *vs.* control.

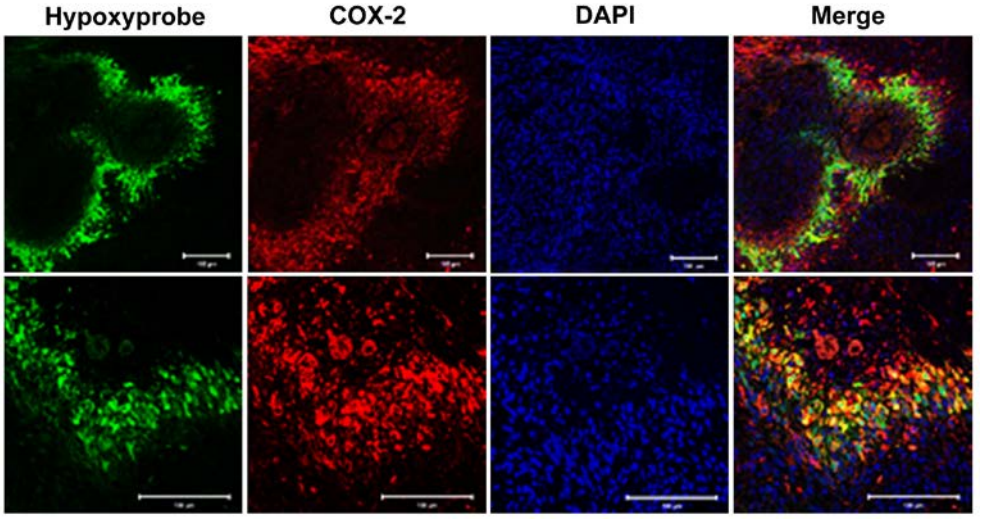

Figure 4.2 COX-2 expression under hypoxia at tumor tissues. Tumor tissues were collected from SCC7-bearing mice after Hypoxyprobe™-1 injection and were further stained with anti-COX-2 antibodies. The relationship between hypoxia and COX-2 expression was observed under confocal laser scanning microscope (scale bar = 200 μm).

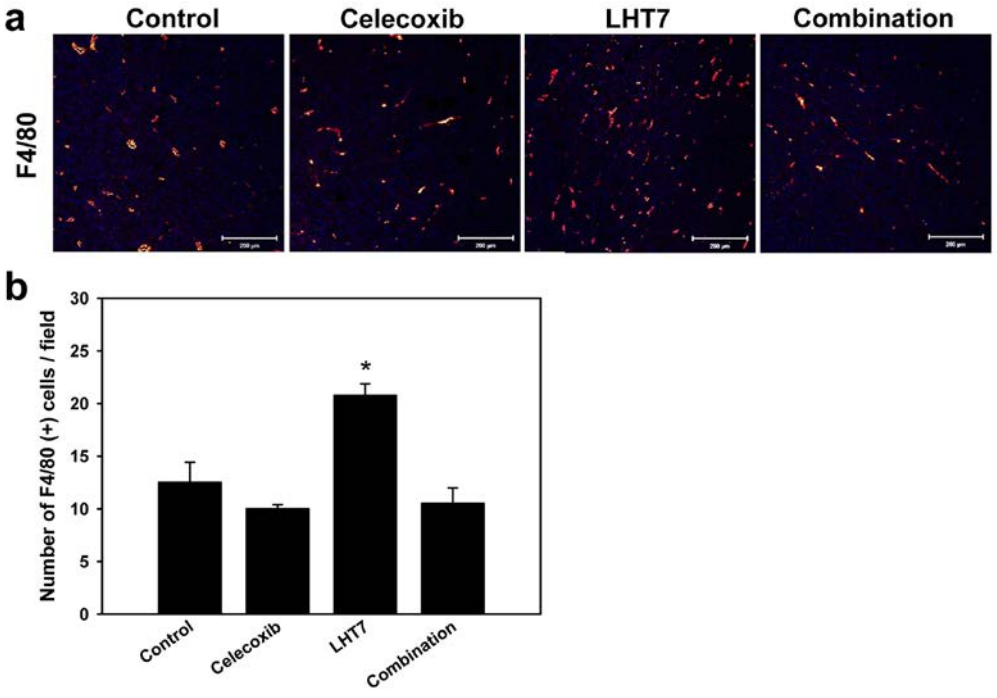

Figure 4.3 The recruitment of macrophages under drug treatment with celecoxib, LHT7 and combination use of celecoxib and LHT7. (A) The drug effect on the recruitment of F4/80-positive macrophages was studied and (B) the intensity was quantitatively compared (scale bar = 200 μm). *$p < 0.05$, *vs.* control.

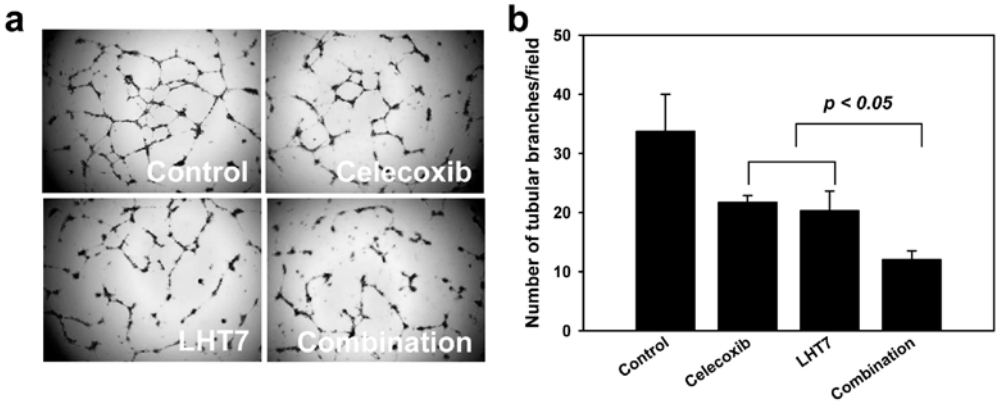

Figure 4.4 The effect of celecoxib and LHT7 on *in vitro* tube formation using HUVECs. (A) The inhibition effect of celecoxib, LHT7, and combination of celecoxib and LHT7 on *in vitro* tubular formation was observed and photographed. (B) Then, the number of branch point per field was counted.

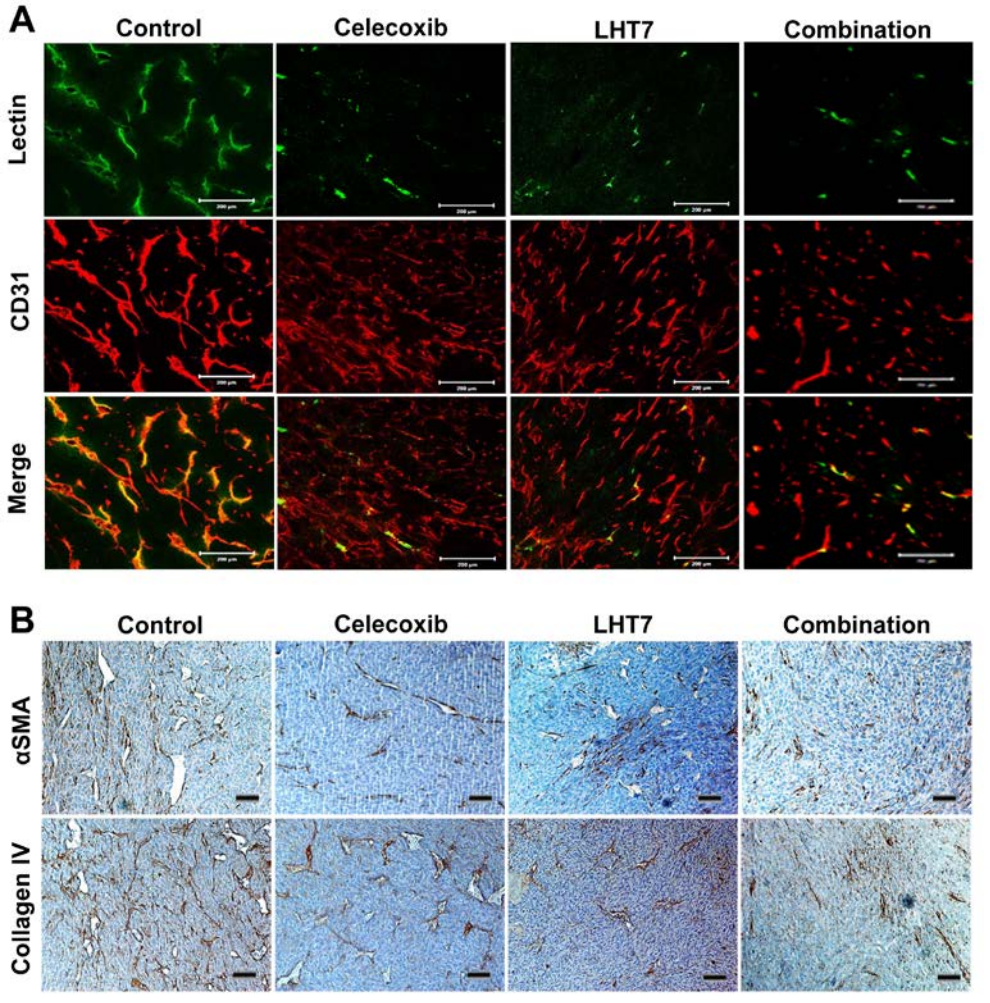

Figure 4.5 The effect of celecoxib and LHT7 on *in vivo* vessel formation and structures. (A) The inhibition effect of celecoxib, LHT7, and combination of celecoxib and LHT7 on vessel formation and structure was studied using SCC7-bearing mice. Tumor vascular structures were imaged by FITC-labelled lectin-perfusion followed by immunofluorescence using PE-conjugated CD31. (B)

The recruitment of mural cells to vascular structure was observed in terms of α-SMA and collagen IV (scale bar = 200 μm).

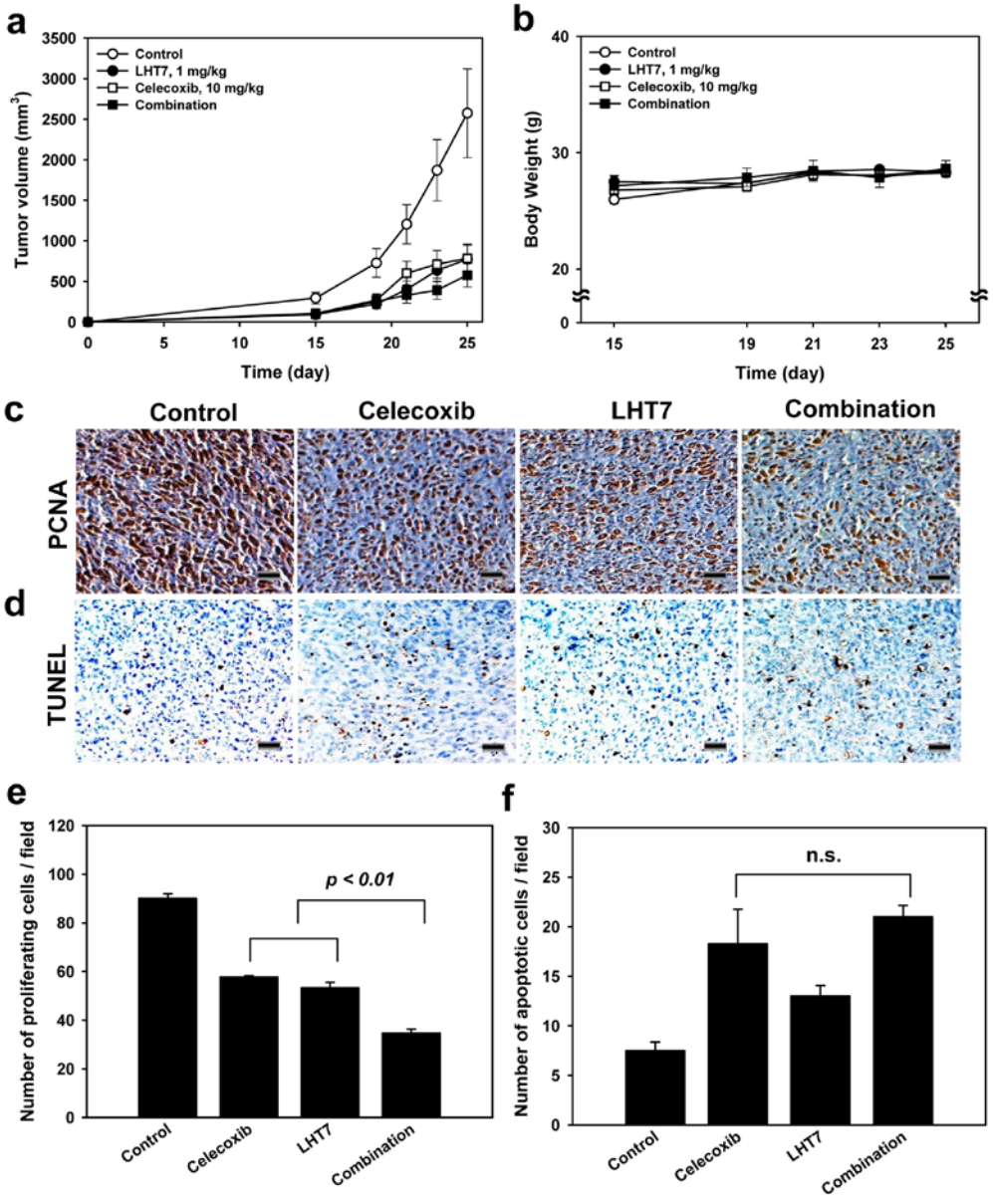

Figure 4.6 The combination effect of celecoxib and LHT7 on tumor growth inhibition. SCC-7 bearing mice were treated with either celecoxib (10 mg/kg/day), or LHT7 (1 mg/kg/2 days), or combination of celecoxib and LHT7. (A) Tumor volume

and (B) body weight change over the time were observed. The tumor tissues were isolated and examined by immunohistochemistry for PCNA (C, E) and TUNEL assay (D, F) (scale bar = 100 μm).

Chapter V. Tumor vasculature targeting following co-delivery of heparin-taurocholate conjugate and suberoylanilide hydroxamic acid using cationic nanolipoplex

5.1. Introduction

Heparin, widely used as an anticoagulant drug, has been studied as an anticancer drug [140] for its inhibition effect on cancer cell proliferation, adhesion, angiogenesis, migration and invasion [38]. However, heparin anticoagulant activity causes adverse effects such as bleeding, which limits its expanded applications. In the previous study, Lee *et al.* reported a low molecular weight heparin (LMWH)-derived angiogenesis inhibitor with a low anticoagulant activity but with high antiangiogenic efficacy [41]. Moreover, the newly developed angiogenesis inhibitor, namely LMWH-taurocholate conjugate (LHT7), would be a promising agent owing to its wide range of inhibition effects on several angiogenic factors such as vascular endothelial growth factor, basic fibroblast growth factor, and platelet-derived endothelial cell growth factor [41]. Considering that the kinds of angiogenic factors that are released from the tumor tend to increase as tumor progresses, multi-targeting antiangiogenic drugs such as LHT7 would be preferred to inhibit tumoral angiogenesis [9, 10].

To increase the biodistribution of antiangiogenic drugs to tumor vasculature, various approaches have been tried to enhance targeting efficiency of anticancer drugs to tumor vasculature using nanoparticles such as nanospheres [141] and liposomes [61]. It has been well-recognized that the nanoparticulate drugs can be distributed more effectively to tumor vasculatures due to the enhanced permeability and retention (EPR) effect, which explains the leaky vascular nature of actively angiogenic tumor tissues [53]. Among various nanoparticles, cationic liposomes have

been reported to provide tumor vasculature targeting property, probably due to the increased exposure of anionic phospholipids on the surfaces of tumor blood vessels [56, 57]. Once arrived at the tumor vascular region, the prolonged retention in tumor vasculature as nanoparticular forms might be beneficial. There exists a strong rationale to deliver angiogenesis inhibitor using nanoparticles as nanoparticular angiogenesis inhibitors can reduce new blood vessels formation following EPR effect-based tumor vasculature targeting [142].

In addition to the tumor vasculature targeting using nanoparticles, the combination therapy of angiogenesis inhibitors with other drugs would be one of the approaches to enhance the anticancer effects. Histone deacetylase inhibitors are one of new class anticancer drugs affecting cell cycles, apoptosis, and protein expressions [143]. Although histone deacetylase inhibitor monotherapy has been demonstrated to be effective in cancer therapy, most clinical trials have used combinations of histone deacetylase inhibitors with various anticancer chemotherapeutics simultaneously or sequentially [144]. Recently, combined treatment of a histone deacetylase inhibitor with an angiogenesis inhibitor was shown to increase the anticancer activity in rat hepatoma [145]. However, most combination studies have used histone deacetylase inhibitors with other drugs without using nanoparticles.

In this study, we hypothesized that the targeting delivery of LHT7 to tumor vasculature using cationic nanoliposomes may enhance the anti-angiogenic activity of LHT7, and that the co-delivery of LHT7 with histone deacetylase inhibitor using the multifunctional cationic nanolipoplex may further increase the therapeutic

anticancer activity of anti-angiogenic drugs after tumor vasculature targeting. To evaluate this hypothesis, we formulated a multifunctional nanolipoplex carrying LHT7 together with a histone deacetylase inhibitor, suberoylanilide hydroxamic acid (SAHA). We utilized the negative charge of LHT7 and slightly soluble property of SAHA to complex LHT7 on the surface of cationic nanoliposomes and to entrap SAHA inside. After the co-delivery of LHT7 and SAHA in nanolipoplexes, the antiangiogenic effect, *in vivo* anticancer activity, and biodistribution of the compounds were evaluated.

5.2. Materials and Methods

5.2.1. Materials

LMWH (Fraxiparin®; average MW 4.5 kDa) was obtained from Nanjing King-Friend Biochemical Pharmaceutical Company Ltd. (Nanjing, China). Taurocholic acid sodium salt (TCA), *N*-hydroxysuccinimide (HOSu), *N*-ethyl-*N´*-(3-dimethylaminopropyl) carbodiimide hydrochloride (EDAC), dimethyl sulfoxide (DMSO), fluorescein isothiocyanate (FITC) and cholesterol were purchased from Sigma-Aldrich Chemical Co. (St. Louis, MO). Dioleyl-*sn*-glycero-3-phosphoethanolamine, 1, 2-distearoyl-sn-glycero-3-phosphoethanolamine-*N*-[methoxy(polyethylene glycol)-2000] (PEG-DSPE) were purchased from Avanti Polar Lipids (Birmingham, AL). SAHA was from Cayman Chemical Co. (Ann Arbor, MI). Cy5.5-NHS was from

Lumiprobe (Hallandale beach, FL). All reagents were analytical grade and were used without further purification.

5.2.2. Synthesis of LHT7, FITC-LHT7, and Cy5.5-LHT7

LHT7 was synthesized according to the previous method [41]. Briefly, ethylenediamine taurocholic acid (5 g) was dissolved in methanol (150 ml) in the presence of sodium hydroxide (5 g). After stirring for 2 hr, the solution was precipitated with cold acetonitrile. This precipitate, sodium ethylenediamine taurocholate (Et-STC), was washed with cold acetonitrile and freeze-dried. LMWH (500 mg) was dissolved in distilled water in the presence of HOSu (126.6 mg). Then, EDAC (310 mg) and Et-STC (686 mg) were added consecutively into this solution. After overnight reaction, the solution was precipitated, washed with cold methanol, and freeze-dried. Finally, the final product, LHT7, was obtained as white powder.

For the synthesis of FITC-labeled LHT7 used in nanolipoplex characterization, first, LHT7 (200 mg) was dissolved in borate buffer at pH 9. Then, this solution was mixed with 20 mg of FITC dissolved in anhydrous DMSO and reacted for 5 hr. The compound was washed with cold methanol twice, and dissolved in distilled water. The solution was purified by dialysis using membrane with molecular cutoff size 2000 Da, and freeze-dried to get the final product, FITC-LHT7. To synthesize Cy5.5-labeled LHT7 used for *in vivo* molecular imaging, LHT7 was oxidized by KIO_4 (3.6 μmol) for 3 hr to introduce an aldehyde group, followed by adding ethyldiamine (21.6 μmol) in the presence of $NaCNBH_3$ (18 μmol). The

mixture was reacted for 2 hr at 40°C and pH 9. This solution was precipitated and washed with cold methanol, followed by dialyzing. The obtained LHT7-NH_2 powder (3.1 μmol) was dissolved in 0.1 M borate buffer (pH 9), and conjugated with Cy5.5-NHS (3.72 μmol) that was dissolved in DMSO through overnight reaction. Finally, the product was purified by precipitation in cold acetone and by phase separation using ethyl acetate. After freeze-drying, the final product, Cy5.5-LHT7, was obtained.

5.2.3. Preparation of LHT7/SAHA nanolipoplex

A nanolipoplex carrying LHT7 and SAHA (LHT7/SAHA nanolipolplex) was prepared by first entrapping SAHA inside cationic nanoliposomes, followed by complexing negatively charged LHT7 onto the surface of SAHA-loaded cationic nanoliposomes (SAHA-L). LHT7 was complexed to the surfaces of cationic SAHA-L by charge-charge interaction (Fig. 5.1). To entrap SAHA inside cationic liposomes, cationic *N', N"*-dioleylglutamide, dioleyl-*sn*-glycero-3-phosphoethanolamine, cholesterol, SAHA, and PEG-DSPE were mixed at a molar ratio of 3:1:1:1:0.06. All lipids and SAHA were dissolved in chloroform and methanol, respectively. After removal of the organic solvents, the resulting thin lipid film was hydrated in 21 mM HEPES-buffered saline (pH 7.4), and extruded three times through 0.2 μm polycarbonate membrane filters using an extruder (Northern Lipids, British Columbia, Canada). Next, anionic LHT7 was

complexed onto SAHA-L at weight ratio of 1:65, and incubated for 10 min at room temperature.

After preparation of LHT7/SAHA nanolipoplex, it was physicochemically characterized with loading efficacy by gel retardation assay using 1% agarose containing 0.5 mg/ml ethidium bromide [Gel Doc System (Bio-Rad Lab., Hercules, CA)], size and zeta potential [ELS-8000 dynamic light scattering instrument (Photal, Osaka, Japan)], and *in vitro* stabilities both in buffer condition (HEPES-buffered saline, 4°C) and in serum condition (50% fetal bovine serum, 37°C) . Furthermore, the biodistributions of LHT7 alone and in LHT7/SAHA nanolipoplex were visualized by molecular imaging, respectively, in a SCC7-bearing mouse [eXplore Optix System (Advanced Research Technologies Inc., Montreal, QC, Canada)]. Then, this LHT7/SAHA nanolipoplex was applied into following *in vivo* studies.

5.2.4. Pharmacokinetic study

The pharmacokinetic profiles of LHT7 alone and in LHT7/SAHA nanolipoplex were determined in rats, respectively. Sprague–Dawley rats (male, 7-weeks of age, 230-250 g) were purchased from Orient Bio. Lab. Animal Inc. (Seungnam, South Korea). Animals were raised under standard pathogen-free conditions of Animal Center for Pharmaceutical Research in Seoul National University. The rats were fed with commercial rodent chow (Samyang Co., Seoul, Korea) and water ad libitum. All animal experiments were conducted according to

standard operating procedures of the Committee for Ethics in Animal Experimentation of Seoul National University.

The SD rats were intravenously administered with LHT7 alone and in LHT7/SAHA nanolipoplex with the dose of 1 and 5 mg/kg for LHT7 and SAHA, respectively. The blood samples (360 μl) were collected into a microcentrifuge tube containing 13 mM sodium citrate (40 μl) at 5, 15, 30 min, 1, 2, 4, 8, 12 hr after dosing, and centrifuged at 2500 xg at 4°C for 15 min. Then, the plasma samples were treated with 0.5% Triton X-100 to solubilize LHT7 from the nanolipoplex. Then, the concentration of LHT7 in the plasma was analyzed by heparin orange assay method [146]. Finally, the non-compartmental pharmacokinetic parameters were calculated with the software program WinNonlin™ (Scientific Consulting Inc., Lexington, KY). The mean residence time (MRT) was calculated by the non-compartmental method dividing the area under the momentum curve (AUMC) with the area under the curve (AUC).

5.2.5. Inhibition effect of LHT7/SAHA nanolipoplex on tumor growth

The anticancer activity of LHT7/SAHA nanolipolplex was studied in xenografted mice. SCC7 (murine squamous cell carcinoma) cells (American Type Culture Collection, Rockville, MD) were cultured in RPMI 1640 medium (Sigma Aldrich, St. Louis, MO) supplemented with 10% fetal bovine serum and 1% penicillin-streptomycin. The cells were cultured at 37°C with 5% CO_2. C3H/HeN

mice (7 week old, male, Orient Bio, Inc., Seungnam, South Korea) were subcutaneously injected to the left flank with 1×10^6 SCC7 cells.

On day 7, when each tumor volume became palpable and reached at the size of about 50–70 mm^3, mice were randomly allocated to five groups for each formulation. Mice were divided into four groups which were each given free LHT7, SAHA-L, and free LHT7 and SAHA-L in sequential order, and LHT7/SAHA nanolipoplex, respectively. For the sequential co-administration group, the mice were injected with LHT7 followed with SAHA-L in 30 min interval. The control group was treated with phosphate-buffered saline (PBS, pH 7.4). The drug dosages for all groups were fixed at 1 mg/kg for LHT7 and 5 mg/kg for SAHA. Tumor size were measured in two dimensions using a slide caliper every two days, and the tumor volume as *a*x*b*x0.5, where *a* is the largest and *b* is the smallest diameters. The mice were treated with drugs for two weeks and sacrificed by over-inhalation of carbon dioxide.

The tumor tissues were collected and evaluated by immune-staining using anti-CD34 antibody and anti-proliferating cell nuclear antigen (PCNA) antibody to indicate blood vessel formation and proliferating cells, respectively. The number of microvessels and proliferating cells were counted by using microscope (Eclipse TE2000-S, Nikon, Japan).

5.2.6. Statistical analysis

All the data were expressed as mean ± SEM. Data were statistically analyzed by the ANOVA. Student-Newman-Keuls was used as a post-hoc method when appropriate. A p value of less than 0.05 was considered to be statistically significant.

5.3. Results

5.3.1. Pharmacokinetic parameters of LHT7

The administration of LHT7 in nanolipoplex significantly affected the pharmacokinetic parameters in rats. When the rats were administered with free LHT7 at dose of 1 mg/kg, LHT7 was not detected in the plasma at 4 hr post-administration. However, after administration of the same dose of LHT7 in nanolipoplex, LHT7 was still detected in blood at 12 hr post-dose (Fig. 5.2). One notable change in pharmacokinetic parameters is a half-life and a MRT of LHT7 after intravenous administration of LHT7/SAHA nanolipoplex (Table 5.1). The half-life of LHT7 was 2.38 ± 1.76 hr for the free form of LHT7 and 4.37 ± 1.71 hr for the LHT7/SAHA nanolipoplex. Moreover, the MRT of LHT7 increased 1.9-fold after the administration using the nanolipoplex formulation, compared to after using the free form.

5.3.2. Inhibition effect of LHT7/SAHA nanolipoplex on tumor growth in SCC7-bearing mice

The therapeutic effect of LHT7 given in different formulations was studied in SCC7-bearing mice. As shown in Fig. 5.3A and B, the highest anticancer efficacy was observed in the LHT7/SAHA nanolipoplex-treated group, where the tumor mass was decreased 60.6% compared to the control. There was a significant difference in the tumor volume on day 21 between the groups treated with LHT7 alone and LHT7/SAHA nanolipoplex (p value < 0.01). However, the therapeutic efficacy of the sequential co-administration group, where the mice were injected with LHT7 and SAHA-L consecutively with the time interval of 30 min, was not significantly different from that of the LHT7-treated group.

Both degree of angiogenesis and cell proliferation at the tumor tissue were evaluated by immnunohistochemistry using anti-CD34 and anti-PCNA antibodies as shown in Fig. 5.4. The number of CD-34 positive blood vessels and PCNA-positive proliferating cells per field were counted by using a microscope, respectively. The number of CD34-positive blood vessels was significantly lowered both in LHT7-treated ($p < 0.05$, vs control) group and LHT7/SAHA nanolipoplex-treated group ($p < 0.01$, vs control). However, the statistical significance was much lower in the LHT7/SAHA nanolipoplex-treated group than LHT7-treated group (Fig. 5.4A, C). In addition, the number of PCNA-positive proliferation cells was significantly lower in the LHT7/SAHA nanolipoplex-treated group compared to the control ($p < 0.01$, vs control) (Fig. 5.4B, D).

5.4. Discussion

In this study, we demonstrated that the delivery of LHT7 in the nanolipoplex formulation could prolong the retention of LHT7 as well as enhance its accumulation in the tumor site. Moreover, co-delivery of LHT7 and a histone deacetylase inhibitor, SAHA, in the nanolipoplex formulation could significantly improve the anticancer effect of LHT7.

In the previous study on physicochemical properties of LHT7/SAHA nanolipoplex, it demonstrated surface charge of 29.1 ± 1.1 mV and particle size of 117.6 ± 2.2 nm. In addition, in the in vitro stability test, LHT7/SAHA nanolipoplex maintained its size for at least 30 days of storage at 4°C in PBS. Moreover, the contents of LHT7 in LHT7/SAHA nanolipoplex did not change upon incubation at 37°C in serum for 24 hr. From these result, it was proven that LHT7/SAHA nanolipoplex satisfies the requirements as a nanoparticle. Moreover, the complexation of LHT7 to SAHA-L affected its biodistribution kinetics and extents to the tumor vasculature. When LHT7 was intravenously administered as a free form, LHT7 was detected in the tumor site starting from 4 hr after its administration. The distribution of free LHT7 to the tumor site peaked at 24 hr after administration, and disappeared at 72 hr. In contrast, LHT7 given in the nanolipoplex formulation was detected at the tumor site starting from 1 hr after its administration. The accumulation of LHT7 at the tumor site was the highest at 24 hr after its administration and it was still detected at 72 hr.

For the formation of nanolipoplex with anionic LHT7, we used *N'*, *N"*-dioleylglutamide as a cationic lipid in liposome compostion. *N'*, *N"*-dioleylglutamide was chosen as a cationic component for its low cytotoxicity and capability to provide effective complexation to negatively charged biomolecule, siRNA [147, 148]. Recently, we reported that *N'*, *N"*-dioleylglutamide-based cationic liposomes provided effective delivery of complexed siRNA in various tumor cells [147]. Based on their recently observed advantages, *N'*, *N"*-dioleylglutamide-based cationic liposome was formulated to entrap SAHA inside liposomes, and to load negatively charged LHT7 via electrostatic interaction.

In the pharmacokinetic study of LHT7 in SD rats, we observed that *in vivo* fate of LHT7 was altered by its administration in nanolipoplex. Considering that half-life and MRT of nanoliposomal LHT7 were longer than those of free LHT7 by 1.83 times and 1.92 times, respectively, we concluded that LHT7 was released from the nanolipoplex in a sustained manner. Therefore, the plasma concentration of LHT7 remained in the therapeutic range for a prolonged period, which led to its improved therapeutic effect. In this study, we imposed steric hindrance on the surface of liposome by adding polyethylene glycol to prolong the circulation time [59, 149]. The surface modification of nanolipoplex surfaces using polyethylene glycol is known to inhibit the rapid recognition by reticuloendothelial system and clearance from the body, which might lead to the prolonged fate of LHT7 in the body. This result indicates the utility of polyethylene glycol-modified cationic nanoliposomes for sustained delivery systems of negatively charged LHT7.

The biodistribution of LHT7 could be modulated by the nanolipoplex formulation. LHT7 in nanolipoplex was selectively localized to tumor vasculature and it resided for a longer time, compared to free LHT7. We supposed that the serum stability and prolonged circulation of LHT7 in nanolipoplex contributed to the enhanced localization and retention in tumor vasculature. The particle size of LHT7/SAHA nanolipoplex was about 120 nm, which satisfied the requirements for selective entrapment by the leaky vascular structure at tumor sites during circulation in the blood. This phenomenon, which is called EPR effect, comes from the very rapid growth of tumoral vessels and makes nano-sized particles between 100 and 200 nm to be captured through the loose connections between endothelium cells [53]. Beside the EPR effect, the positive surface charges of LHT7/SAHA nanolipoplex may affect the enhanced distribution of LHT to tumor vasculature, as newly formed vessels at the tumor site are known to abnormally overexpress negative charged proteins [56, 57]. The dominant existence of negative proteins in tumor vasculature microenvironments was favorable for the retention of cationic LHT7/SAHA nanolipoplex in tumor vasculature, after its enhanced arrival by EPR effect [58, 150]. Even though LHT7/SAHA nanolipoplex still had positive surface charge as a final drug formulation, there was no sign of behavioral changes observed after intravenous injection.

Both tumor growth inhibition data (Fig. 5.3) and the immunohistochemistry (Fig. 5.4) data supported the enhanced antitumor and antiangiogenesis effects of LHT7 after treatment in nanolipoplex. The *in vivo* tumor growth inhibition data

revealed that LHT7/SAHA nanolipoplex showed the highest therapeutic effect, compared to LHT7 or to SAHA-L alone. In addition, the expression of CD34 and PCNA was also significantly decreased in the LHT7/SAHA nanolipoplex-treated group. In this study, SAHA was used for the combination therapy with LHT7. SAHA is a histone deacetylase inhibitor, and known to intervene cell-cycle arrest, angiogenesis, immune modulation and apoptosis in cancer [17, 18]. Ultimately, we observed that those two drugs work together in inhibition of angiogenesis and cell proliferation, which led to the synergistic combination effect. Previously, the co-treatment of angiogenesis inhibitor with a histone deacetylase inhibitior was shown to enhance the anticancer efficacy in hepatoma model [14].

These results indicated the importance of multifunctional nanolipoplex of LHT7 for synergistic effects after combination therapy with SAHA. Although LHT7/SAHA nanolipoplex substantially inhibited tumor growth compared to when LHT7 alone was administered, the co-administration of LHT7 and SAHA-L in a sequential manner did not show significantly different anticancer effects compared to when LHT7 alone was administered. The different effect observed between the sequential co-administration of LHT7 and SAHA liposome and LHT7/SAHA nanolipoplex group might be due to the lower distribution of free LHT7 injected to the tumor vasculature in advance as evidenced in the biodistribution study. Moreover, the rapid elimination of free LHT in blood may contribute to the lower distribution to the tumor vasculature, limiting the antitumor effect. Considering the fact that the EPR effect is derived from the abnormal vascular structures as mentioned above, it

was expected that LHT7/SAHA nanolipoplex would be a suitable drug carrier for selective delivery of angiogenesis inhibitors to the tumor vasculature.

The enhanced antitumor effect of LHT7 in nanolipoplex might be further explained by the antiangiogenic effect. It is observed that LHT7 in nanolipoplex was selectively accumulated in the tumor site at 24 hrs post-dose. Once arriving at the tumor site, LHT7 may be constantly released from the nanolipoplex and cause antiangiogenic effects in a sustained and constant manner. Consequently, the local microenvironmental effect brought on by LHT7, in return, enhances the chance of both LHT7 and SAHA to exert their anticancer effects effectively at the tumor site. This positive contribution of LHT7 in tumor vasculature provides a clue for further designing of anti-angiogenesis studies. Hence, by formulating angiogenesis inhibitors in the nanolipoplex, the therapeutic effect of angiogenesis inhibitors may be enhanced and their toxicity reduced more effectively by EPR.

5.5. Conclusions

Our results indicate that the formulation of LHT7 in nanolipoplex could prolong the retention time and enhance tumor vasculature targeting. Moreover, the co-delivery of LHT7 with a histone deacetylase inhibitor SAHA in nanolipoplex provided the synergistic antitumor effects although the consequent co-treatment of LHT7 and SAHA-L did not reveal any synergistic activity. Furthermore, the systemic administration of LHT7 in nanolipoplex could decrease the numbers of abnormal blood vessels in tumor vasculature more effectively than LHT7 in free form.

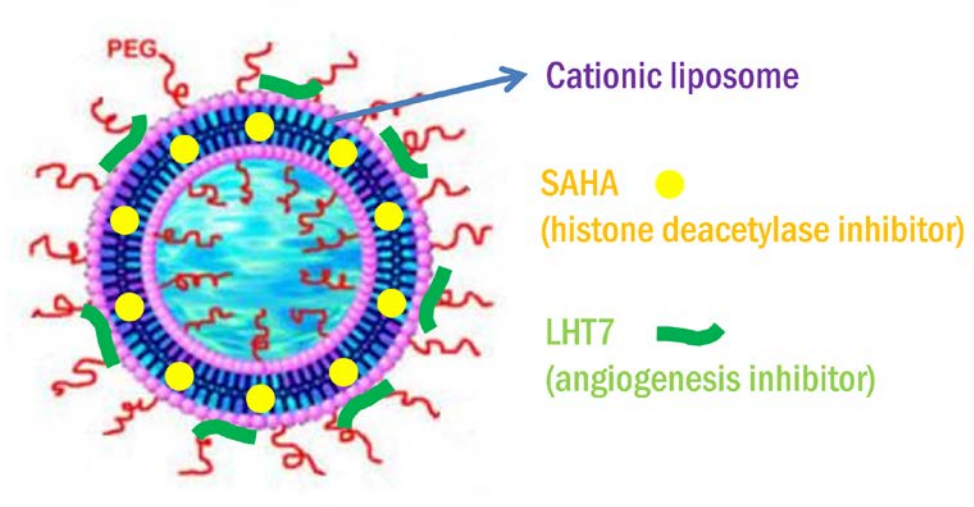

Figure 5.1 Schematic structure of LHT7/SAHA nanolipoplex

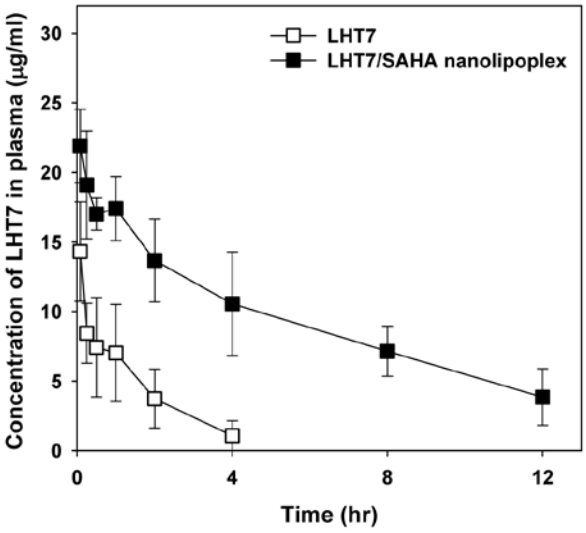

Figure 5.2 Plasma concentration vs. time profiles of LHT7. LHT7 in free form or in nanolipoplex were intravenously administered to SD rats. The concentrations of LHT7 in the blood were measure by heparin orange assay. The results are expressed as the mean ± SEM (n=3)

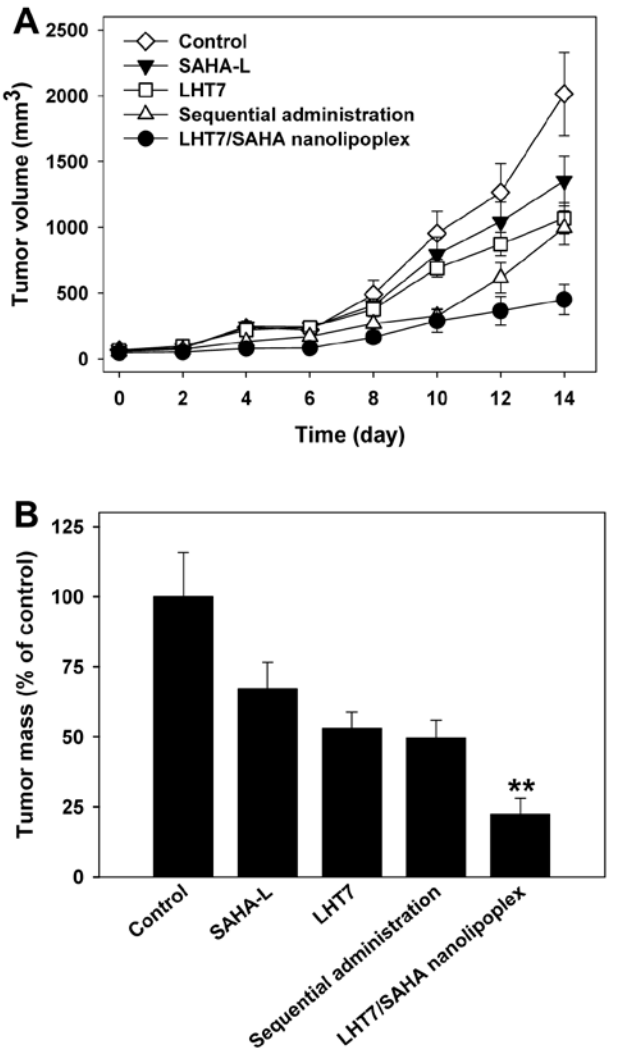

Figure 5.3 *In vivo* antitumor effects in SCC7-bearing mice. (A) SCC7-bearing mice were intravenously treated with PBS, SAHA-L, LHT7, the sequential co-administration of SAHA-L and LHT7, or LHT7/SAHA nanolipoplex. The tumor volume was measured at various time points post-dose. (B) Comparative tumor mass

presented as percent of control after 14 days. Data were expressed as mean ± SEM (n = 6 ~ 7). **$p < 0.01$ *vs.* LHT7-treated group.

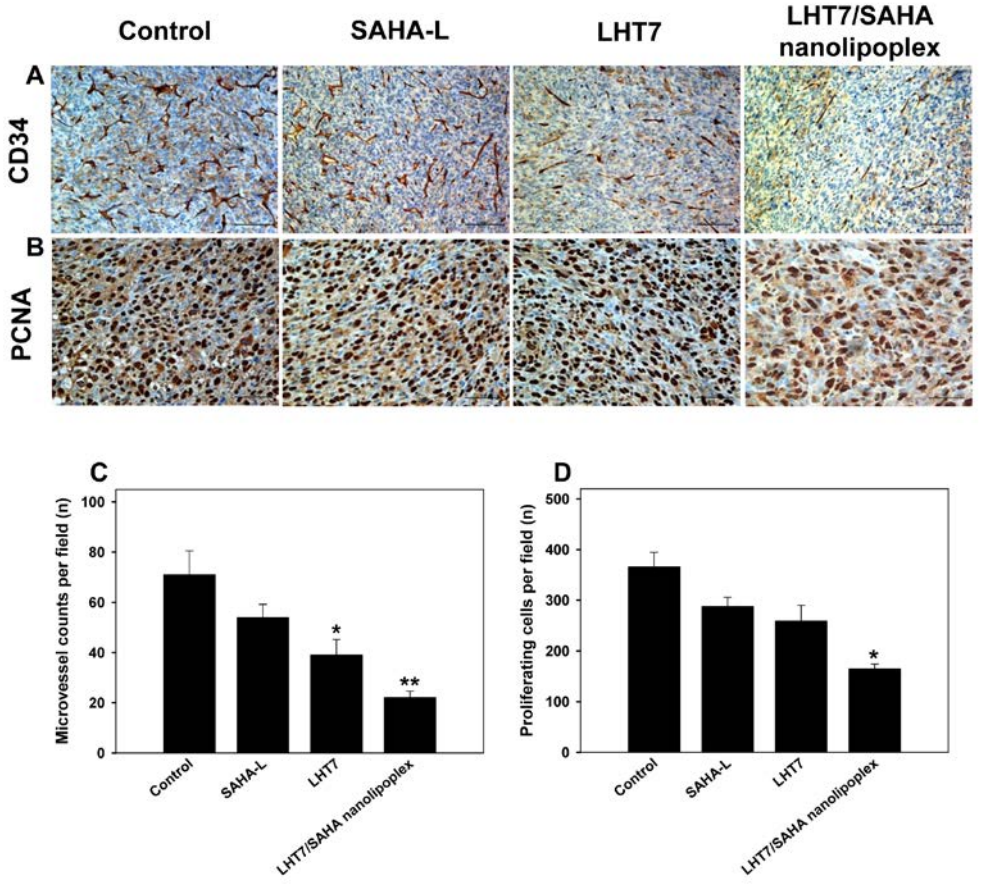

Figure 5.4 Immunohistochemistry of tumor tissues isolated from mice treated with LHT7/SAHA nanolipoplex. (A) Microphotographs of anti-CD34 antibody immunostaining against microvessels on the isolated tumor tissue sections of various groups. (B) Microphotographs of anti-PCNA antibody immunostaining against proliferating cells on the isolated tumor tissue sections of various groups. (C) The numbers of anti-CD34 immunostained microvessels on the isolated tumor tissues. Data were expressed as mean ± SEM (n=3). (D) The numbers of PCNA

immunostained proliferating cells on the isolated tumor tissues. Data were expressed as mean ± SEM (n=3). *$p < 0.05$ *vs.* control. **$p < 0.01$ *vs.* control

Table 5.1 Pharmacokinetic parameters after intravenous administration of LHT7 in free or nanolipoplex to rats (n=3).

	Formulation	
	LHT7	LHT7/SAHA nanolipoplex
AUC (mg·hr/ml)	41.35 ± 29.39	149.81 ± 30.69
Cl (ml/hr/kg)	15.30 ± 15.12	0.0074 ± 0.0017
AUMC (mg·hr^2/ml)	334.57 ± 318.24	1261.06 ± 675.24
V_{ss} (ml/kg)	22.13 ± 22.03	0.047 ± 0.0095
MRT (hr)	3.86 ± 2.98	7.42 ± 2.81
Half-life (hr)	2.38 ± 1.76	4.37 ± 1.71

*AUC, area under the curve; Cl, clearance; AUMC, area under the momentum curve; Vss, volume of distribution at steady state, MRT, mean residence time

Chapter VI. Conclusions

In this study, we have studied on cancer chemoprevention and chemotherapy by using different kind of LMWH-bile acid conjugates as angiogenesis inhibitors and utilizing vascular structure targeted-drug delivery system.

In Chapter II of this study, we introduce a newly developed oral heparin derivative named as LHTD4, where LMWH is conjugated with 7 molecule of taurocholic acid and a tetermeric deoxycholic adic, for use as an oral angiogenesis inhibitor. LHTD4 demonstrated its antiangiogenic activity both *in vitro* and *vivo*. In particular, it still retained its antiangiogenic activity after oral administration, which contributes to the retardation of lung cancer progression in animal model. Its bioavailability and therapeutic efficacy indicate that LHTD4 could be applied as an antiangiogenic drug in the clinics. Above all, because of high patient convenience of intake guaranteed by its route of administration, we expect that LHTD4LHTD4 can serve well in cancer chemoprevention requiring chronic administration.

In Chapter III of this study, the combination effect of celecoxib, a selective COX-2 inhibitor, and newly developed oral angiogenesis inhibitor named as LHD4, where LMWH is conjugated with deoxycholic acid at molar ration of 1:4, on chemoprevention was evaluated to achieve a clinically rational regimen for cancer chemoprevention with improved efficacy and safety. We showed, using an AOM and DSS-induced colorectal carcinogenesis animal model, that the combination use of celecoxib, a selective COX-2 inhibitor, and LHD4, an angiogenesis inhibitor, could

significantly enhance chemoprevention of colorectal cancer in terms of polyp formation and malignancy development. In addition, we also introduced a newly developed angiogenesis inhibitor, which can be absorbed via oral route, as a promising chemopreventive agent. This new regimen is a clinically rational strategy for overcoming the chemopreventive limitations of celecoxib treatment alone.

In Chapter IV of this study, we have studied the COX-2 inhibition effect on antiangiogneic therapy using multitargeting angiogeneies inhibitor named as LHT7, where LMWH is conjugated with taurocholic acid at molar ration of 1:7. We found that COX-2 inhibition might enhance the therapeutic effect of antiangiogenic drugs both by inhibiting the inflammatory reactions induced by hypoxia and by altering the vascular stabilization that is mediated by assembly with mural cells. Our results indicate that the new anti-angiogenic regimen combined with a selective COX-2 inhibitor could be applied in the clinics to prevent the evasive resistance to cancer treatment that comes from the chronic anti-angiogenic therapy. Thus, we expect that this new regimen improve the overall clinical therapeutic efficacy by prolonging the progression-free period and overall survival rate of cancer patients.

In Chapter V of this study, we have studied on the tumor vascular structure-targeted delivery of antiangiogenic drug. We prepared a cationic nanolipocomplex by co-loading LHT7 and SAHA into lipid nanoparticle. We found that the formulation of LHT7 in nanolipoplex could prolong the retention time and

enhance tumor vasculature targeting. Moreover, the co-delivery of LHT7 with suberoylanilide hydroxamic acid (SAHA), a histone deacetylase inhibitor, in nanolipoplex provided the synergistic antitumor effects although the consequent co-treatment of LHT7 and SAHA-L did not reveal any synergistic activity. Furthermore, the systemic administration of LHT7 in nanolipoplex could decrease the numbers of abnormal blood vessels in tumor vasculature more effectively than LHT7 in free form. These results suggested the potential of LHT7/SAHA nanolipoplex for enhanced tumor vasculature targeting, and the importance of nanolipoplex-mediated co-delivery with a histone deacetylase inhibitor for maximal anticancer effect.

Taken all, a series of LMWH-bile acids conjugates as angiogenesis inhibitors could be promising and clinically available cancer chemopreventive and therapeutic agents in the future. In addition, the antiangiogenic potency of LMWH-bile acids conjugates might be further improved by utilizing a functionalized drug delivery system such as tumor vascular targeting carrier.

References

[1] Carmeliet P, Jain RK. Angiogenesis in cancer and other diseases. Nature. 2000;407:249-57.

[2] Chung AS, Lee J, Ferrara N. Targeting the tumour vasculature: insights from physiological angiogenesis. Nat Rev Cancer. 2010;10:505-14.

[3] Weis SM, Cheresh DA. Tumor angiogenesis: molecular pathways and therapeutic targets. Nat Med. 2011;17:1359-70.

[4] Ferrara N, Kerbel RS. Angiogenesis as a therapeutic target. Nature. 2005;438:967-74.

[5] Folkman J. Tumor angiogenesis: therapeutic implications. N Engl J Med. 1971;285:1182-6.

[6] Marmé D, Fusenig N. Tumor Angiogenesis: Basic Mechanisms and Cancer Therapy: Springer; 2007.

[7] Calabrese C, Poppleton H, Kocak M, Hogg TL, Fuller C, Hamner B, Oh EY, Gaber MW, Finklestein D, Allen M, Frank A, Bayazitov IT, Zakharenko SS, Gajjar A, Davidoff A, Gilbertson RJ. A perivascular niche for brain tumor stem cells. Cancer Cell. 2007;11:69-82.

[8] Holzel M, Bovier A, Tuting T. Plasticity of tumour and immune cells: a source of heterogeneity and a cause for therapy resistance? Nat Rev Cancer. 2013;13:365-76.

[9] Cao Y. Antiangiogenic cancer therapy. Semin Cancer Biol. 2004;14:139-45.

[10] Relf M, LeJeune S, Scott PA, Fox S, Smith K, Leek R, Moghaddam A, Whitehouse R, Bicknell R, Harris AL. Expression of the angiogenic factors vascular endothelial cell growth factor, acidic and basic fibroblast growth factor, tumor growth factor beta-1, platelet-derived endothelial cell growth factor, placenta growth factor, and pleiotrophin in human primary breast cancer and its relation to angiogenesis. Cancer Res. 1997;57:963-9.

[11] Davis DW, Herbst RS, Abbruzzese JL. Antiangiogenic Cancer Therapy: Taylor & Francis; 2010.

[12] Dieter Marmé NF. Tumor Angiogenesis: Basic Mechanisms and Cancer

Therapy Springer; 2007.

[13] Catalano V, Turdo A, Di Franco S, Dieli F, Todaro M, Stassi G. Tumor and its microenvironment: a synergistic interplay. Semin Cancer Biol. 2013;23:522-32.

[14] Ellis LM, Hicklin DJ. VEGF-targeted therapy: mechanisms of anti-tumour activity. Nat Rev Cancer. 2008;8:579-91.

[15] Sennino B, McDonald DM. Controlling escape from angiogenesis inhibitors. Nat Rev Cancer. 2012;12:699-709.

[16] Bergers G, Hanahan D. Modes of resistance to anti-angiogenic therapy. Nat Rev Cancer. 2008;8:592-603.

[17] Bottsford-Miller JN, Coleman RL, Sood AK. Resistance and escape from antiangiogenesis therapy: clinical implications and future strategies. J Clin Oncol. 2012;30:4026-34.

[18] Loges S, Mazzone M, Hohensinner P, Carmeliet P. Silencing or fueling metastasis with VEGF inhibitors: antiangiogenesis revisited. Cancer Cell. 2009;15:167-70.

[19] Prevention of cancer in the next millennium: Report of the Chemoprevention Working Group to the American Association for Cancer Research. Cancer Res. 1999;59:4743-58.

[20] Blackburn EH. Cancer interception. Cancer Prev Res (Phila). 2011;4:787-92.

[21] Sporn MB, Dunlop NM, Newton DL, Smith JM. Prevention of chemical carcinogenesis by vitamin A and its synthetic analogs (retinoids). Fed Proc. 1976;35:1332-8.

[22] Bode AM, Dong Z. Cancer prevention research - then and now. Nat Rev Cancer. 2009;9:508-16.

[23] Gravitz L. Chemoprevention: First line of defence. Nature. 2011;471:S5-S7.

[24] De Flora S, Ferguson LR. Overview of mechanisms of cancer chemopreventive agents. Mutat Res. 2005;591:8-15.

[25] De Flora S, Izzotti A, D'Agostini F, Balansky RM, Noonan D, Albini A. Multiple points of intervention in the prevention of cancer and other

mutation-related diseases. Mutat Res. 2001;480-481:9-22.

[26] Sporn MB, Liby KT. Cancer chemoprevention: scientific promise, clinical uncertainty. Nat Clin Pract Oncol. 2005;2:518-25.

[27] William WN, Jr., Heymach JV, Kim ES, Lippman SM. Molecular targets for cancer chemoprevention. Nat Rev Drug Discov. 2009;8:213-25.

[28] Sporn MB, Suh N. Chemoprevention: an essential approach to controlling cancer. Nat Rev Cancer. 2002;2:537-43.

[29] Sporn MB. Combination chemoprevention of cancer. Nature. 1980;287:107-8.

[30] Sporn MB, Hong WK. Concomitant DFMO and sulindac chemoprevention of colorectal adenomas: a major clinical advance. Nature Clinical Practice. Oncology. 2008;5:628-9.

[31] Meyskens FL, Jr., McLaren CE, Pelot D, Fujikawa-Brooks S, Carpenter PM, Hawk E, Kelloff G, Lawson MJ, Kidao J, McCracken J, Albers CG, Ahnen DJ, Turgeon DK, Goldschmid S, Lance P, Hagedorn CH, Gillen DL, Gerner EW. Difluoromethylornithine plus sulindac for the prevention of sporadic colorectal adenomas: a randomized placebo-controlled, double-blind trial. Cancer Prev Res (Phila). 2008;1:32-8.

[32] Lippman SM, Hong WK. Cancer prevention by delay. Commentary re: J. A. O'Shaughnessy et al., Treatment and Prevention of Intraepithelial Neoplasia: An Important Target for Accelerated New Agent Development. Clin. Cancer Res., 8: 314-346, 2002. Clinical Cancer Research. 2002;8:305-13.

[33] Mukhtar H. Chemoprevention: making it a success story for controlling human cancer. Cancer Lett. 2012;326:123-7.

[34] Albini A, Sporn MB. The tumour microenvironment as a target for chemoprevention. Nat Rev Cancer. 2007;7:139-47.

[35] Bergers G, Benjamin LE. Tumorigenesis and the angiogenic switch. Nat Rev Cancer. 2003;3:401-10.

[36] Lever R, Page CP. Novel drug development opportunities for heparin. Nat Rev Drug Discov. 2002;1:140-8.

[37] Weitz JI. Low-molecular-weight heparins. N Engl J Med. 1997;337:688-98.

[38] Mousa SA, Petersen LJ. Anti-cancer properties of low-molecular-weight heparin: preclinical evidence. Thromb Haemost. 2009;102:258-67.

[39] Zacharski LR, Ornstein DL. Heparin and cancer. Thromb Haemost. 1998;80:10-23.

[40] Park JW, Jeon OC, Kim SK, Al-Hilal TA, Jin SJ, Moon HT, Yang VC, Kim SY, Byun Y. High antiangiogenic and low anticoagulant efficacy of orally active low molecular weight heparin derivatives. J Control Release. 2010;148:317-26.

[41] Lee E, Kim YS, Bae SM, Kim SK, Jin S, Chung SW, Lee M, Moon HT, Jeon OC, Park RW, Kim IS, Byun Y, Kim SY. Polyproline-type helical-structured low-molecular weight heparin (LMWH)-taurocholate conjugate as a new angiogenesis inhibitor. Int J Cancer. 2009;124:2755-65.

[42] Chung SW, Lee M, Bae SM, Park J, Jeon OC, Lee HS, Choe H, Kim HS, Lee BS, Park RW, Kim SY, Byun Y. Potentiation of anti-angiogenic activity of heparin by blocking the ATIII-interacting pentasaccharide unit and increasing net anionic charge. Biomaterials. 2012;33:9070-9.

[43] Adulnirath A, Chung SW, Park J, Hwang SR, Kim JY, Yang VC, Kim SY, Moon HT, Byun Y. Cyclic RGDyk-conjugated LMWH-taurocholate derivative as a targeting angiogenesis inhibitor. J Control Release. 2012;164:8-16.

[44] Bae SM, Kim JH, Chung SW, Byun Y, Kim SY, Lee BH, Kim IS, Park RW. An apoptosis-homing peptide-conjugated low molecular weight heparin-taurocholate conjugate with antitumor properties. Biomaterials. 2013;34:2077-86.

[45] Al-Hilal TA, Park J, Alam F, Chung SW, Park JW, Kim K, Kwon IC, Kim IS, Kim SY, Byun Y. Oligomeric bile acid-mediated oral delivery of low molecular weight heparin. J Control Release. 2014;175:17-24.

[46] Al-Hilal TA, Chung SW, Alam F, Park J, Lee KE, Jeon H, Kim K, Kwon IC, Kim IS, Kim SY, Byun Y. Functional transformations of bile acid transporters induced by high-affinity macromolecules. Sci Rep. 2014;4:4163.

[47] F. Alam, T.A. Al-Hilal, S.W. Chung, D. Seo, F. Mahmud, H.S. Kim, S.Y. Kim, Byun Y. Oral delivery of a potent anti-angiogenic heparin conjugate by chemical conjugation and physical complexation using deoxycholic acid. Biomaterials. 2014;***In press***.

[48] Davis ME, Chen ZG, Shin DM. Nanoparticle therapeutics: an emerging treatment modality for cancer. Nat Rev Drug Discov. 2008;7:771-82.

[49] Schroeder A, Heller DA, Winslow MM, Dahlman JE, Pratt GW, Langer R, Jacks T, Anderson DG. Treating metastatic cancer with nanotechnology. Nat Rev Cancer. 2012;12:39-50.

[50] Zhao G, Rodriguez BL. Molecular targeting of liposomal nanoparticles to tumor microenvironment. Int J Nanomedicine. 2013;8:61-71.

[51] Yoncheva K, Momekov G. Antiangiogenic anticancer strategy based on nanoparticulate systems. Expert Opin Drug Deliv. 2011;8:1041-56.

[52] Dass CR. Improving anti-angiogenic therapy via selective delivery of cationic liposomes to tumour vasculature. Int J Pharm. 2003;267:1-12.

[53] Matsumura Y, Maeda H. A new concept for macromolecular therapeutics in cancer chemotherapy: mechanism of tumoritropic accumulation of proteins and the antitumor agent smancs. Cancer Res. 1986;46:6387-92.

[54] Cabral H, Matsumoto Y, Mizuno K, Chen Q, Murakami M, Kimura M, Terada Y, Kano MR, Miyazono K, Uesaka M, Nishiyama N, Kataoka K. Accumulation of sub-100 nm polymeric micelles in poorly permeable tumours depends on size. Nat Nanotechnol. 2011;6:815-23.

[55] Lian T, Ho RJ. Trends and developments in liposome drug delivery systems. J Pharm Sci. 2001;90:667-80.

[56] Zwaal RF, Schroit AJ. Pathophysiologic implications of membrane phospholipid asymmetry in blood cells. Blood. 1997;89:1121-32.

[57] Ran S, Downes A, Thorpe PE. Increased exposure of anionic phospholipids on the surface of tumor blood vessels. Cancer Res. 2002;62:6132-40.

[58] Krasnici S, Werner A, Eichhorn ME, Schmitt-Sody M, Pahernik SA, Sauer B, Schulze B, Teifel M, Michaelis U, Naujoks K, Dellian M. Effect of the surface charge of liposomes on their uptake by angiogenic tumor vessels. Int J Cancer. 2003;105:561-7.

[59] Abu Lila AS, Ishida T, Kiwada H. Targeting anticancer drugs to tumor vasculature using cationic liposomes. Pharm Res. 2010;27:1171-83.

[60] Ho EA, Ramsay E, Ginj M, Anantha M, Bregman I, Sy J, Woo J, Osooly-Talesh M, Yapp DT, Bally MB. Characterization of cationic liposome formulations designed to exhibit extended plasma residence times and tumor vasculature targeting properties. J Pharm Sci. 2010;99:2839-53.

[61] Abu Lila AS, Ishida T, Kiwada H. Recent advances in tumor vasculature targeting using liposomal drug delivery systems. Expert Opin Drug Deliv. 2009;6:1297-309.

[62] Kuesters GM, Campbell RB. Conjugation of bevacizumab to cationic liposomes enhances their tumor-targeting potential. Nanomedicine (Lond). 2010;5:181-92.

[63] Murase Y, Asai T, Katanasaka Y, Sugiyama T, Shimizu K, Maeda N, Oku N. A novel DDS strategy, "dual-targeting", and its application for antineovascular therapy. Cancer Lett. 2010;287:165-71.

[64] Niers TM, Klerk CP, DiNisio M, Van Noorden CJ, Buller HR, Reitsma PH, Richel DJ. Mechanisms of heparin induced anti-cancer activity in experimental cancer models. Critical Reviews in Oncology/Hematology. 2007;61:195-207.

[65] Mousa SA, Petersen LJ. Anti-cancer properties of low-molecular-weight heparin: preclinical evidence. Thrombosis and Haemostasis. 2009;102:258-67.

[66] Zacharski L, Ornstein D, Mamourian A. Low-molecular-weight heparin and cancer. Seminars in Thrombosis and Hemostasis. 2000;26:69-77.

[67] Park K, Lee GY, Kim YS, Yu M, Park RW, Kim IS, Kim SY, Byun Y. Heparin-deoxycholic acid chemical conjugate as an anticancer drug carrier and its antitumor activity. Journal of Controlled Release. 2006;114:300-6.

[68] Lee DY, Kim SK, Kim YS, Son DH, Nam JH, Kim IS, Park RW, Kim SY, Byun Y. Suppression of angiogenesis and tumor growth by orally active deoxycholic acid-heparin conjugate. Journal of Controlled Release. 2007;118:310-7.

[69] Lee DY, Park K, Kim SK, Park RW, Kwon IC, Kim SY, Byun Y. Antimetastatic effect of an orally active heparin derivative on experimentally induced metastasis. Clinical Cancer Research. 2008;14:2841-9.

[70] Lee E, Kim YS, Bae SM, Kim SK, Jin S, Chung SW, Lee M, Moon HT, Jeon OC, Park RW, Kim IS, Byun Y, Kim SY. Polyproline-type helical-structured low-molecular weight heparin (LMWH)-taurocholate conjugate as a new angiogenesis inhibitor. International Journal of Cancer. 2009;124:2755-65.

[71] Park JW, Jeon OC, Kim SK, Al-Hilal TA, Jin SJ, Moon HT, Yang VC, Kim SY, Byun Y. High antiangiogenic and low anticoagulant efficacy of orally active low molecular weight heparin derivatives. Journal of Controlled Release. 2010;148:317-26.

[72] Lee S, Lee J, Lee DY, Kim SK, Lee Y, Byun Y. A new drug carrier, Nalpha-deoxycholyl-L: -lysyl-methylester, for enhancing insulin absorption in the intestine. Diabetologia. 2005;48:405-11.

[73] Jeon OC, Hwang SR, Al-Hilal TA, Park JW, Moon HT, Lee S, Park JH, Byun Y. Oral Delivery of Ionic Complex of Ceftriaxone with Bile Acid Derivative in Non-human Primates. Pharmaceutical Research. 2013;30:959-67.

[74] Park JW, Hwang SR, Jeon OC, Moon HT, Byun Y. Enhanced oral absorption of ibandronate via complex formation with bile acid derivative. Journal of Pharmaceutical Sciences. 2013;102:341-6.

[75] Albini A, Tosetti F, Li VW, Noonan DM, Li WW. Cancer prevention by targeting angiogenesis. Nat Rev Clin Oncol. 2012;9:498-509.

[76] Albini A, Noonan DM, Ferrari N. Molecular pathways for cancer angioprevention. Clinical Cancer Research. 2007;13:4320-5.

[77] Bergers G, Benjamin LE. Tumorigenesis and the angiogenic switch. Nature Reviews. Cancer. 2003;3:401-10.

[78] Sporn MB, Newton DL. Chemoprevention of cancer with retinoids. Federation Proceedings. 1979;38:2528-34.

[79] Gerhauser C. Cancer Chemoprevention and Nutri-Epigenetics: State of the Art and Future Challenges. Topics in Current Chemistry. 2012.

[80] Karoor V, Le M, Merrick D, Dempsey EC, Miller YE. Vascular endothelial growth factor receptor 2-targeted chemoprevention of murine lung tumors. Cancer Prev Res (Phila). 2010;3:1141-7.

[81] Keith RL, Miller YE, Gemmill RM, Drabkin HA, Dempsey EC, Kennedy TC, Prindiville S, Franklin WA. Angiogenic squamous dysplasia in bronchi of individuals at high risk for lung cancer. Clinical Cancer Research. 2000;6:1616-25.

[82] Siegel R, Naishadham D, Jemal A. Cancer statistics, 2013. CA: A Cancer Journal for Clinicians. 2013;63:11-30.

[83] Tong L, Spitz MR, Fueger JJ, Amos CA. Lung carcinoma in former smokers. Cancer. 1996;78:1004-10.

[84] Silva MT, Galvao TF, Zimmerman IR, Pereira MG, Lopes LC. Non-aspirin

Non-steroidal Anti-inflammatory Drugs for the Primary Chemoprevention of Non-gastrointestinal Cancer: Summary of Evidence. Current Pharmaceutical Design. 2012;18:4047-70.

[85] Hwang SR, Seo DH, Al-Hilal TA, Jeon OC, Kang JH, Kim SH, Kim HS, Chang YT, Kang YM, Yang VC, Byun Y. Orally active desulfated low molecular weight heparin and deoxycholic acid conjugate, 6ODS-LHbD, suppresses neovascularization and bone destruction in arthritis. J Control Release. 2012;163:374-84.

[86] Orita H, Coulter J, Tully E, Kuhajda FP, Gabrielson E. Inhibiting fatty acid synthase for chemoprevention of chemically induced lung tumors. Clinical Cancer Research. 2008;14:2458-64.

[87] Nikitin AY, Alcaraz A, Anver MR, Bronson RT, Cardiff RD, Dixon D, Fraire AE, Gabrielson EW, Gunning WT, Haines DC, Kaufman MH, Linnoila RI, Maronpot RR, Rabson AS, Reddick RL, Rehm S, Rozengurt N, Schuller HM, Shmidt EN, Travis WD, Ward JM, Jacks T. Classification of Proliferative Pulmonary Lesions of the Mouse: Recommendations of the Mouse Models of Human Cancers Consortium. Cancer Research. 2004;64:2307-16.

[88] Lippman SM, Ki Hong W. Cancer Prevention by Delay. Clinical Cancer Research. 2002;8:305-13.

[89] Ji-young Kim FA, Seung Woo Chung, Jooho Park, Ok Cheol Jeon, Sang Yoon Kim, Woo Chan Son, Youngro Byun. Combinational chemoprevention effect of celecoxib and an oral anti-angiogenic LHD4 on colorectal carcinogenesis in mice. Anti-Cancer Drugs. 2014;*In press*.

[90] Sporn MB, Suh N. Chemoprevention: an essential approach to controlling cancer. Nature Reviews. Cancer. 2002;2:537-43.

[91] Balkwill F, Charles KA, Mantovani A. Smoldering and polarized inflammation in the initiation and promotion of malignant disease. Cancer Cell. 2005;7:211-7.

[92] Burstein E, Fearon ER. Colitis and cancer: a tale of inflammatory cells and their cytokines. Journal of Clinical Investigation. 2008;118:464-7.

[93] Aggarwal BB, Gehlot P. Inflammation and cancer: how friendly is the relationship for cancer patients? Current Opinion in Pharmacology. 2009;9:351-69.

[94] Chan AT. Aspirin and chemoprevention of cancer: reaching beyond the colon.

Gastroenterology. 2012;143:1110-2.

[95] Nam KT, Hahm KB, Oh SY, Yeo M, Han SU, Ahn B, Kim YB, Kang JS, Jang DD, Yang KH, Kim DY. The selective cyclooxygenase-2 inhibitor nimesulide prevents Helicobacter pylori-associated gastric cancer development in a mouse model. Clinical Cancer Research. 2004;10:8105-13.

[96] Segawa E, Hashitani S, Toyohara Y, Kishimoto H, Noguchi K, Takaoka K, Urade M. Inhibitory effect of sulindac on DMBA-induced hamster cheek pouch carcinogenesis and its derived cell line. Oncology Reports. 2009;21:869-74.

[97] Arber N, Eagle CJ, Spicak J, Racz I, Dite P, Hajer J, Zavoral M, Lechuga MJ, Gerletti P, Tang J, Rosenstein RB, Macdonald K, Bhadra P, Fowler R, Wittes J, Zauber AG, Solomon SD, Levin B. Celecoxib for the prevention of colorectal adenomatous polyps. New England Journal of Medicine. 2006;355:885-95.

[98] Koki AT, Masferrer JL. Celecoxib: a specific COX-2 inhibitor with anticancer properties. Cancer Control. 2002;9:28-35.

[99] Menakuru SR, Brown NJ, Staton CA, Reed MW. Angiogenesis in pre-malignant conditions. British Journal of Cancer. 2008;99:1961-6.

[100] Goodlad RA, Ryan AJ, Wedge SR, Pyrah IT, Alferez D, Poulsom R, Smith NR, Mandir N, Watkins AJ, Wilkinson RW. Inhibiting vascular endothelial growth factor receptor-2 signaling reduces tumor burden in the ApcMin/+ mouse model of early intestinal cancer. Carcinogenesis. 2006;27:2133-9.

[101] Korsisaari N, Kasman IM, Forrest WF, Pal N, Bai W, Fuh G, Peale FV, Smits R, Ferrara N. Inhibition of VEGF-A prevents the angiogenic switch and results in increased survival of Apc+/min mice. Proceedings of the National Academy of Sciences of the United States of America. 2007;104:10625-30.

[102] Lee Y, Nam JH, Shin HC, Byun Y. Conjugation of low-molecular-weight heparin and deoxycholic acid for the development of a new oral anticoagulant agent. Circulation. 2001;104:3116-20.

[103] Albini A, Tosetti F, Benelli R, Noonan DM. Tumor Inflammatory Angiogenesis and Its Chemoprevention. Cancer Res. 2005;65:10637-41.

[104] Ono M. Molecular links between tumor angiogenesis and inflammation: inflammatory stimuli of macrophages and cancer cells as targets for therapeutic strategy. Cancer Science. 2008;99:1501-6.

[105] Tanaka T, Kohno H, Suzuki R, Yamada Y, Sugie S, Mori H. A novel inflammation-related mouse colon carcinogenesis model induced by azoxymethane and dextran sodium sulfate. Cancer Science. 2003;94:965-73.

[106] Boivin GP, Washington K, Yang K, Ward JM, Pretlow TP, Russell R, Besselsen DG, Godfrey VL, Doetschman T, Dove WF, Pitot HC, Halberg RB, Itzkowitz SH, Groden J, Coffey RJ. Pathology of mouse models of intestinal cancer: consensus report and recommendations. Gastroenterology. 2003;124:762-77.

[107] Ma YL, Peng JY, Zhang P, Liu WJ, Huang L, Qin HL. Immunohistochemical analysis revealed CD34 and Ki67 protein expression as significant prognostic factors in colorectal cancer. Med Oncol. 2010;27:304-9.

[108] Tamimi RM, Lagiou P, Adami HO, Trichopoulos D. Prospects for chemoprevention of cancer. Journal of Internal Medicine. 2002;251:286-300.

[109] Sporn MB, Suh N. Chemoprevention of cancer. Carcinogenesis. 2000;21:525-30.

[110] Sporn MB, Liby KT. Cancer chemoprevention: scientific promise, clinical uncertainty. Nature Clinical Practice. Oncology. 2005;2:518-25.

[111] De Flora S, Ferguson LR. Overview of mechanisms of cancer chemopreventive agents. Mutation Research. 2005;591:8-15.

[112] Kim CY, Kim J, Han K, Kim S, Park K, Byun Y. Toxicity screening after repeated dose of a newly developed oral heparin derivative in male cynomolgus monkeys. Journal of Toxicological Sciences. 2007;32:411-20.

[113] Bergers G, Javaherian K, Lo KM, Folkman J, Hanahan D. Effects of angiogenesis inhibitors on multistage carcinogenesis in mice. Science. 1999;284:808-12.

[114] Kim HS, Kundu JK, Lee JS, Oh TY, Na HK, Surh YJ. Chemopreventive effects of the standardized extract (DA-9601) of Artemisia asiatica on azoxymethane-initiated and dextran sulfate sodium-promoted mouse colon carcinogenesis. Nutr Cancer. 2008;60 Suppl 1:90-7.

[115] Kundu JK, Surh YJ. Inflammation: gearing the journey to cancer. Mutation Research. 2008;659:15-30.

[116] Wu X, Lippman SM. An intermittent approach for cancer chemoprevention.

Nature Reviews. Cancer. 2011;11:879-85.

[117] Leahy KM, Ornberg RL, Wang Y, Zweifel BS, Koki AT, Masferrer JL. Cyclooxygenase-2 inhibition by celecoxib reduces proliferation and induces apoptosis in angiogenic endothelial cells in vivo. Cancer Research. 2002;62:625-31.

[118] Swamy MV, Patlolla JM, Steele VE, Kopelovich L, Reddy BS, Rao CV. Chemoprevention of familial adenomatous polyposis by low doses of atorvastatin and celecoxib given individually and in combination to APCMin mice. Cancer Research. 2006;66:7370-7.

[119] Fischer SM, Hawk ET, Lubet RA. Coxibs and other nonsteroidal anti-inflammatory drugs in animal models of cancer chemoprevention. Cancer Prev Res (Phila). 2011;4:1728-35.

[120] Sahin M, Sahin E, Gumuslu S. Cyclooxygenase-2 in cancer and angiogenesis. Angiology. 2009;60:242-53.

[121] Coussens LM, Werb Z. Inflammation and cancer. Nature. 2002;420:860-7.

[122] Greenhough A, Smartt HJ, Moore AE, Roberts HR, Williams AC, Paraskeva C, Kaidi A. The COX-2/PGE2 pathway: key roles in the hallmarks of cancer and adaptation to the tumour microenvironment. Carcinogenesis. 2009;30:377-86.

[123] Lee A, Frischer J, Serur A, Huang J, Bae JO, Kornfield ZN, Eljuga L, Shawber CJ, Feirt N, Mansukhani M, Stempak D, Baruchel S, Glade Bender J, Kandel JJ, Yamashiro DJ. Inhibition of cyclooxygenase-2 disrupts tumor vascular mural cell recruitment and survival signaling. Cancer Res. 2006;66:4378-84.

[124] Gupta GP, Nguyen DX, Chiang AC, Bos PD, Kim JY, Nadal C, Gomis RR, Manova-Todorova K, Massague J. Mediators of vascular remodelling co-opted for sequential steps in lung metastasis. Nature. 2007;446:765-70.

[125] Fisher JC, Gander JW, Haley MJ, Hernandez SL, Huang J, Chang YJ, Johung TB, Guarnieri P, O'Toole K, Yamashiro DJ, Kandel JJ. Inhibition of cyclo-oxygenase 2 reduces tumor metastasis and inflammatory signaling during blockade of vascular endothelial growth factor. Vasc Cell. 2011;3:22.

[126] Ebos JM, Lee CR, Cruz-Munoz W, Bjarnason GA, Christensen JG, Kerbel RS. Accelerated metastasis after short-term treatment with a potent inhibitor of tumor angiogenesis. Cancer Cell. 2009;15:232-9.

[127] Paez-Ribes M, Allen E, Hudock J, Takeda T, Okuyama H, Vinals F, Inoue M, Bergers G, Hanahan D, Casanovas O. Antiangiogenic therapy elicits malignant progression of tumors to increased local invasion and distant metastasis. Cancer Cell. 2009;15:220-31.

[128] Wang X, Zhang L, O'Neill A, Bahamon B, Alsop DC, Mier JW, Goldberg SN, Signoretti S, Atkins MB, Wood CG, Bhatt RS. Cox-2 inhibition enhances the activity of sunitinib in human renal cell carcinoma xenografts. Br J Cancer. 2013;108:319-26.

[129] Wu G, Luo J, Rana JS, Laham R, Sellke FW, Li J. Involvement of COX-2 in VEGF-induced angiogenesis via P38 and JNK pathways in vascular endothelial cells. Cardiovasc Res. 2006;69:512-9.

[130] Gupta RA, Dubois RN. Colorectal cancer prevention and treatment by inhibition of cyclooxygenase-2. Nat Rev Cancer. 2001;1:11-21.

[131] Ulrich CM, Bigler J, Potter JD. Non-steroidal anti-inflammatory drugs for cancer prevention: promise, perils and pharmacogenetics. Nat Rev Cancer. 2006;6:130-40.

[132] Gately S, Kerbel R. Therapeutic potential of selective cyclooxygenase-2 inhibitors in the management of tumor angiogenesis. Prog Exp Tumor Res. 2003;37:179-92.

[133] Rapisarda A, Melillo G. Role of the hypoxic tumor microenvironment in the resistance to anti-angiogenic therapies. Drug Resist Updat. 2009;12:74-80.

[134] Ebos JM, Lee CR, Kerbel RS. Tumor and host-mediated pathways of resistance and disease progression in response to antiangiogenic therapy. Clin Cancer Res. 2009;15:5020-5.

[135] Murdoch C, Giannoudis A, Lewis CE. Mechanisms regulating the recruitment of macrophages into hypoxic areas of tumors and other ischemic tissues. Blood. 2004;104:2224-34.

[136] Na YR, Yoon YN, Son DI, Seok SH. Cyclooxygenase-2 inhibition blocks M2 macrophage differentiation and suppresses metastasis in murine breast cancer model. PLoS One. 2013;8:e63451.

[137] Nakanishi Y, Nakatsuji M, Seno H, Ishizu S, Akitake-Kawano R, Kanda K, Ueo T, Komekado H, Kawada M, Minami M, Chiba T. COX-2 inhibition alters the phenotype of tumor-associated macrophages from M2 to M1 in ApcMin/+ mouse polyps. Carcinogenesis. 2011;32:1333-9.

[138] Nakao S, Kuwano T, Tsutsumi-Miyahara C, Ueda S, Kimura YN, Hamano S, Sonoda KH, Saijo Y, Nukiwa T, Strieter RM, Ishibashi T, Kuwano M, Ono M. Infiltration of COX-2-expressing macrophages is a prerequisite for IL-1 beta-induced neovascularization and tumor growth. J Clin Invest. 2005;115:2979-91.

[139] Carmeliet P, Jain RK. Molecular mechanisms and clinical applications of angiogenesis. Nature. 2011;473:298-307.

[140] Castelli R, Porro F, Tarsia P. The heparins and cancer: review of clinical trials and biological properties. Vasc Med. 2004;9:205-13.

[141] Patra CR, Bhattacharya R, Wang E, Katarya A, Lau JS, Dutta S, Muders M, Wang S, Buhrow SA, Safgren SL, Yaszemski MJ, Reid JM, Ames MM, Mukherjee P, Mukhopadhyay D. Targeted delivery of gemcitabine to pancreatic adenocarcinoma using cetuximab as a targeting agent. Cancer Res. 2008;68:1970-8.

[142] Zhang Q, Bindokas V, Shen J, Fan H, Hoffman RM, Xing HR. Time-course imaging of therapeutic functional tumor vascular normalization by antiangiogenic agents. Mol Cancer Ther. 2011;10:1173-84.

[143] Ma X, Ezzeldin HH, Diasio RB. Histone deacetylase inhibitors: current status and overview of recent clinical trials. Drugs. 2009;69:1911-34.

[144] Lee MJ, Kim YS, Kummar S, Giaccone G, Trepel JB. Histone deacetylase inhibitors in cancer therapy. Curr Opin Oncol. 2008;20:639-49.

[145] Ganslmayer M, Zimmermann A, Zopf S, Herold C. Combined inhibitors of angiogenesis and histone deacetylase: efficacy in rat hepatoma. World J Gastroenterol. 2011;17:3623-9.

[146] Wang S, Chang YT. Discovery of heparin chemosensors through diversity oriented fluorescence library approach. Chem Commun (Camb). 2008:1173-5.

[147] Suh MS, Shim G, Lee HY, Han SE, Yu YH, Choi Y, Kim K, Kwon IC, Weon KY, Kim YB, Oh YK. Anionic amino acid-derived cationic lipid for siRNA delivery. J Control Release. 2009;140:268-76.

[148] Lee S, Shim G, Kim S, Kim YB, Kim CW, Byun Y, Oh YK. Enhanced transfection rates of small-interfering RNA using dioleylglutamide-based magnetic lipoplexes. Nucleic Acid Ther. 2011;21:165-72.

[149] Meng M, Liu Y, Wang YB, Wang JC, Zhang H, Wang XQ, Zhang X, Lu WL, Zhang Q. Increase of the pharmacological and pharmacokinetic efficacy of negatively charged polypeptide recombinant hirudin in rats via parenteral route by association with cationic liposomes. J Control Release. 2008;128:113-9.

[150] Thurston G, McLean JW, Rizen M, Baluk P, Haskell A, Murphy TJ, Hanahan D, McDonald DM. Cationic liposomes target angiogenic endothelial cells in tumors and chronic inflammation in mice. J Clin Invest. 1998;101:1401-13.

국문초록

혈관 신생 억제 작용을 기반으로 한 화학적 암 예방 및 치료를 위한 헤파린 유도체의 개발에 관한 연구

암의 발달 과정에 있어서 혈관 신생 작용의 중요성은 많은 연구에서 보고된바 있다. 일반적으로 혈관 신생이란 암 조직의 크기가 1-2 ㎣ 에 이르렀을 때, 산소와 영양분의 공급을 위해 기존 혈관으로부터 새로운 혈관이 파생되어 성장하는 것을 말한다. 이 과정에서 관여하게 되는 여러 다양한 세포 전달 물질 및 성장 인자는 암 치료에 있어서 중요한 표적 물질이 된다. 그 결과, 다양한 기전을 바탕으로 한 수많은 종류의 혈관 신생 억제제가 개발되어 왔으며, 임상적으로 적용되고 있다. 그러나 최근 여러 보고에 따르면, 혈관 신생은 암의 초기 발생단계, 즉 세포 과증식 및 이형성과 같은 전암 상태에서 이미 시작된다고 한다. 이러한 특징은 혈관 신생을 표적으로 한 화학적 암 예방의 가능성을 또한 제시하고 있다. 화학적 암 예방이란, 약리학적 기능을 가진 물질을 이용하여 암의 초기 단계에서부터 그 진행을 지연시키거나, 억제하고, 더 나아가 되돌리는

것으로, 암의 발생을 억제하기 위한 중요한 수단으로 인식되고 있다. 혈관 신생 작용을 억제함으로써, 전암 병변이 암 조직으로 진행되는 것을 예방할 수 있을 뿐만 아니라, 암 조직이 더 악성화되는 것을 효과적으로 방지할 수 있을 것이다. 한편으로, 암 조직 부위 혈관을 표적으로 하는 약물 전달체를 개발 및 이용할 경우, 약물에 의한 독성 부작용은 줄일 수 있는 반면 약물의 혈관 신생 억제 작용은 더욱 효과적으로 증가 시킬 수 있을 것이다.

저분자량 헤파린은 평균 분자량 5000 Da 정도의 다분산성의 산성뮤코다당류의 한 종류로서, 한 분자 내 여러 개의 황산기를 가지고 있으며, 대표적인 항응고 약물로써 임상에서 널리 사용되어 왔다. 한편으로, 저분자량 헤파린은 정전기적 상호작용을 바탕으로 하여 다양한 종류의 성장 인자 및 세포 전달 물질과의 결합력을 보인다. 이러한 성질을 바탕으로 하여 저분자량 헤파린의 항암효과에 대한 연구 또한 활발하게 진행되어 왔다. 이러한 연구의 일환으로, 저분자량 헤파린과 담즙산의 화학적 결합체를 혈관 신생 억제제로서 개발 및 적용하고자 하는 연구가 활발하게 진행되어 왔다. 이러한 화학적 결합 및 수식을 통하여, 항응고 효과로 인한 출혈과 같은 부작용은 최소화 하는 반면, 혈관 신생 억제에 의한 치료 효과는 극대화 되었다고 보고 되었다. 기존의 여러 연구에서 다양한 종류의 저분자량 헤파린-담즙산 결합체의 혈관 신생 억제를 통한

항암 효과가 증명 되었으며, 또한 약물 분자 내 기능기의 도입을 통하여 다양한 투여 경로를 통하여 흡수가 가능하게 되었다.

본 연구의 제 2장에서는, 새롭게 개발된 경구형 헤파린 유도체(LHTD4)의 혈관 신생 억제 효과를 규명하고, 또한 이를 이용하여 폐암 동물 모델에서의 암 예방 효과를 연구하였다. 먼저 혈관 내피 세포 및 마트리겔을 이용하여 LHTD4의 혈관 신생 억제 효과를 확인하였으며, LHTD4에 의하여 혈관 성장 인자에 의한 수용체의 인산화가 효과적으로 저해됨을 확인하였다. 더 나아가 사람 폐암 세포가 이식된 동물 모델을 이용하여 혈관 신생 억제에 의한 암 조직의 성장 억제 효과를 확인하였다. 마지막으로, 화학적 발암 동물모델에서의 폐암 예방 효과 연구에서, LHTD4에 의하여 폐 조직에서의 결절 형성 및 혈관 생성이 효과적으로 감소됨을 확인하였다. 이러한 결과를 바탕으로, LHTD4는 경구형 혈관 신생 억제제로서, 폐암의 화학적 암 예방 제제로서의 적용이 가능할 것이라 기대된다.

본 연구의 제 3장에서는, 대표적인 항염증 약물인 쎄레콕시브와 새롭게 개발된 경구형 헤파린 유도체(LHD4)의 병용에 의한 대장암 예방 효과를 연구하였다. 대장 표적형 화학적 발암 물질을 이용한 동물 모델을 이용하여, 17주간 약물을 투여한 후 대장 조직을 떼어내어 두 약물의

대장암 예방 효과를 평가하였다. 그 결과 약물에 의하여 대장 조직에서의 폴립 형성 및 폴립 조직 내의 암 진행 정도, 혈관 생성, 염증 진행 정도가 유의적으로 감소되었으며, 두 약물의 병용 시 가장 효과적으로 억제됨을 확인하였다. 이러한 결과를 바탕으로, 혈관 신생 및 염증 반응을 동시 저해 가능한 두 약물의 병용요법은 임상적으로도 유효한 대장암의 화학적 암 예방법이 될 것으로 기대된다.

본 연구의 제 4장에서는, 본 연구에서는 혈관 신생 억제제(LHT7)를 이용한 항암 치료에 있어서 2형 시클로옥시게나아제 (cyclooxygenase-2)의 억제 효과를 연구하였다. 먼저 암세포를 이식한 동물 모델에서 혈관 신생 억제제를 투여한 경우, 암 조직 크기의 성장은 효과적으로 저해되는 반면 이로 인해 암 조직 내 산소 분압은 감소하는 것으로 확인되었다. 그 결과, 암조직 내 저산소 부위에서 특이적으로 2형 시클로옥시게나아제의 발현이 증가하는 것으로 확인되었다. 또한 LHT7을 투여한 동물의 암조직에서의 대식세포의 수는 증가하였으며, 이는 쎄레콕시브의 병용 투여로 인하여 효과적으로 억제되었다. 한편으로, 혈관 내피 세포와 동물 모델을 이용하여 LHT7과 쎄레콕시브의 병용효과가 혈관 생성 정도에 미치는 영향을 평가하였다. 그 결과, 두 약물의 병용으로 인하여 혈관의 생성 및 구조 안정화가 더욱 현저하게 저해됨을 확인하였다. 그러나 암 조직의 크기 성장 억제에 있어서는 이러한 두

약물의 병용 사용으로 인한 상승효과가 나타나지 않는 것으로 확인되었다. 이러한 결과를 바탕으로 2형 시클로옥시게나아제의 억제는 혈관 신생 억제제의 사용시 발생하는 2형 시클로옥시게나아제를 매개로 한 치료 저항 기전을 효과적으로 억제시켜주며, 또한 혈관 신생 억제제의 효과를 증가시켜 줄 것으로 기대된다.

마지막으로 본 연구의 제 5장에서는, 혈관 신생 억제제(LHT7)의 혈관 부위 표적형 전달을 위한 약물 전달체를 개발하였다. 정전기적 상호작용을 바탕으로 하여, 양이온성을 띄는 지질성 나노 입자의 표면에 음이온성의 LHT7을 결합시켰다. 더 나아가 지질성 나노 입자의 내부에는 히스톤 탈아세틸화효소(histone deaceytylase)의 억제를 기전으로 하는 항암제인 SAHA (suberoylanilide hydroxamic acid)를 봉입하였다. 이러한 제제화를 통하여 LHT7의 약물동태학적 특성은 현저하게 개선되었으며, 암 부위 표적 효과 또한 확인할 수 있었다. 또한 지질성 나노 복합체를 이용하여 두 약물을 동시에 제제화 함으로써(LHT7/SAHA nanolipoplex), 두 가지 약물의 병용으로 인한 치료 상승 효과 또한 얻을 수 있었다. 이러한 결과를 바탕으로, 본 연구는 혈관 신생 억제제 및 병용 약물의 혈관 표적 부위로 동시 전달이 가능한 약물 전달체로서의 지질성 나노 복합체의 개발 가능성을 제시하였다.

이러한 연구들을 통하여, 앞으로 혈관 신생 억제 작용을 가지는 다양한 저분자량 헤파린-담즙산 유도체의 화학적 암 예방 및 치료제로서의 임상적 적용을 기대해본다. 더 나아가 이러한 치료 효과는 혈관 부위 표적성을 가지는 약물 전달체를 이용함으로써 더욱 증가 시킬 수 있을 것이라고 기대된다.

주요어: 혈관 신생, 헤파린 유도체, 화학적 암 예방, 화학적 암 치료, 2형 시클로옥시게나아제, 약물 병용 요법, 나노 복합체

학번: 2009-30460